THESE DE DOCTORAT

Présentée en vue de l'obtention du grade de
DOCTEUR D'AIX-MARSEILLE UNIVERSITE

Sciences de l'Environnement Terrestre

par

Marta KERBER SCHÜTZ

LE ROLE DES BACTERIES HYDROGENOTROPHES ET FERRI-REDUCTRICES SUR LE PROCESSUS DE CORROSION EN CONTEXTE DE STOCKAGE GEOLOGIQUE

THE ROLE OF HYDROGENOTROPHIC IRON-REDUCING BACTERIA ON THE CORROSION PROCESS IN THE CONTEXT OF GEOLOGICAL DISPOSAL

Soutenue publiquement le 13 décembre 2013
- Château de Cadarache -

Membres du jury:

Mme. Régine BASSEGUY	LGC, Université de Toulouse	Rapporteur
M. Christian MUSTIN	LIEC, Université de Lorraine	Rapporteur
M. Pierre ROCHETTE	CEREGE, Aix-Marseille Université	Examinateur
M. Achim ALBRECHT	Andra	Examinateur
M. Bernard TRIBOLLET	LISE, UPMC-Paris 6	Examinateur
M. Damien FERON	CEA Saclay	Invité
M. Olivier BILDSTEIN	CEA Cadarache	Invité
M. Michel SCHLEGEL	CEA Saclay	Co-directeur de thèse
Mme. Marie LIBERT	CEA Cadarache	Directrice de thèse

« Dans la vie, rien n'est à craindre, tout est à comprendre »

Marie Curie

Dedication

To Paulo and Marilda,
the greatest examples in my life

ACKNOWLEDGEMENTS

First, I would like to thank the BIOCOR ITN project and the European Community for the financial support.

I wish to express my greatest thanks to my supervisor, Marie Libert, who gave me the opportunity to work and learn about the fascinating world of microbiology. Thanks for making me feel welcome in France and for the patience with a "non-French speaker" and "non-microbiologist" as well as for the constant guidance, advice and encouragement.

I would also like to extend my thanks to my co-supervisor, Michel Schlegel, for his support, constructive comments and discussions.

I take this opportunity to thank all members of the LMTE laboratory. You were my family when I arrived in France and I will carry you all in my heart! Thank you for teaching me the everyday joys of the French life style as well as for the patience and the help to improve my understanding *en français*. A special thanks to Olivier Bildstein and Jean-Eric Lartigue for their significant contribution and support towards this work and fruitful discussions.

I must thank Catherine Berthomieu and the LIPM team for receiving me so well during the last years of my PhD work. I felt very welcomed and you were always there for me when I needed! Many thanks for the friendship and for the good working atmosphere!

I also send my best gratitude to Régine Sellier who introduced me to the microbiological methods. Michel Lillo and Paul Soreau for the help with the ICP-OES analysis. Françoise Pillier who patiently helped me with the SEM analysis. Daniel Borschneck for the help with the XRD analysis. Sylvie Pierrisnard for the help with IC analysis. Gilles de Luca and Patrick Carrier for the help with the anaerobic glovebox.

Many thanks to Jérémy Royer and Claire Riot with whom I had the opportunity to work with during their undergraduate internship. Thanks for keeping the enthusiasm and for never giving up in the difficult moments!

I am grateful to the members of the jury for having accepted to participate on the evaluation of this work, especially to Régine Basséguy and Christian Mustin for their work as referees.

I would also like to thank Bernard Tribollet and Vincent Vivier for their support with the surface analysis at the LISE laboratory. A special thanks to Rebeca Moreira… *Rebequita*, it was a pleasure to work with you and I hope to keep our friendship even after the "BIOCOR era"!

Many thanks to all the BIOCOR team for providing many special moments during our meetings. I had the opportunity to meet incredible people that I will take as friends for the rest of my life!

I would like to extend my thanks to Michel Jullien who helped me a lot in my adaptation phase in France. I could always count on you to feel at home with our *soirées à la brésilienne*! Thank you for the advices and encouragements.

A special thanks to all the friends that have made these three years much easier and pleasant, in particular to Loïc, Valérie, Amélie, Camille, Mohamed, Romain and Maria Rosa. Thanks for the friendship and for standing by me all this time!

I am most grateful to my parents, Paulo and Marilda, for their love and support. They always encouraged my personal and professional growth. Many thanks to all my family and friends who trust and believe that I can always go further!

Finally, I want to express my deepest thanks to Vinícius for his constant support and encouragement in my professional carrier. Thank you for taking the challenge of facing a new life in France by my side! I hope that this is just the beginning of a long and happy journey together!

PREFACE

This thesis is undertaken under the BIOCOR ITN research project (website: www.biocor.eu); a Marie Curie Initial Training Network funded by the European Community's Seventh Framework (FP7) 2008 "People" Programme, under grant agreement n° 238579. The PhD work was performed at the Laboratory for Modelling Transfers in the Environment (LMTE), Service of Transfer Modelling and Nuclear Measurement (SMTM), Department of Nuclear Technology (DTN), Alternative Energies and Atomic Energy Commission (CEA) at Cadarache from September 2010 to August 2013. Part of the work was performed at the Laboratory of Protein Metal Interactions (LIPM), Department of Plant Biology and Environmental Microbiology (SBVME), Institute of Environmental Biology and Biotechnology (iBEB), CEA Cadarache.

This work was widely disseminated through publication of articles and participation in conferences/congresses:

- **Articles:**

SCHÜTZ, M. K.; MOREIRA, R.; BILDSTEIN, O.; LARTIGUE, J-E.; SCHLEGEL, M. L.; TRIBOLLET, B.; VIVIER, V.; LIBERT, M. (2013). *Combined geochemical and electrochemical methodology to quantify corrosion of carbon steel by bacterial activity*. Accepted for publication in the Bioelectrochemistry journal (doi: 10.1016/j.bioelechem.2013.07.003).

SCHÜTZ, M. K.; LIBERT, M.; SCHLEGEL, M. L.; LARTIGUE, J-E.; BILDSTEIN, O. (2013). *Dissimilatory iron reduction in the presence of hydrogen: a case study of microbial activity and nuclear waste disposal*. Procedia Earth and Planetary Science 7: 409–412.

- **Participation in conferences and congresses:**

SCHÜTZ, M. K.; LIBERT, M.; SCHLEGEL, M. L. *Metallic Corrosion within Nuclear Waste Repositories: A Source of H_2 and Fe oxyhydroxides for Microbial Activities*, EUROCORR 2013: "Corrosion Control for a Blue Sky", 2013, Estoril, Portugal. (Oral presentation)

SCHÜTZ, M. K.; LIBERT, M.; SCHLEGEL, M. L.; LARTIGUE, J-E.; BILDSTEIN, O. *Dissimilatory Iron Reduction in the Presence of Hydrogen: A Case Study of Microbial Activity and Nuclear Waste Disposal*, Fourteenth International Symposium on Water-Rock Interaction (WRI 14), 2013, Avignon, France. (Oral presentation)

SCHÜTZ, M. K.; LIBERT, M.; LARTIGUE, J-E.; BILDSTEIN, O.; SCHLEGEL, M. L. *Microbial Impact on Corrosion Products: The Role of Hydrogen and Magnetite on Nuclear Waste Geological Disposal*, 5th International Meeting: "Clays in Natural and Engineered Barriers for Radioactive Waste Confinement", 2012, Montpellier, France. (Poster presentation)

SCHÜTZ, M. K.; LIBERT, M.; SCHLEGEL, M. L. *Impact of Iron-Reducing Bacteria on the carbon steel corrosion: implications for the safe disposal of High Level Nuclear Waste*, EUROCORR 2012: "Safer World through better Corrosion Control", 2012, Istanbul, Turkey. (Oral presentation)

SCHÜTZ, M. K.; LIBERT, M.; SCHLEGEL, M. L. *Possible development of Iron-Reducing Bacteria using corrosion products within nuclear waste geological disposal facilities*, EUROCORR 2011: "Developing Solutions for the Global Challenge", 2011, Stockholm, Sweden. (Oral presentation)

SCHÜTZ, M. K.; LIBERT, M.; SCHLEGEL, M. L. *Influence of Iron-reducing Bacteria which use Hydrogen of Biocorrosion*, 18ème Congrès des Doctorants en Sciences de l'Environnement, 2011, Aix en Provence, France. (Poster presentation)

- **Other articles closely related to the topic of the thesis and co-authored, but not totally comprised in this manuscript, are listed below:**

LIBERT, M.; SCHÜTZ, M. K.; ESNAULT, L.; BILDSTEIN, O. (2013). *Are underground clay disposal conditions favorable for microbial activity and biocorrosion?* Procedia Earth and Planetary Science 7: 73–76.

LIBERT, M.; SCHÜTZ, M. K.; ESNAULT, L.; FERON, D.; BILDSTEIN, O. (2013). *Impact of microbial activity on the radioactive waste disposal: long term prediction of biocorrosion processes*. Accepted for publication in the Bioelectrochemistry journal (doi: 10.1016/j.bioelechem.2013.10.001).

MOREIRA, R.; SCHÜTZ, M. K.; LIBERT, M.; TRIBOLLET, B.; VIVIER, V. (2013). *Influence of hydrogen-oxidizing bacteria on the corrosion of low carbon steel: Local electrochemical investigations*. Accepted for publication in the Bioelectrochemistry journal (doi: 10.1016/j.bioelechem.2013.10.003).

TABLE OF CONTENTS

LIST OF FIGURES

LIST OF TABLES

LIST OF ABBREVIATIONS

Andra: national radioactive waste management agency

ASTM: American society for testing and materials

ATR: attenuated total reflection

BET: Brunauer, Emmett and Teller

BSE: backscattered electrons

CEA: alternative energies and atomic energy commission

CFZ: connected fracture zone

COx: Callovo-Oxfordian argillite

CR: corrosion rate

DMSO: dimethyl sulfoxide

EDTA: ethylenediaminetetraacetic acid

EDX: energy dispersive X-ray

EPS: extracellular polymeric substances

FTIR: Fourier-transform infrared spectroscopy

GC: gas chromatography

HLNW: high level nuclear waste

HOB: hydrogen-oxidizing bacteria

IC: ion chromatography

ICP-OES: inductively coupled plasma optical emission spectrometry

IR: infrared

IRB: iron-reducing bacteria

IRSN: institute for radiological protection and nuclear safety

LB: Luria Bertani Broth

MIC: microbiologically influenced corrosion

NTA: nitrilotriacetic acid

RM: Raman microspectroscopy

SCE: saturated calomel electrode

SE: secondary electrons

SEM: scanning electron microscopy

SHE: standard hydrogen electrode

SOB: sulfur-oxidizing bacteria

SRB: sulfate-reducing bacteria

TMAO: trimethylamine N-oxide

URL: underground research laboratory

UV-Vis: ultraviolet–visible

WL: weight loss

XRD: X-ray diffraction

INTRODUCTION

Nuclear power generation, nuclear fuel cycle and the use of radioactive materials in the industry and medicine produce radioactive waste that are classified according to the radioactivity content and its half-life. Compared to other kinds of industrial waste, the radioactive waste have the advantage to be self-degrading due to the radioactive decay process which allows to decrease their toxicity with time. Moreover, the volume of waste is small, and thus confinement strategy can be used to isolate them from the environment. In that, they differ from the fossil fuel waste (combustion gases) which are usually dispersed directly into the atmosphere. The biggest challenge concerning nuclear waste management is to ensure a safe long-term confinement.

Among the types of radioactive waste, the high level nuclear waste (HLNW) are the most hazardous one, as it is made essentially of spent fuel or of reprocessing residues (fission and activation products). Since the radioactive decay process can take hundreds of thousands of years in the HLNW, they must be stored and disposed in a way that provides adequate protection for man and ecosystems against the risks associated with these waste.

The disposal in deep stable geological repositories (e.g. salt domes, granite structures and some types of argillaceous formations) is the generally recognised solution for HLNW management in many countries (Finland, France, Germany, Japan, Sweden, Russia, United Kingdom and United States). The strategy is based on a multi-barrier system involving several natural and/or engineered barriers designed to ensure long-term confinement.

In France, for example, HLNW are embedded in a glass matrix, stored in stainless steel containers, and then conditioned in carbon steel overpacks that are emplaced in a metallic sheath (liner) in a deep argillaceous formation. The liner serves as a ground support which enables a reversible disposal and where the packages can be emplaced and, if necessary, retrieved. The overpack is hermetically sealed and provides the mechanical integrity of the waste package. The function of this metallic material is also to limit water ingress from the geological formation, which can trigger corrosion and hence degradation of the HLNW package (Andra, 2005a). The groundwater is considered as the main factor liable to alter waste containers.

Because of the economic and environmental impact, the assessment of the long-term behavior of the radioactive waste and disposal materials is required to demonstrate the safety of this strategy and to assure the future geological disposal. The impact of abiotic parameters (e.g. temperature, pressure) on corrosion has already been integrated in the safety assessments (Andra, 2005a). In contrast, the impact of microbial processes is still an

open issue and must be further investigated in order to provide biological parameters for long-term prediction of biocorrosion phenomena.

It is known that microorganisms can adapt and survive even in the extreme conditions that will prevail during the repository lifetime (i.e. radiation, high temperature) (Meike and Stroes-Gascoyne, 2000; Pedersen, 2002). Moreover, under anoxic conditions, corrosion process produces H_2 gas and Fe(II,III)-bearing minerals, such as magnetite (Fe_3O_4). Both corrosion products can provide energetic substrates for anaerobic microbial development: H_2 as electron donor and Fe(III) as electron acceptor for redox reactions. It is noteworthy that H_2 is an important substrate, especially in repository environments containing low amounts of biodegradable organic matter. Water-saturated conditions and the availability of these corrosion products can thus promote the activities of hydrogen-oxidizing bacteria (HOB) and iron-reducing bacteria (IRB) within nuclear waste repository. However, the role of IRB on corrosion processes is still under discussion. Several studies have demonstrated either inhibitory or enhancing effects on corrosion depending on the environmental conditions (Dubiel *et al.*, 2002; Herrera and Videla, 2009; Lee and Newman, 2003; Mehanna *et al.*, 2008; Potekhina *et al.*, 1999). Bacterial-enhanced corrosion may be associated with the destabilization/dissolution of passivating oxide layers (i.e. magnetite) by structural Fe(III) reduction, which in turn exposes the metallic material to the corrosive environment and reactivates corrosion (Esnault *et al.*, 2011).

The research problem of this study is defined by asking open questions with respect to the potential impacts of HOB and IRB activities on the nuclear waste geological disposal:

- can HOB and IRB affect corrosion rates and modify the nature and amount of corrosion products?
- can HOB and IRB influence on the passivating properties of magnetite by structural Fe(III) reduction?
- can H_2 resulting from corrosion serve as energetic substrate?

The challenge of predicting the biocorrosion phenomena on long-term and under geological disposal conditions calls for an integrative approach, coupling *in situ* and laboratory experiments, study of archaeological analogues and modelling (Libert *et al.*, 2013). In our scientific approach we focus on laboratory experiments in order to understanding the phenomena, to identify the physicochemical mechanisms, and to determine the key parameters controlling the corrosion rate (over short periods of time). The main objective of this study is to evaluate the role of HOB and IRB activities on anoxic corrosion process by using geochemical indicators. *Shewanella oneidensis* strain MR-1 was

chosen as model organism of HOB and IRB, and both abiotic and biotic conditions were investigated. The experimental approach consists of three main setups:

(i) experiments with magnetite and H_2 aiming at verifying if bacteria can use H_2 to reduce structural Fe(III) from magnetite;
(ii) experiments with metallic iron powder in order to enhance the surface area and hence the iron corrosion and H_2 production;
(iii) experiments with carbon steel coupon (type A37) aiming at evaluating the corrosion process in more "realistic conditions" in terms of the type of material and reactive surface area.

This study is divided into six chapters. **Chapter 1** provides general background information on the nuclear waste geological disposal, microbial activity in deep geological formations, aqueous metallic corrosion and biocorrosion phenomena. **Chapter 2** gives a description of experimental methods and procedures used in this study. **Chapter 3** deals with a preliminary study on reactional parameters that can likely influence on the activity of *Shewanella oneidensis* and consequently Fe(III) reduction. **Chapter 4** discusses the results related to the Fe(III) bioavailability in magnetite and the influence of H_2 concentration on the Fe(III) reduction. **Chapter 5** addresses the results related to the impact of HOB and IRB activities on anoxic corrosion process for both iron powder and carbon steel coupons. Finally, a summary of the principal findings of this study with perspectives can be found in **chapter 6**.

CHAPTER 1: BACKGROUND OF THE STUDY

This thesis is undertaken under the BIOCOR ITN research project (website: www.biocor.eu). BIOCOR is a Marie Curie Initial Training Network (ITN) funded by the EU Seventh Framework "People" Programme. BIOCOR ITN aims at developing a new profile of researcher, capable of addressing all aspects of scientific and industrial problems related to biocorrosion. The project is oriented towards major industrial concerns and based on a "problem-oriented approach" from real field cases of biocorrosion from two major sectors: the oil/gas and energy industries. The research topics are based on three different research sub-programmes: the oil and gas water injection and production structures (RSP1&2), the cooling circuits in power plants (RSP3) and the nuclear waste underground disposal (RSP4). This PhD work takes part of the RSP4.

1.1 High Level Nuclear Waste Geological Disposal

Nuclear power provides 80% of the electricity production in France and, accordingly, generates substantial amounts of radioactive waste. With regard to the nuclear waste management in France, the general principles were initially set by the law of 30 December 1991 and later modified by the law of 28 June 2006. These principles establish deep geological disposal as the solution for management of intermediate/high level and long lived nuclear waste. Moreover, the law also requires that the disposal should be reversible for at least 100 years. An underground facility, called as Cigéo, is now in the industrial design phase in France. It is planned to submit the licence application for evaluation in 2015, and to ask later for commissioning by 2025. In this context, the National Radioactive Waste Management Agency (Andra) has been responsible for assessing the feasibility of the deep geological disposal of nuclear waste in France since the law of 30 December 1991. The Alternative Energies and Atomic Energy Commission (CEA) is the steering body in charge of research on their temporary storage and conditioning (Andra, 2005a).

Nuclear waste are classified according to their radiation level (very low, low, intermediate and high) and to the half-life (short- or intermediate-lived: < 30 years; long-lived: > 30 years) of the main radionuclides (Andra, 2005a). In France, the high level nuclear waste (HLNW) (or C-type nuclear waste) represents 0.2% of the total volume of nuclear waste but provides 97% of the total radioactivity. According to Andra (2012), 4000 m^3 of HLNW in 2020 and 5400 m^3 in 2030 are expected to be disposed in a deep repository as illustrated in Figure 1.

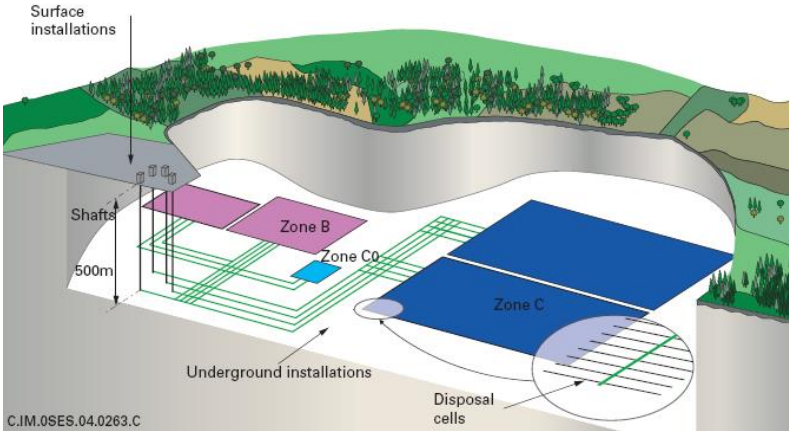

Figure 1: Schematic illustration of nuclear waste geological disposal with the areas devoted to intermediate level waste (or B-type nuclear waste) and high level waste (or C-type nuclear waste) (Andra, 2005a).

The generally accepted strategy to manage the HLNW is the disposal of waste packages in a deep underground repository (about 500 m deep) in stable geological formations (e.g. clay or granitic medium) (Bennett and Gens, 2008). This concept is known as a multi-barrier system which has been designed to prevent the migration of radionuclides that could be harmful to ecosystems and human health. It involves the use of several natural and/or engineered barriers (Figure 2) capable of confining the radioactivity for several thousand years.

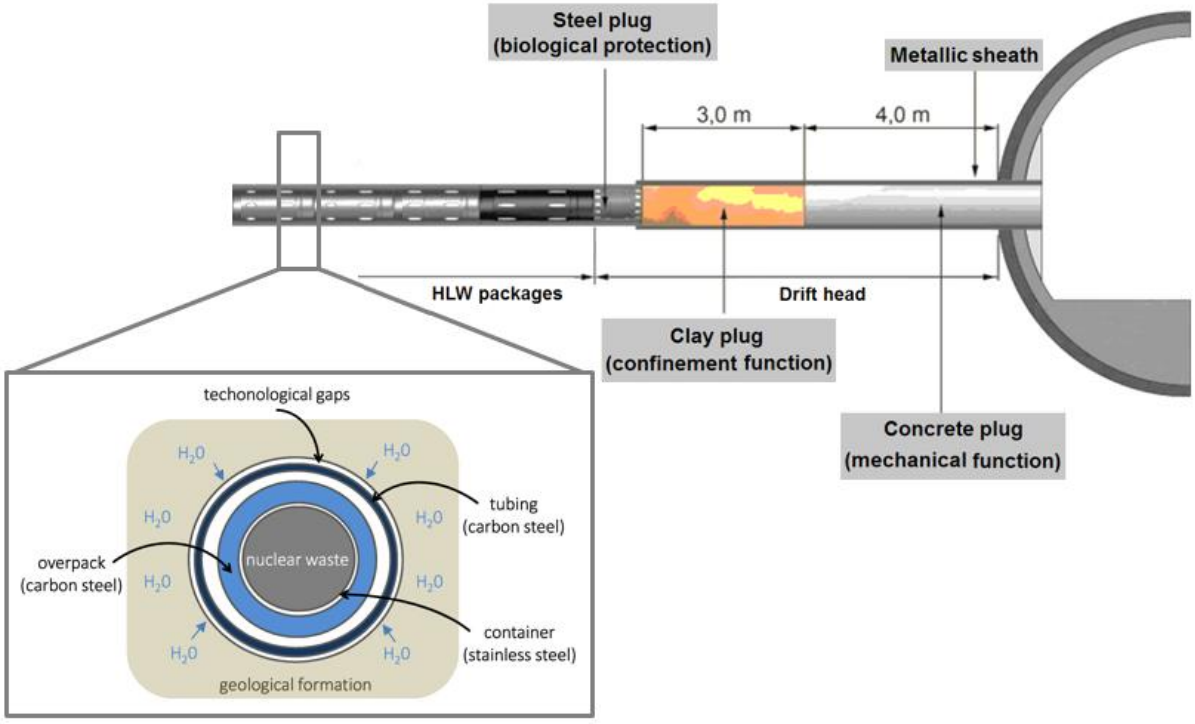

Figure 2: Longitudinal cross section of the HLNW disposal cells: the image in detail shows the different metallic packages of the multi-barrier system (modified from Andra, 2005a).

Each of these barriers provides a unique and stand-alone level of protection — if any of the barriers deteriorate, the next one will come into play. Multi-barrier systems have been widely considered in a number of countries in Europe, Asia and North America and the approach of the concept differs depending upon the type of nuclear waste and the geology of the available sites.

The long-term behavior of HLNW depends on the properties of the waste repository, but also on the nature of the HLNW itself. In France, HLNW are solidified as a glass, encapsulated in a container with different metallic packages and then placed into underground disposal cells (Andra, 2005a).

The multi-barrier system aims at minimizing water migration around the metallic packages (tubing, overpack, and container) because corrosion in water-saturated conditions is the major vector liable to alter the waste container. Note that materials selection for the packages is based on their properties, behavior and predictable nature of their corrosion processes.

The natural barrier (geological formation) presents a key part of the disposal system due to the intrinsic properties that provide good confining properties, such as low porosity and permeability, low hydraulic conductivity, high radionuclide sorption capacity, and swelling of clay minerals. In France, Andra has studied the Callovo-Oxfordian (COx) argillite of the Meuse/Haute-Marne site within the Bure Underground Research Laboratory (URL). This argillaceous formation has been considered as potential host-rock for future nuclear waste disposal because it displays the desired confining properties (Andra, 2005a). In addition, the Institute for Radiological Protection and Nuclear Safety (IRSN) has been carrying out research in the Toarcian argillite within the Tournemire URL in Southern Aveyron, France. The Tournemire URL is a tunnel crossing a 250 m thick Toarcian formation with adjacent drifts excavated in 1996, 2003 and 2008. This URL has been developed only for expertise purpose, and there is no intention of disposing nuclear waste in this site at any time in the future. COx and Toarcian argillites present similar physico-chemical properties.

In this context, the assessment of the long-term behavior of the nuclear waste and disposal materials is required in order to demonstrate the safety of this strategy and to assure the future geological disposal. The study of the phenomena linked to corrosion becomes therefore crucial to evaluate the containment capacity of the metallic materials (Bennett and Gens, 2008; Cattant *et al.*, 2008; Duquette *et al.*, 2009; Feron *et al.*, 2008; Landolt *et al.*, 2009). Modelling has been widely applied as approach for long-term predictions. Either laboratory experiments or archaeological artifacts, which were exposed to corrosive environments over a long time, may provide parameters (e.g. kinetics, physico-chemical) for testing and validating models. Modelling efforts indicate that a

water flow of 10^{-2} L.m^{-2}.year^{-1} (assuming to be uniform) limits the metallic corrosion rate to 3 µm.year^{-1}, which means 3 mm of metal corroded in 1000 years. For flows below 10^{-3}-10^{-2} L.m^{-2}.year^{-1}, the corrosion rate appears to be limited by the water flow in the geological formation. A water flow above 0.1-1 L.m^{-2}.year^{-1} no longer limits the corrosion rate (Feron *et al.*, 2008). The corrosion phenomenon under geological conditions is discussed in more detail in the section 1.3 of this chapter.

1.2 Microbial Activity in Deep Geological Formations

1.2.1 Microbial diversity, survival and potential effects

Several studies demonstrate that bacteria and archaea are present in most of the deep geological formations already investigated (Boivin-Jahns *et al.*, 1996; Mauclaire *et al.*, 2007; Poulain *et al.*, 2008; Stroes-Gascoyne *et al.*, 2011; Urios *et al.*, 2012). For example, a study performed by Urios *et al.* (2012) pointed out the cultivable microbial diversity at different zones of the Tournemire URL. The investigated zones comprised *(i)* the wall of the drift excavated in 1996; *(ii)* a connected fractured zone (CFZ) (0-0.38 m from the wall) which is characterized as a damaged zone due to the excavation of underground structures; *(iii)* a deeper undisturbed zone (3.50–3.80 m from the wall); and *(iv)* a zone intersected by a geological fault (6–6.22 m from the wall). According to this study, the microbial diversity can depend on oxygen (O_2) and humidity conditions, and also on space availability (Table 1).

Table 1: Example of microbial diversity in a deep geological formation (Tournemire case) (Urios et al., 2012).

Zone	Microbial diversity			
	Sulfate-reducers	Anaerobic heterotrophs	Aerobic heterotrophs	Aerobic oligotrophs
Undisturbed zone	-	+	-	-
CFZ	-	+	+	+
Faulted area	+	+	+	+
Drift wall	+	+	+	+

- : absence; + : presence

As shown in Table 1, the microbial diversity is higher in the faulted area and drift wall. Moreover, the presence of anaerobic/aerobic and heterotrophs/oligotrophs

microorganisms in the CFZ can be expected. It is important to note that the introduction of non-indigenous microorganisms due to human activities within nuclear waste repository cannot be excluded during the construction and operational phases.

It is known that microorganisms can use different pathways for their survival in extreme conditions, like in the near field of HLNW packages. The most resistant form of survival is the formation of endospores by certain Gram-positive and sulfate-reducing bacteria (SRB). Many microorganisms can just scale down their metabolism to an absolute minimum level when there is an energetic and/or nutritional deficiency. Therefore, it is possible that microorganisms survive initially in the presence of irradiation, desiccation, heat or high pH until the conditions for their growth and activity become favorable again (Meike and Stroes-Gascoyne, 2000; Pedersen, 2002).

Taking into account their survival capability and adaptation even in extreme conditions, the impact of microbial activities within nuclear waste repository definitively needs to be investigated in order to determine if biological parameters should be integrated in safety assessments of geological disposal.

As shown in Figure 3, the physico-chemical conditions within underground repository change with time.

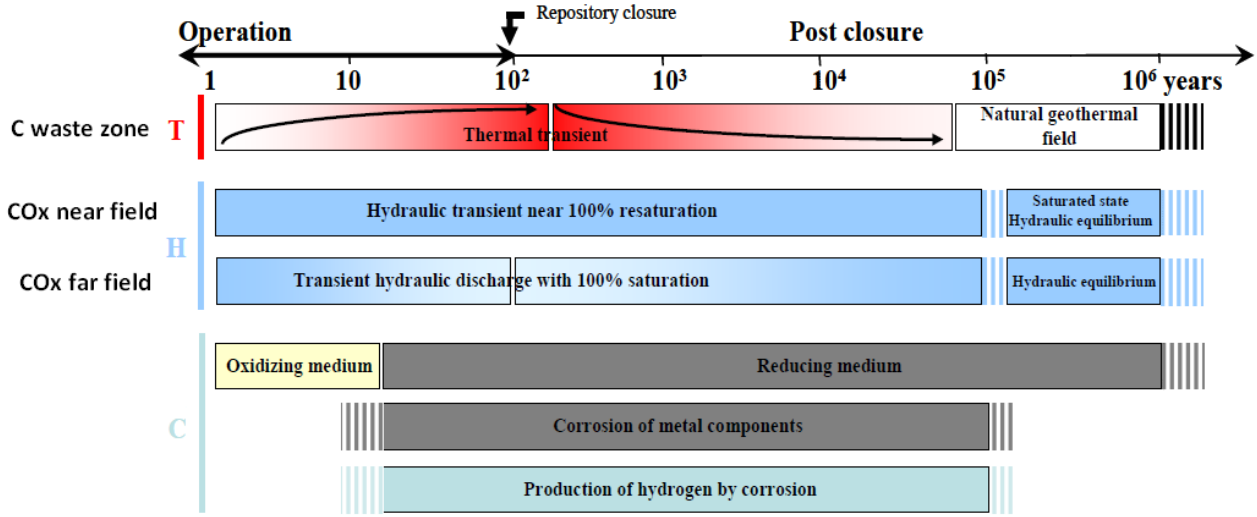

* near field is defined as the host-rock in contact with (or near) the waste package whose properties have been affected by the presence of the repository, like the connected fractured zone (CFZ).

* far field is defined as the geosphere (including the biosphere) beyond the near field.

Figure 3: Phenomenological evolution within the HLNW repository: T for thermal; H for hydraulic; and C for corrosion (modified from Andra, 2005b).

Initially, the conditions will be hot (maximum temperature of 90°C) and oxidizing. The temperature will then decrease and the conditions will change to anoxic because the irradiation is reduced by radioactive decay process and O_2 is consumed, for example, by

aerobic corrosion and/or aerobic microbial activities. A re-saturation of the repository by water coming from the geological formation will occur with concomitant corrosion of metallic packages as well as degradation of other disposal materials.

Table 2 shows the evolution of physico-chemical conditions as a function of time within HLNW repository (Andra, 2005a) compared to the conditions favorable to bacterial activity (line highlighted in blue) (Motamedi *et al.*, 1996; Pedersen *et al.*, 1995).

Table 2: Comparison of physico-chemical conditions within HLNW repository with bacterial activity optimal conditions.

Time (years)	Temperature (°C)	Irradiation (Sv/h)	Water saturation
bacteria			
-	*20-45 / 70*	*< 60*	*> 0.96*
~10	90[a] - 75[b] - 65[c]	100	0.8
100	65[a] - 61[b] - 58[c]	50	0.97
500	50[a] - 47[b] - 46[c]	0.8	0.97
1,000	40[a] - 40[b] - 40[c]	0.5	0.98
10,000	27[a] - 27[b] - 27[c]	0.4	0.99
30,000	25[a] - 25[b] - 25[c]	0.1	0.99

[a]: overpack; [b]: CFZ; [c]: claystone

As shown in Table 2, it is expected that after approximately 100 years, decreased irradiation, lower temperatures and substantial water resaturation will permit bacterial development. It is important to note that even though growth and activity of microorganisms in compacted clay medium are still a matter of debate, especially due to the small pore size in the nanometer range (Fredrickson *et al.*, 1997; Stroes-Gascoyne *et al.*, 2010), such a growth will certainly be possible in the CFZ (presence of heterogeneities, cracks) and in the technological gaps (void space between metallic packages, see Figure 2).

Therefore, since microorganism development may occur under HLNW disposal conditions, the potential effects of such microbial activity must be investigated. In this way, several aspects have been studied, such as tolerance of microorganisms to extreme conditions, microbial gas production, biocorrosion of metallic packages, and radionuclides migration (including effects of biofilms) (Behrends *et al.*, 2012; Keith-Roach and Livens, 2002; Libert *et al.*, 2013; Lloyd and Renshaw, 2005; Pedersen, 2000; Pedersen, 2002; Stroes-Gascoyne and Sargent, 1998; Stroes-Gascoyne and West, 1996; West *et al.*, 2002). For instance, microbial activities may interfere with the migration of radionuclides through geological formations by different processes: *(i)* microbial redox reactions; *(ii)* production of extracellular polymers which may act as ligands, forming dissolved complexes with

dissolved radionuclides, and thus preventing their sorption by geological medium, or biofilms which may act as barriers to radionuclide sorption on mineral surfaces or, alternatively, may favor sorption through the formation of ternary surface complexes; and *(iii)* incorporation of trace amounts of radionuclides into the cell structure which enables their retention and subsequent release when microorganisms decompose (Keith-Roach and Livens, 2002; Pedersen, 2002; West *et al.*, 2002).

Moreover, studies have shown that iron-reducing bacteria (IRB) can alter *(i)* passivating oxide layers (especially magnetite) at the corroded metal surface by structural Fe(III) reduction (Dong *et al.*, 2000; Esnault *et al.*, 2011; Herrera and Videla, 2009; Kostka and Nealson, 1995), which could reactivate the corrosion process; and *(ii)* smectite phases from argillaceous formations, destabilizing clay minerals and affecting confining properties of the natural barrier (Esnault *et al.*, 2013a; Kostka *et al.*, 2002; Kostka *et al.*, 1996; Kostka *et al.*, 1999; Liu *et al.*, 2012).

1.2.2 Microbial growth and metabolism

1.2.2.1 Effect of physico-chemical conditions

Microorganisms are able to survive and grow in a wide range of environments (i.e. soil, water, acidic hot springs, and deep portions of Earth's crust). They exhibit a great diversity morphological and physiological capable to tolerate even extreme physico-chemical conditions as already mentioned.

Most life forms are dependent on O_2 for survival and growth, and they are called *aerobes*. However, some *anaerobes* microorganisms are able to survive in the absence of O_2 and some do not even tolerate its presence (Gottschalk, 1986; Hogg, 2005).

Regarding the temperature, most of the microorganisms grow slowly at low temperatures because the enzymes efficiency decreases, the lipids tend to harden and the membrane and cytoplasm fluidity decrease. Growth rates increase with temperature until an optimum is reached. Above this optimal temperature, a decrease of microbial activity may occur by denaturation of enzymes, promoting a decline of the growth rate and ultimately death of the microorganisms. Most of the microorganisms achieve optimal growth at temperatures around 20-40°C and they are classified as *mesophiles*. *Thermophile* microorganisms are capable of growing within a temperature range of 40-80°C; *extreme thermophiles* may tolerate temperatures higher than 100°C. In contrast, some *psychrophiles* can grow at 0°C (Gottschalk, 1986; Hogg, 2005).

Regarding the pH, most of the microorganisms better grow around the neutrality (pH ~ 7), and thus are classified as *neutrophiles*. Microorganisms that prefer slightly alkaline conditions (pH ~ 11) are named as *alkalophiles*, and the ones which tolerate acidic conditions (pH < 5.5) are classified *acidophiles* (Gottschalk, 1986).

One of the most limiting conditions for microbial growth, besides the available space, is the water availability which is usually expressed as water activity (a_w). Most of the microorganisms grow better at water activities around 0.98 or higher, but they can support variations in the range of 0.8-0.9. At low water activities they must expend extra efforts to grow (Pedersen *et al.*, 1995).

1.2.2.2 Nutritional and energetic substrates

All living organisms need nutritional and energetic substrates (Figure 4). Nutritional substrates are required for synthesis of cell components and energetic substrates for energy production. Energy is generated by transferring electrons through the cell membrane (ATP synthase), which provides energy carrier molecules such as adenosine-5'-triphosphate (ATP). Therefore, a growth medium must supply all of the needed substrates required for cellular growth and for their reproduction and maintenance.

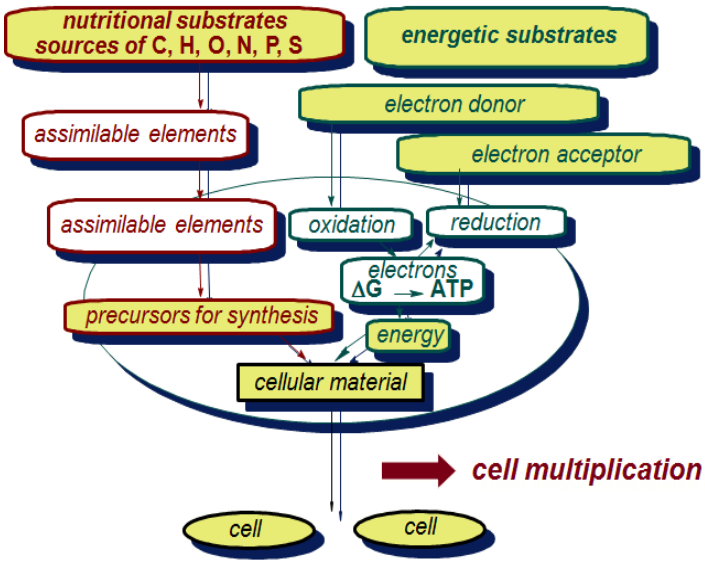

Figure 4: Nutritional and energetic substrates for microbial metabolism.

The nutriments must contain those chemical elements that are constituents of the cellular materials (i.e. C, H, O, N, P, S) and that are needed for enzymatic activities and transport systems. Other elements in small amounts are also required for the cells, such as

Ca, Fe, K, Mg, Zn, Mn, Mo, Se, Co, Cu, Ni and Na (Gottschalk, 1986; Hogg, 2005). A number of bacteria do not have the ability to synthesize all the organic compounds needed for growth, and depend on certain growth factors, such as vitamins and amino acids. As the growth factors have not been identified yet for all microorganisms, yeast extract and peptone are generally added to the growth medium as cheap sources of these factors in laboratory experiments (Gottschalk, 1986; Hogg, 2005).

The microorganisms can be classified according to their carbon source for biomass synthesis. *Autotrophic* microorganisms obtain carbon from carbon dioxide (CO_2) and *heterotrophic* from organic compounds. *Phototrophic* microorganisms use the photosynthesis process to convert light energy into chemical energy. C*hemotrophic* microorganisms obtain energy from oxidation-reduction (redox) reactions with external chemical compounds, which means that these microorganisms require an electron donor (reducer) and an electron acceptor (oxidizer). Depending on the nature of the electron donor compounds, the microorganisms are classified as *chemoorganotrophs* (organic compounds) or *chemolithotrophs* (inorganic compounds) (Gottschalk, 1986; Hogg, 2005).

Studies have shown that host-rocks can provide several nutrients needed for microorganism growth (Gaucher *et al.*, 2004; Vinsot *et al.*, 2008). Such nutrients may be found either as soluble species in the interstitial waters or as insoluble (solid-associated) forms. The soluble nutrients are assimilated directly by microorganisms. In contrast, insoluble nutrients can be recovered only by specific mechanisms, such as solubilisation. In addition, the introduction of exogenic materials (i.e. steel, glass) within nuclear waste repository will change the nutrient and energetic inventory of the original (pristine) environment. Corrosion is the mainly phenomenon responsible for providing new substrates, especially energetic by production of Fe(II,III) (hydr)oxides and dihydrogen (H_2). It is noteworthy that the nutrients provided by the host-rock as well as disposal materials and the environmental conditions will control the type of metabolisms which are likely to develop and their activity.

1.2.2.2.1 Iron: an element of biological importance

Iron (Fe) is the fourth most abundant element in Earth's crust and can be found in a variety of rocks and soil minerals. The common oxidation states in natural systems are (0) (in meteorites), (II) and (III). Under oxidizing conditions, the ferrous form Fe(II) readily oxidizes to the ferric form Fe(III), and vice-versa under reducing conditions. Fe(III) is usually found as phyllosilicates (e.g. nontronite), hydroxides ($Fe(OH)_3$), oxyhydroxides (FeOOH) and oxides (Fe_2O_3) (Ehrlich and Newman, 2008). However, significant

concentrations of soluble Fe(III) species may be obtained by complexation with strong chelators (Pierre *et al.*, 2002).

All living organisms require Fe for their metabolism (i.e. proteins synthesis). Specifically, Fe(III) is involved in microbial metabolism by two main Fe(III)-reducing processes: *(i) dissimilatory* iron reduction corresponds to an enzymatic Fe(III) reduction as a form of respiration, mostly anaerobic, in which Fe(III) serves as a dominant or exclusive terminal electron acceptor for energy production; and *(ii) assimilatory* iron reduction occurs when Fe(III) is reduced during uptake or incorporation into specific cellular components. Relatively large quantities of Fe are reduced in dissimilatory reduction, whereas only very small amounts are taken up by assimilatory reduction (Ehrlich and Newman, 2008; Lee and Newman, 2003).

The Fe(II)/Fe(III) redox cycling was an important biogeochemical process on early Earth, and probably still is today in some anoxic environments (Ehrlich and Newman, 2008). Evidences suggest that Fe(III) reduction was a very early form of microbial respiration on Earth (Lovley, 2002; Lovley, 2005).

Dissimilatory Fe(III) reduction: bacteria-substrate electron transfer

A number of laboratory studies have been performed with iron-reducing bacteria, such as *Geobacter metallireducens*, *Geobacter sulfurreducens*, *Shewanella oneidensis* and *Desulfuromonas acetoxidans* in order to understand microbial Fe(III) reduction as respiration form (Ehrlich and Newman, 2008; Gralnick and Newman, 2007).

Fe(III) from soluble complexes (i.e. ferric citrate) can be readily used for respiration. However, uncomplexed Fe(III) has a very low solubility and is usually present as insoluble substrate at pH conditions typically found in the environment (i.e. weakly acidic to weakly basic). The mechanisms by which IRB reduce Fe(III) from insoluble substrates have been extensively studied and the literature suggests that several pathways can be used to transfer electrons to Fe(III) (Gralnick and Newman, 2007; Luu and Ramsay, 2003; Nevin and Lovley, 2002).

Figure 5 illustrates four potential mechanisms for Fe(III) reduction from an insoluble substrate. Figure 5(a) illustrates the direct contact of proteins located on the cell surface (green oval) with the substrate for electron transfer. Figure 5(b) shows a cellular appendage (e.g. fimbriae or pili/nanowires) which forms a bridge between the cell and the substrate, catalyzing electron transfer. Figure 5(c) shows the action of a chelator (yellow oval) dissolving and transporting Fe(III) to the cell for subsequent reduction. Finally, Figure 5(d) shows that reduction can be performed at distance using an electron shuttle (green

oval) which catalyzes the transfer of electrons between the cell and the substrate (Gralnick and Newman, 2007).

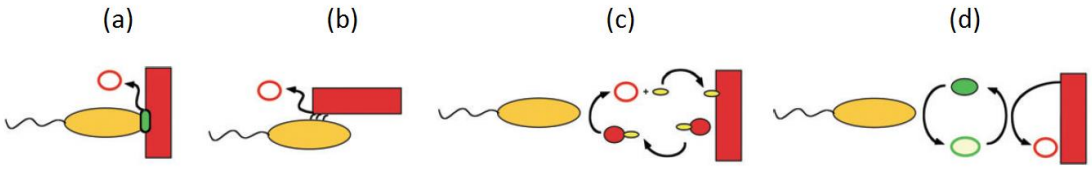

Figure 5: Mechanisms for microbial Fe(III) reduction from insoluble substrates: (a) direct contact; (b) cellular appendage; (c) chelator; and (d) electron shuttle. Red rectangle for Fe(III) insoluble substrate and open red circle for reduced product [Fe(II)] (Gralnick and Newman, 2007).

Electron-shuttling compounds are particularly important when Fe(III) solids are occluded in pore spaces which are too small for IRB access (e.g. clay formations), or in biofilms in which the majority of cells are not in direct contact with the substrate surface. They can be naturally found in some sedimentary environments as humic substances and quinones. Several studies demonstrated that the presence of these compounds in environments with low amounts of organic matter can stimulate Fe(III) reduction (Castro *et al.*, 2013; Lovley *et al.*, 1999; Newman and Kolter, 2000). Usually, the proteins involved in the electron transfer are localized on the outer membrane of Gram-negative bacteria. For example, *c*-type cytochromes play a major role in the Fe(III) reduction in *Shewanella* species (Gralnick, 2012; Lower *et al.*, 2001; Wigginton *et al.*, 2007).

Microbial Fe(III) reduction may affect the environment in different ways. On the one hand, it may provide a pathway for degradation of organic contaminants in groundwater under anoxic conditions. For instance, it was demonstrated that *Geobacter metallireducens* can oxidize common contaminants, such as toluene, phenol, *p*-cresol and benzoate to CO_2 coupled to Fe(III) reduction. On the other hand, toxic trace elements are able to adhere on Fe(III)-bearing minerals, and upon microbial Fe(III) reduction, these elements may be released into the environment. Passivating oxide layers are also strongly affected by bioreduction, and ultimately can fail to protect metal surface against corrosion upon Fe(III) reduction (Fredrickson and Gorby, 1996). The microorganisms can use a wide range of electron donors for Fe(III) reduction, such as lactate (organic) and H_2 (inorganic). The focus of this study is H_2.

1.2.2.2.2 Dihydrogen: an energetic substrate

Several microorganisms are able to metabolize H_2 as electron donor for energy production, known as hydrogenotrophic or hydrogen-oxidizing bacteria (HOB) (Table 3).

Table 3: Metabolic processes of hydrogen-oxidizing bacteria in the presence of different electron acceptors (Libert et al., 2011).

Autotrophic metabolic processes	Microorganisms species	ΔG^0 (kJ/mol electron) 25°C
$2\ H_2 + O_2 \rightarrow 2\ H_2O$	aerobic hydrogen bacteria (*Ralstonia sp.*)	-119
$5\ H_2 + 2\ NO_3^- + 2\ H^+ \rightarrow N_2 + 6\ H_2O$	denitryfing bacteria (*Paracoccus denitrificans*)	-118
$H_2 + 2\ Fe(OH)_3 + 4\ H^+ \rightarrow 2\ Fe^{2+} + 6\ H_2O$	iron-reducing bacteria (*Shewanella sp.*)	-91
$4\ H_2 + SO_4^{2-} + 2\ H^+ \rightarrow H_2S + 4\ H_2O$	sulfate-reducing bacteria (*Desulfovibrio sp.*)	-24
$4\ H_2 + CO_2 \rightarrow CH_4 + 2\ H_2O$	methanogens bacteria (*Methanobacterium sp.*)	-22
$4\ H_2 + 2\ CO_2 \rightarrow CH_3COOH + 2\ H_2O$	acetogens bacteria (*Acetobacterium* sp.)	-18

H_2 is known as one of the most energetic substrates for redox processes in deep terrestrial subsurface environments (Gales *et al.*, 2004; Lin *et al.*, 2005). The availability of this substrate can sustain the development of chemolithotrophic bacteria (able to grow using mineral carbon) within nuclear waste repositories (Libert *et al.*, 2011) that are generally poor or devoid of biodegradable organic matter (e.g. < 1% in Tournemire and 1.4% in Bure sites) (Deniau *et al.*, 2008).

Several processes (abiotic and biotic) may supply H_2, such as *(i)* active volcanism or seismic activity in deep faults of the Earth's crust; *(ii)* serpentinization; *(iii)* microbial fermentation; *(iv)* radiolytic dissociation of water during the radioactive decay of natural radionuclides; and *(v)* anoxic aqueous metallic corrosion (Gales *et al.*, 2004; Libert *et al.*, 2011; Lin *et al.*, 2005).

Moreover, a wide range of electron acceptors can be coupled to H_2 oxidation, such as oxygen, nitrate, ferric iron, sulfate, carbon dioxide or radionuclides. As shown in Figure 6, the redox conditions of the environment will determine in a particular order the electron acceptors to be used by bacteria for H_2 oxidation (Libert *et al.*, 2011).

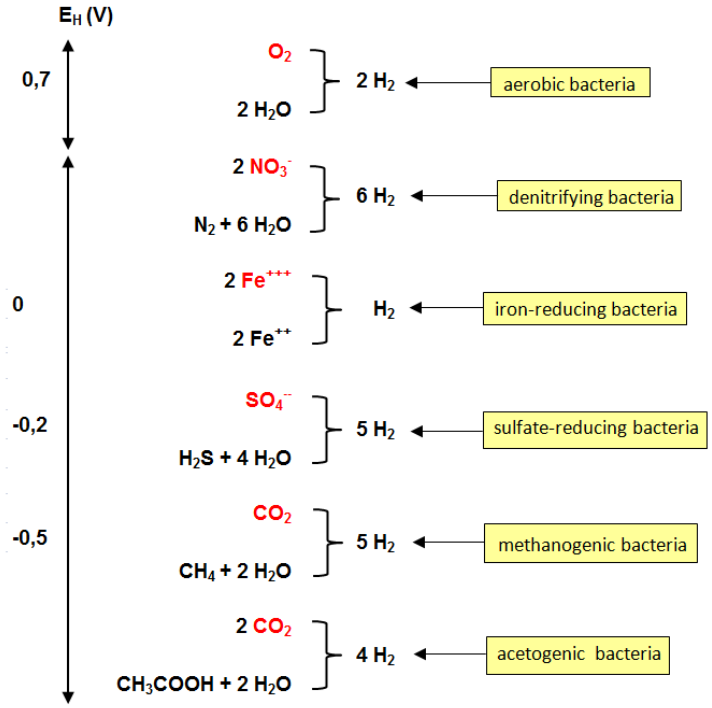

Figure 6: Reactions catalyzed by hydrogen-oxidizing bacteria according to redox conditions shown on the vertical distribution (redox potential versus SHE) (Libert et al., 2011).

The role of hydrogenase enzymes

The role of hydrogenase enzymes must be detailed in this study since our focus is H_2 as electron donor. Besides that, some studies have demonstrated that the sole presence of hydrogenases (without bacteria) can increase the corrosion of stainless steel by direct electron transfer (Da Silva *et al.*, 2002; Mehanna *et al.*, 2008).

These enzymes are responsible for H_2 oxidation in anaerobic or aerobic environments. They can also catalyze the reversible reduction of protons into molecular H_2 (Vignais and Billoud, 2007), according to the equation 1.1.

$$2\ H^+ + 2\ e^- \rightleftharpoons H_2(g) \qquad \textbf{(1.1)}$$

Most of the known hydrogenases are Fe-S proteins and they can be categorized into two phylogenetically distinct classes, according to metal contents of their active sites: [Ni-Fe] hydrogenases and [Fe-Fe] hydrogenases (Figure 7).

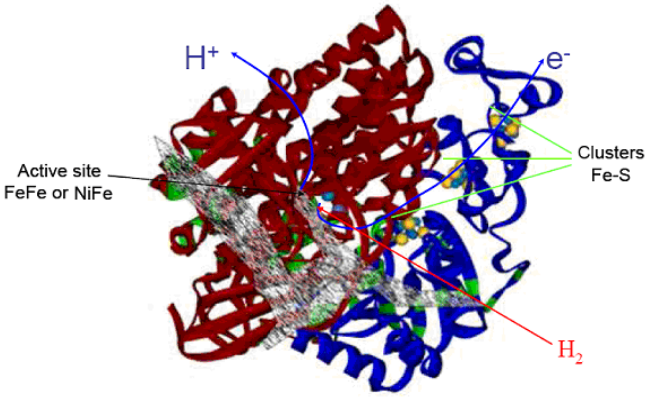

Figure 7: Structure of hydrogenase enzymes (Volbeda et al., 1995).

[Fe-Fe] hydrogenases are typically H_2-forming, while [Ni-Fe] hydrogenases may catalyze either H_2 uptake or formation. Usually, in the presence of an electron acceptor, the hydrogenase will act as a H_2 uptake enzyme, while in the presence of an electron donor of low redox potential, it may use the protons from water as electron acceptors and release H_2 (Frey, 2002; Meshulam-Simon *et al.*, 2007; Vignais and Billoud, 2007).

In both [Ni-Fe] and [Fe-Fe] hydrogenases, the catalytic sites are deeply buried inside of the respective proteins. This indicates that the components of the catalytic reaction (electrons, hydrons and molecular H_2) have to shuttle over several nanometers between these sites and the protein surface. Studies indicate that molecular H_2 could use a hydrophobic cavity and channels network observed in these hydrogenases as shuttle (Frey, 2002; Volbeda *et al.*, 1995).

[Ni-Fe] hydrogenases are found in a variety of anaerobic and facultative heterotrophic bacteria, cyanobacteria and archaea. In contrast, [Fe-Fe] hydrogenases are usually found in strict anaerobic bacteria, such as *Clostridium* and *Desulfovibrio* spp. (Meshulam-Simon *et al.*, 2007).

1.3 Aqueous Metallic Corrosion: A Source of Fe(II,III) (hydr)oxides and H_2

Corrosion is defined as a degradation of a metallic material to ionic species due to physico-chemical interaction with environment. Thus, it is a process coupling the oxidation of metal (anodic reaction, metal dissolution) and the reduction of an oxidizing agent (cathodic reaction) in the presence of an electrolyte. These reactions are illustrated by the equations 1.2-1.6 for iron.

(anodic reaction) $Fe^0 \rightarrow Fe^{2+} + 2\ e^-$ **(1.2)**

(cathodic reaction under *oxidizing* conditions) $O_2 + 2\ H_2O + 4\ e^- \rightarrow 4\ OH^-$ **(1.3)**

(cathodic reactions under *anoxic* conditions) $2\ H_2O + 2\ e^- \rightarrow 2\ OH^- + H_2$ **(1.4)**

or

$2\ H^+ + 2\ e^- \rightarrow H_2$ **(1.5)**

(overall reaction under *anoxic* conditions) $Fe^0 + 2\ H_2O \rightarrow Fe^{2+} + 2\ OH^- + H_2$ **(1.6)**

According to the overall reaction (eq. 1.6), 1 mole of H_2 gas can be generated for each mole of Fe corroded in anoxic hydrated environments. The H_2 generation has been studied in order to evaluate its possible effects within nuclear waste repository (Talandier *et al.*, 2006; Turnbull, 2009). Recently, Moreira (2013) performed electrochemical experiments by means of chronoamperometry to study the influence of local H_2 generation on the corrosion of carbon steel. High amounts of H_2 (0.5 mol) were generated locally in a small volume ($3.9x10^{-8}$ L) between a microelectrode and a carbon steel working electrode. The results showed an increase by a factor of 7 in the charge for steel corrosion in comparison with experiments without local H_2 generation. A modification in the surface reactivity and pH, by the generation of an electroactive species, can likely explain the increase in the corrosion (Moreira, 2013).

H_2 can either be absorbed by the metallic packages and then diffuse through the metal (process known as H_2 embrittlement) or diffuse away through the geological formation which could adversely affect sealing properties (e.g. by production of fissures due to pressure build-up). Usually, two criteria are taken into account to evaluate the impact of H_2 gas on the pressure of the geological formation: *(i)* an estimation of the rates of H_2 gas generation; and *(ii)* a two-phase flow transport modelling considering the physical properties of the host-rock, such as water saturation, gas permeability and effective diffusion. According to early models, the main phase of H_2 generation is the first 5,000 years for HLNW, assuming very low corrosion rates (a few microns per year) (Andra, 2005a).

Taking into account the variation on the physico-chemical conditions during the repository lifetime (oxidizing and then anoxic), the following corrosion products can be expected (eqs. 1.7-1.14) (David, 2001):

	$4\ Fe^0 + 3\ O_2 \rightarrow 2\ Fe_2O_3$	**(1.7)**
aerobic corrosion	$4\ Fe^0 + 6\ H_2O + 3\ O_2 \rightarrow 4\ Fe(OH)_3$	**(1.8)**
	$2\ Fe^0 + H_2O + 3/2\ O_2 \rightarrow 2\ FeOOH$	**(1.9)**
transition phase	$4\ Fe_2O_3 + Fe \rightarrow 3\ Fe_3O_4$	**(1.10)**
	$2\ Fe(OH)_3 + 4\ Fe + 2\ H_2O \rightarrow 2\ Fe_3O_4 + 5\ H_2$	**(1.11)**
anaerobic corrosion	$3\ Fe^0 + 4\ H_2O \rightarrow Fe_3O_4 + 4\ H_2$	**(1.12)**
	$Fe^0 + 2\ H_2O \rightarrow Fe(OH)_2 + H_2$	**(1.13)**
	$3\ Fe(OH)_2 \rightarrow Fe_3O_4 + 2\ H_2O + H_2$	**(1.14)**

Generally ferrous hydroxide ($Fe(OH)_2$) is not thermodynamically stable. Therefore, it will be transformed progressively to magnetite (Fe_3O_4) via the Schikkor reaction (eq. 1.14) (Odziemkowski *et al.*, 1998). Presence of certain impurities (e.g. Ni, Cu, Co) either from metallic packages or from interstitial water can catalyze this reaction. An increase in the temperature (above ~ 60°C) also promotes magnetite formation (the conversion is only 10-20% complete at room temperature) (Platts *et al.*, 1994).

The corrosion products will precipitate at the metal surface and form one or more layers which, depending on their chemistry and morphology, can act as passivating layers (i.e. magnetite) leading to lower corrosion rates and hence H_2 gas production. In this way, the most aggressive forms of corrosion (e.g. localized, stress corrosion cracking) will occur during the initial transient conditions of the repository, and more predictable forms of corrosion (e.g. generalized) will take place later. However, changes in the environmental conditions (e.g. pH, redox potential, CO_2 pressure) can affect the stability of passivating layers and, therefore, the overall susceptibility of the metal to corrosion.

Potential (Eh)-pH diagrams (known also as Pourbaix diagrams) are very useful to evaluate the stability of corrosion products in equilibrium with a given system, but the major limitation is that corrosion rates cannot be derived from the diagrams. Figure 8 shows the Eh-pH diagrams for the Fe-C-H_2O and Fe-PO_4-H_2O systems.

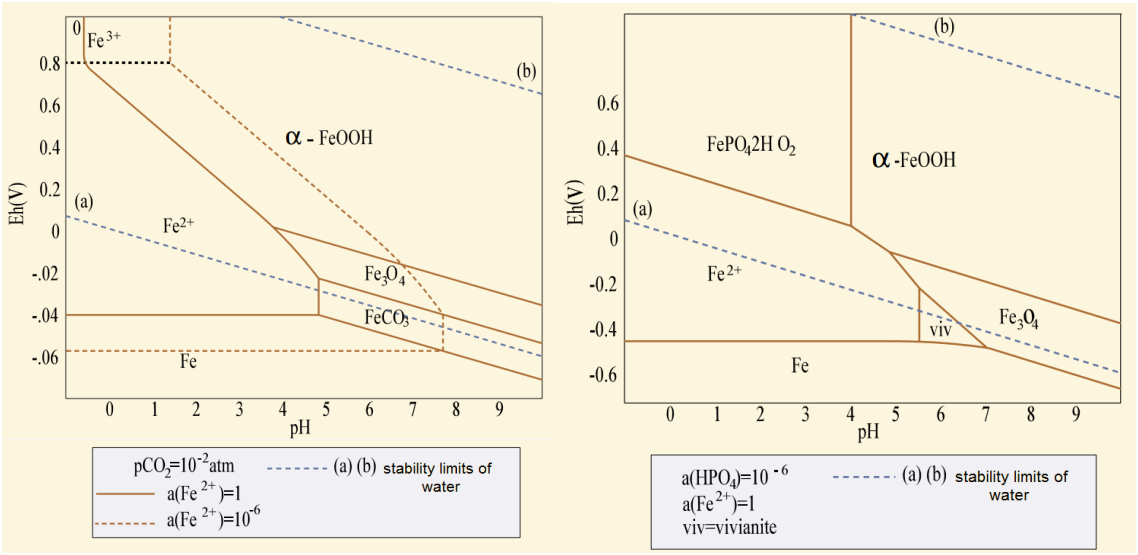

Figure 8: Eh-pH diagrams of Fe-C-H_2O and Fe-PO_4-H_2O systems at 25°C with goethite as mineral phase in equilibrium (David, 2001).

Taking the challenge to understanding and predicting the corrosion phenomena in the framework of nuclear waste geological disposal, an integrative approach becomes necessary. As mentioned previously, archaeological artifacts, modelling and laboratory experiments are key elements for this attempt.

The most frequent corrosion products observed on iron archaeological artifacts are goethite (α-FeOOH) and magnetite (Neff *et al.*, 2004). In particular conditions, carbonate-containing phases (siderite, $FeCO_3$; chukanovite, $Fe_2(OH)_2CO_3$) can be identified (Saheb *et al.*, 2008; Schlegel *et al.*, 2010).

Bildstein *et al.* (2006) pointed out by means of modelling that iron oxides (essentially magnetite) and small amounts of siderite can precipitate at the container interface in contact with COx argillite, over a period of 10,000 years at 50°C. Esnault *et al.* (2013b) claim that magnetite precipitation as well as phosphorus-containing phases (vivianite, $Fe_3(PO_4)_2 \cdot 8H_2O$) can occur over a period of 100,000 years at 90°C.

Combarieu *et al.* (2007) showed by means of laboratory experiments with pure iron samples in the presence of COx argillite (anoxic, 90°C, 1 or 6 months) that the main corrosion products are magnetite and iron-rich serpentine and/or chlorite-like phases as result of the destabilization of clay minerals by the corrosion reaction. In addition, integrated laboratory experiments have been performed in order to analyze the mineralogical properties of iron-clay interface (anoxic, 90°C, 8 months) (Martin *et al.*, 2008; Schlegel *et al.*, 2008). Both studies pointed out the presence of an internal layer made of magnetite at the metal surface, and then an external layer of Fe-phyllosilicate. A clay transformation layer is also observed, and it is composed of predominantly Ca-rich siderite (Figure 9).

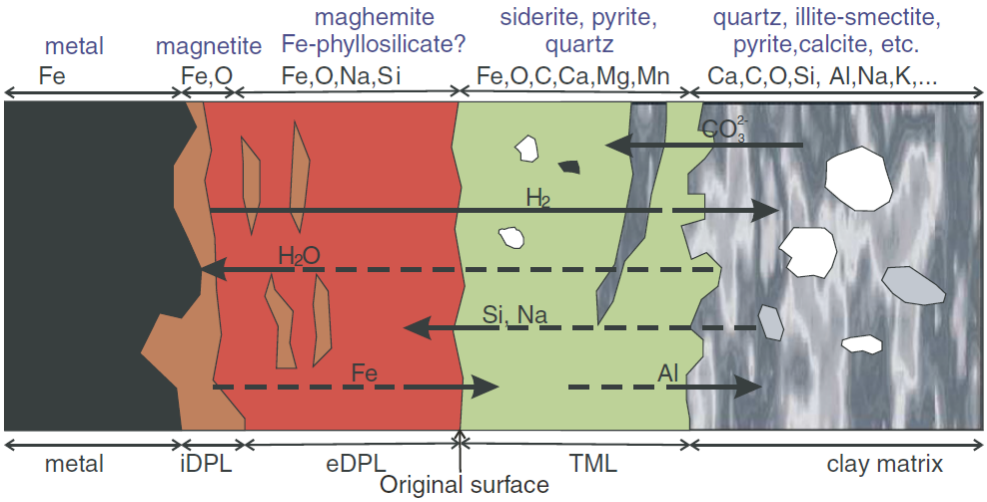

Figure 9: Outline of elemental transfers at the iron-clay corroded interface in the case of COx argillite: dense product layer (DPL); and transformed medium layer (TML). Major elements (in black) and mineral phases (in blue) are indicated at the top of the figure (Schlegel et al., 2008).

King and Stroes-Gascoyne (2000) have compiled data of corrosion rates of carbon steel obtained by weight loss technique at different experimental conditions simulating geological conditions, as shown in Table 4.

Table 4: Examples of corrosion rate found under geological conditions (modified from King and Stroes-Gascoyne, 2000).

Material	Conditions	Exposure time (months)	Corrosion rate (µm.y^{-1})	Reference
1035 carbon steel	compacted FoCa clay[a], saturated with deaerated Na/HCO_3-based groundwater, pH 8.0, 25°C	6	4-5	(Papillon *et al.*, 2003)
1035 carbon steel	compacted FoCa clay, saturated with deaerated Na/HCO_3-based groundwater, pH 8.0, 25°C	8	7-8 (+ pitting)	
carbon steel (as received)	synthetic interstitial Boom clay water, 170°C	6	1.3	(Debruyn *et al.*, 1991)
carbon steel	*in situ* test in direct contact with Boom clay[b], possibly some initial trapped air, 90°C	21	7.7	(Kursten *et al.*, 1996)
carbon steel	*in situ* test in direct contact with Boom clay, possibly some initial trapped air, 90°C	84	4.7	

[a]: FoCa clay has been a candidate backfill material for geological repositories.

[b]: Boom clay is currently investigated as a potential host-rock for a geological repository at Mol site in Belgium.

Constant long-term corrosion rates can be attributed to the presence of magnetite layer with a steady-state thickness and a constant porosity at the metal surface. Therefore, the dissolution of magnetite may be, in this case, the process-enhancing of

corrosion (King, 2007). In some cases, siderite can also form a protective layer slowing down the corrosion rate (Farelas *et al.*, 2010; Gao *et al.*, 2011; Kermani and Morshed, 2003). However, such protective effect can be limited if siderite does not cover the metal surface. As shown in Figure 10, studies with archaeological analogues have indicated that corrosion rates decrease with time probably due to the presence of protective layers.

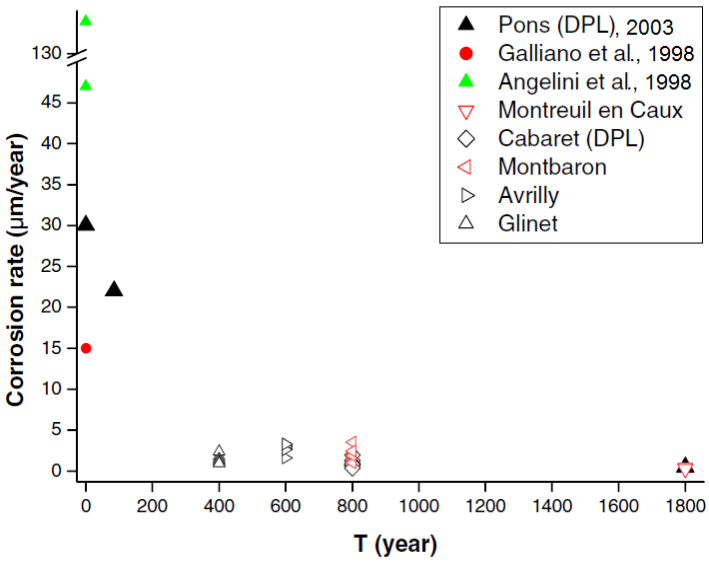

Figure 10: Comparison of inferred corrosion rates from archaeological artifacts examined by the authors (open symbols) and from literature data (full symbols) (Neff et al., 2006).

In order to introduce the next section of this chapter, it is important to keep in mind that corrosion will provide many nutritional and energetic substrates for the development of microorganisms within nuclear waste repository. In particular, magnetite and H_2 are both corrosion products, and they can be used as potential energetic substrates (Figure 11).

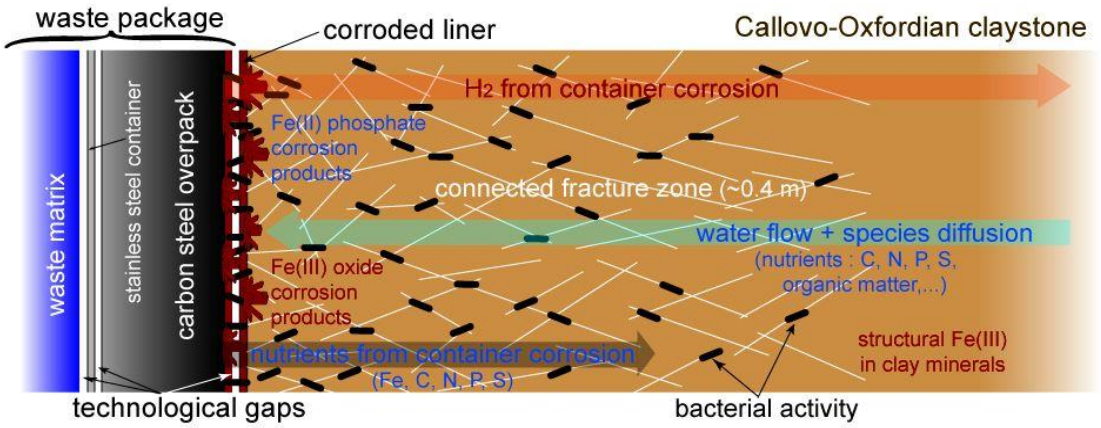

Figure 11: Schematic view of the near field of a HLNW disposal cell indicating the location of potential microbial activity and the flux of nutrients and energetic substrates (not to the scale) (Libert et al., 2013).

A study performed by Urios *et al.* (2013) pointed out a wide microbial diversity at iron-clay interfaces (Table 5). Steel coupon samples were reacted over a period of 10 years inside the Toarcian argillite under *in situ* conditions. The authors stress that the microbial diversity is dependent on the steel type and the *in situ* environmental conditions.

Table 5: Example of microbial diversity found at iron-clay interfaces in a deep geological formation (Tournemire case) (Urios et al., 2013).

Microbial diversity					
Methanogens	Sulfate-reducers	Iron-reducers	Nitrate-reducers	Anaerobic heterotrophs	Aerobic heterotrophs
-	+	+	+	+	+

- : absence; + : presence

1.4 Biocorrosion: The Impact of Microbial Activity

It is widely accepted that microorganisms can affect corrosion processes due to their impact (directly or indirectly) on the chemical and physical characteristics at the metal/environment interface (Beech and Gaylarde, 1999; Stott, 1993; Videla and Herrera, 2005). Corrosion associated with the action of microorganisms is known as either microbiologically influenced corrosion (MIC) or biocorrosion. It is important to note that biocorrosion is not a new corrosion mechanism, but it integrates the role of microorganisms in the corrosion processes. Usually, this type of corrosion is more aggressive than corrosion itself because it frequently occurs as pitting. Moreover, an oxic-anoxic environment leads to greater corrosion due to the development of both aerobic and anaerobic microorganisms.

Microbial activity within biofilms formed on metal surfaces can affect the kinetics of cathodic and/or anodic reactions (Jones and Amy, 2002) and can also considerably modify the properties of protective layers (Beech *et al.*, 2000; Esnault *et al.*, 2011). Biofilm is a gel of water (up to 97%) contained in a matrix of extracellular polymeric substances (EPS) made of bacterial cells, DNA, proteins, nutrients, metabolic products and other elements from the environment. Biofilm formation results from an accumulation process, which involves initial bacterial attachment, maturation and detachment (Flemming and Wingender, 2010). A wide range of microorganisms can coexist in the biofilm, notably species with the ability to *(i)* reduce oxygen, sulfate and Fe(III); *(ii)* oxidize sulfide and Fe(II); *(iii)* ferment; and *(iv)* produce acids. Thus, biofilms are characterized by a strong chemical and reactional heterogeneity.

It has been shown in the literature that the role of microorganisms in corrosion process is still not clear in that they can either accelerate or inhibit corrosion. In both cases, the mechanisms are always linked to a marked modification of the environmental conditions at the metal surface by microbial activity.

On the one hand, an inhibitory effect is usually associated with O_2 consumption (a corrosive agent). The O_2 removal slows down the cathodic reaction at the metal surface, which in turn slow down the metal oxidation. In addition, the biofilm matrix could either stabilize pre-existing protective films on the metal surface or form a transport barrier that can prevent the penetration of corrosive agents (e.g. O_2, chloride, sulfides) (Dubiel *et al.*, 2002; Lee and Newman, 2003; Potekhina *et al.*, 1999; Videla and Herrera, 2009). Studies have shown that microorganisms within the films must be alive for the biofilms to inhibit corrosion. Indeed, when antibiotics were added to kill the bacteria in the biofilm, pitting corrosion occurred within a few hours (Zuo *et al.*, 2005).

On the other hand, an inducing effect is usually associated with corrosive properties of some metabolic products. For instance, sulfur-oxidizing bacteria (SOB) are capable of producing sulfuric acid (H_2SO_4) by oxidizing sulfur compounds. Regarding SRB species, it has been stressed that a combination of mechanisms can induce corrosion: *(i)* the direct electron uptake from metal; and *(ii)* the biogenic production of corrosive hydrogen sulfide (H_2S) (Beech, 2003; Potekhina *et al.*, 1999; Venzlaff *et al.*, 2013). Regarding IRB species, the main mechanism proposed to accelerate corrosion is by reducing structural Fe(III) from passivating oxide layers (i.e. magnetite) (Esnault *et al.*, 2011; Herrera and Videla, 2009; Lee and Newman, 2003; Potekhina *et al.*, 1999). Changes in the stability of the passivating layers are always controlled by environmental conditions, which may consequently influence in the biofilm effect (corrosive or protective).

1.4.1 Corrosion by sulfate-reducing bacteria

Sulfate-reducing bacteria (SRB) have been reported to be the main group responsible for anaerobic corrosion, especially in environments with high sulfate concentration (e.g. seawater). This is why most of the corrosion mechanisms already hypothesized are related to SRB.

SRB perform dissimilatory reduction of sulfur compounds, such as sulfate (SO_4^{-2}), sulfite (SO_3^{-2}) and thiosulfate ($S_2O_3^{-2}$) to sulfide (S^{-2}) (Beech, 2003). Certain SRB (i.e. *Desulfovibrio* sp.) are able to use H_2 as electron donor for sulfate reduction under reducing conditions, and although SRB are often considered to be strictly anaerobic, it has been demonstrated that some genera tolerate O_2 (Beech and Gaylarde, 1999).

The production of H_2S often indicates the activity and presence of SRB in natural habitats. The presence of H_2S is obvious by its characteristic smell and black precipitation of ferrous sulfide (FeS) when iron minerals are present.

Some studies about the impact of SRB on steel corrosion under geological disposal conditions have pointed out that corrosion rate is increased 2-3 times compared to control experiments (El Hajj *et al.*, 2010; Philp *et al.*, 1991).

El Mendili *et al.* (2013) stressed that the thickness of corrosion layer is dependent on the presence or absence of O_2 in the system (Figure 12). Corrosion was less severe in aerobic conditions compared to strict anaerobic conditions due to the formation of magnetite as corrosion product.

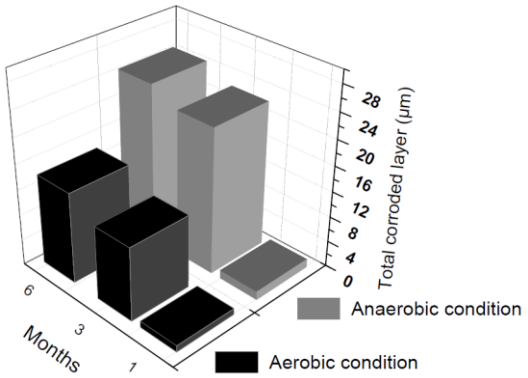

Figure 12: Thickness of the total corrosion layer for steel under aerobic and anaerobic conditions (El Mendili et al., 2013).

In the presence of SRB, nanocrystalline mackinawite (FeS) was identified as the only corrosion product within the first month of anaerobic exposure. With increasing exposure time, nanocrystalline mackinawite evolved into polycristalline pyrrhotite ($Fe_{(1-x)}S$), which exhibited good protective properties against corrosion (an increase of only 5 µm on the corroded layer was observed between the third and sixth month) (El Mendili *et al.*, 2013).

1.4.2 Corrosion by iron-reducing bacteria

The impact of iron-reducing bacteria (IRB) on corrosion processes has been only marginally investigated compared to SRB. IRB can couple oxidation of organic (e.g. lactate and acetate) or inorganic (e.g. H_2) substrates with Fe(III) reduction. In the environment, IRB may outcompete both SRB and methanogenic bacteria for H_2 as electron donor. In some cases, H_2 concentration may serve as an indicator of the predominant metabolism in anoxic sediments (Fredrickson and Gorby, 1996).

The role of IRB on corrosion processes is still under discussion. Several studies have demonstrated inhibitory or enhancing effects (Dubiel *et al.*, 2002; Herrera and Videla, 2009; Lee and Newman, 2003; Mehanna *et al.*, 2008; Potekhina *et al.*, 1999).

On the one hand, an enhancing effect is associated with the destabilization/ dissolution of passivating oxide layers (i.e. magnetite) by structural Fe(III) reduction under anoxic conditions, which in turn exposes the metal surface to the corrosive environment and reactivates corrosion (Esnault *et al.*, 2011; Little *et al.*, 1998). For instance, Beech *et al.* (2000) demonstrated that the chemical elements within the passivating layer of stainless steel 316 and its thickness markedly changed by exposing to *Pseudomonas* species compared with the unexposed steel. On the other hand, under aerobic conditions, Fe(II) produced by Fe(III) reduction may be oxidized by O_2, which forms a protective way against O_2 attack on the metal surface (Dubiel *et al.*, 2002).

Lee and Newman (2003) propose a scheme showing both inhibitory and enhancing effects of facultative IRB on metal surface in a dynamic system, as shown in Figure 13.

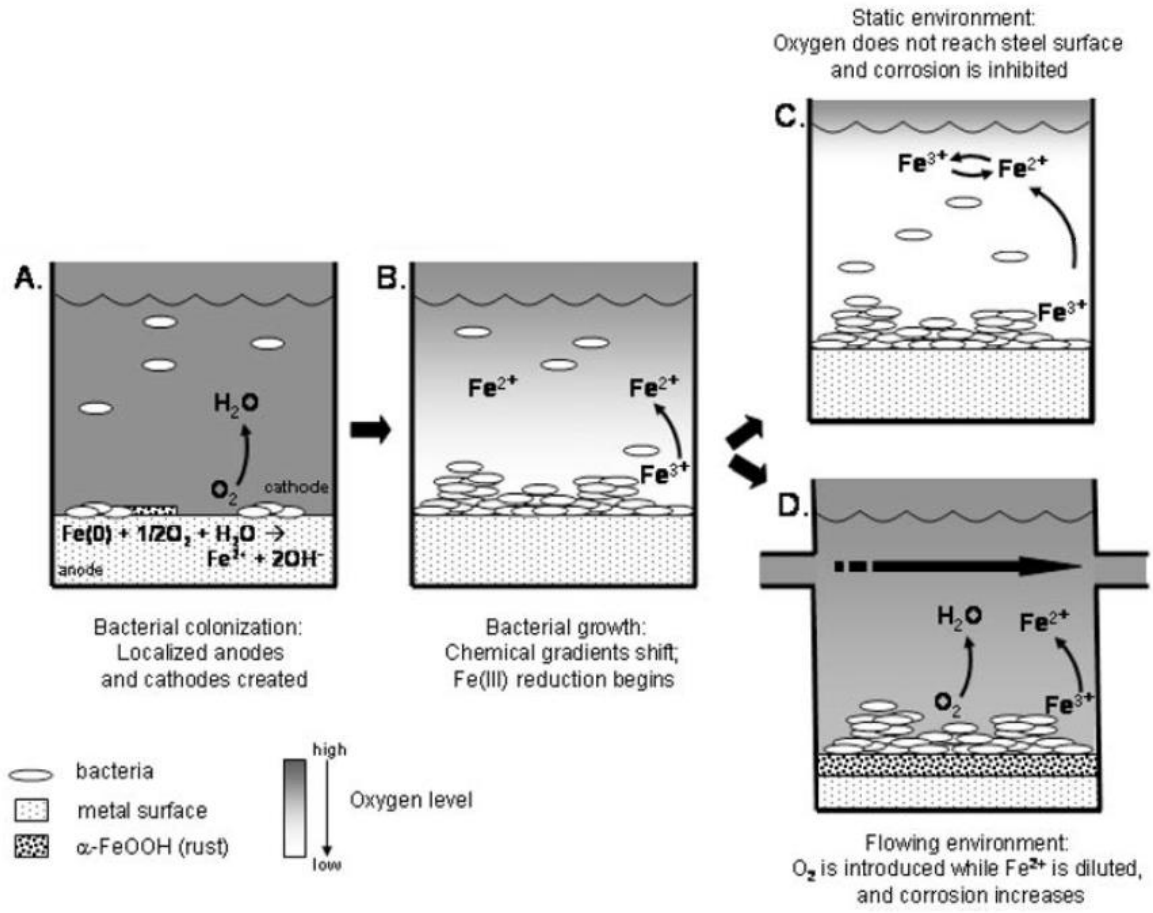

Figure 13: Developmental process of microbiologically influenced corrosion or corrosion inhibition with facultative iron-reducing bacteria: (a) and (d) inducing effects; (b) transitory condition; and (c) inhibitory effect (Lee and Newman, 2003).

Figure 13(a) shows bacterial colonization at the metal surface and O_2 consumption by aerobic respiration, leading to the creation of localized anodes and cathodes that accelerate corrosion. Figure 13(b) shows biofilm growth which eliminates localized anodes and cathodes. As O_2 is consumed, the bacteria turn to Fe(III) respiration and Fe(II) diffuses into the bulk fluid as it is produced. Figure 13(c) shows that in an anoxic static environment, the iron respiration creates a chemical shield of diffuse Fe(II) that reduces any O_2 diffusing from the atmosphere. Fe(II) is oxidized to Fe(III) which can again be reduced by bacterial respiration, and thus corrosion is inhibited. Figure 13(d) shows that in an environment with fluid flow, Fe(II) is diluted out while O_2 is introduced, accelerating the corrosion process.

Studies performed by De Windt *et al.* (2003) with iron beads showed that H_2 consumption by *Shewanella oneidensis* strain MR-1, precipitation of corrosion products on the cell surface and cell density play a significant role on corrosion processes. A significant H_2 consumption could only be detected at cell densities of 10^6 cells.mL^{-1} or higher. The corrosion products were identified as vivianite particles with a diameter changing with the cell density (medium with 173 mM of phosphate).

Moreira (2013) stressed that corrosion rate of carbon steel is significantly increased in the presence of hydrogenotrophic IRB and with local H_2 generation. However, over a time period of 5 days, the form of corrosion remains as generalized and not localized.

Recently, it was evidenced that depending on the medium composition IRB can inhibit corrosion by formation of a vivianite layer on carbon steel surface (Coy, 2013; Lee *et al.*, 2010). Coy (2013) evidenced that only in the presence of *Geobacter sulfurreducens* a protective vivianite layer was formed in a way that could stabilize the corrosion potential even after intrusion of air in the system (medium with 5 mM of phosphate).

Shewanella oneidensis: a model organism to biocorrosion studies with IRB

Iron-reducing bacteria have been discovered in a diverse range of aquatic sediments, soils and other subsurface environments. The most intensively studied IRB are *Shewanella* species. They are widely used in laboratory due to advantages that make their study easier for the researchers. *Shewanella* is related to *Escherichia*, a bacterium well known to microbiologists. Therefore, the same tools and techniques already developed for *Escherichia* can be used for *Shewanella*.

Regarding the MIC studies and molecular understanding of Fe(III) reduction, *Shewanella oneidensis* strain MR-1 is considered a model organism because its genome has been completely sequenced (Dubiel *et al.*, 2002).

This bacterium (formally *Alteromonas putrefaciens* and *Shewanella putrefaciens*) was first isolated from sediments of the Oneida Lake (New York, USA). Studies with strain MR-1 allowed demonstrating for the first time that the reduction of Fe(III) or Mn(IV) oxides can be coupled to the bacterial growth and energy generation (Myers and Nealson, 1988; Nealson and Saffarini, 1994).

Shewanella oneidensis is a mesophilic, Gram-negative, non-fermentative and facultative anaerobic γ-Proteobacterium. A wide range of compounds can be used as terminal electron acceptors under anoxic conditions, such as: fumarate, dimethyl sulfoxide (DMSO) and trimethylamine N-oxide (TMAO); elemental sulfur, thiosulfate, nitrate (NO^{3-}) and nitrite (NO^{2-}); metal ions, Fe(III), Mn(IV) and Cr(VI); and radionuclides, U(VI). Electron donors can include H_2 and metabolic end-products of primary fermenting bacteria, such as lactate and formate (Figure 14) (Nealson *et al.*, 2002; Venkateswaran *et al.*, 1999).

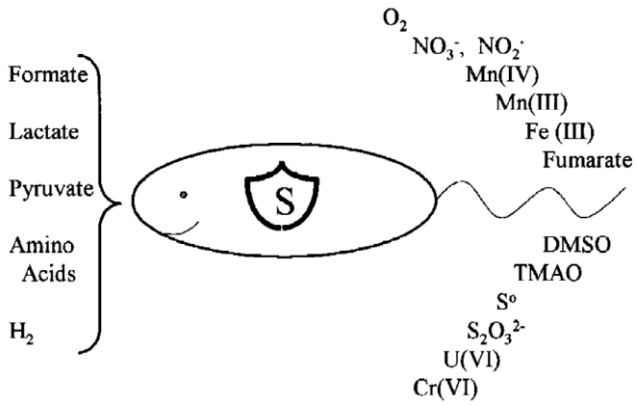

Figure 14: Energy flow in Shewanella oneidensis strain MR-1 (Nealson et al., 2002).

It has been shown that *Shewanella oneidensis* strain MR-1 can use different mechanisms to access Fe(III). In the case which involves contact with Fe(III) from insoluble substrates, the bacteria may produce fimbriae, pili or nanowires (cellular appendages) as conductors for electrons. Moreover, *Shewanella* can also release flavin mononucleotide, riboflavin and riboflavin 5′-phosphate, which could act as electron shuttles for bioreduction of sparingly soluble Fe(III) (hydr)oxides (Ehrlich and Newman, 2008).

1.4.3 Bioreduction of Fe(III) (hydr)oxides

Fe(II)-Fe(III) redox cycling represents the major energy flux on Earth's surface. However, Fe(III) (hydr)oxides are characterized by low solubility. In this way, dissolution mechanisms must take place for the cycling of Fe, such as: *(i)* dissolution promoted by

surface protonation; *(ii)* ligand-promoted dissolution; and *(iii)* reductive dissolution mainly by biological processes.

The mechanism by surface protonation involves the chemisorption of protons at the Fe(III) (hydr)oxide surface, which weakens the Fe-O bonds by polarization promoting the detachment of structural Fe(III) from the mineral. The rate of dissolution by protonation is highly dependent on pH conditions (higher dissolution at acidic conditions). This mechanism can be further enhanced by organic acids (e.g. oxalic and citric acid) or anions (e.g. Cl^-) which also adsorb to the Fe(III) (hydr)oxide surface (Grygar, 1995; Oulkadi, 2013; Panias *et al.*, 1996). Under anaerobic conditions, reductive dissolution is the most prominent mechanism (Cornell and Schwertmann, 2003). In this case, the microbial activity takes an important role. Indeed, IRB species are considered to be the primary agent in the reductive dissolution in sedimentary environments (Lovley, 2002; Lovley, 2005).

Microbial reduction (or bioreduction) is a complex process which involves bacterial cells, Fe(III) (hydr)oxides, aqueous-phase components and secondary mineral phases that can be formed as result of Fe(III) bioreduction. Moreover, the rate and extent of bioreduction depend on several conditions, such as bacterial strain, cell density, characteristics of the insoluble substrate (crystallinity, surface area), solution composition and flow-through or batch incubation. In this way, some early studies are discussed in order to improve the understanding of how different biogeochemical parameters may influence on the bioreduction.

Kostka and Nealson (1995) were the first to demonstrate Fe(III) bioreduction from synthetic magnetite coupled to growth and respiration (glucose as electron donor). Their study showed that the optimal conditions for dissolution of magnetite are pH 5-6.2 at 37°C in the presence of *Shewanella putrefaciens* strains MR-1 and MR-4. Dissolution rate varied according to initial cell concentration; the optimum dissolution was reached with 10^5 cells.mL^{-1}. They argued that dissolution can be limited by the saturation of magnetite surface with cell densities above 10^5 cells.mL^{-1}.

Urrutia *et al.* (1999) studied the influence of aqueous ligands (e.g. NTA and EDTA) and solid-phase ligands (e.g. aluminium oxide and layered silicate minerals) on the rate and extent of Fe(III) bioreduction from synthetic goethite in the presence of *Shewanella alga* strain BrY (H_2 as electron donor). Both solid-phase ligands were able to serve as sinks for removal of biogenic Fe(II), which significantly increases the extent of bioreduction. In contrast, among the aqueous ligands, only nitrilotriacetic acid (NTA) led to greater bioreduction. They explain this result indicating that Fe(II)-EDTA complexes can be easier absorbed on the goethite/bacterial cell surfaces compared to Fe(II)-NTA complexes, which in turn blocks active surface sites for further bioreduction.

Dong *et al.* (2000) studied the impact of growth medium composition and strain type on the rate and extent of magnetite bioreduction (lactate as electron donor). The extent of bioreduction in a bicarbonate-buffered medium (inorganic buffer) was greater than in a PIPES-buffered medium (organic buffer). One reason is the ability of bicarbonate to form complexes with Fe(II) ions, which again serve as a sink for removal of biogenic Fe(II). Under the same experimental conditions, *Shewanella putrefaciens* strain CN32 reduced more Fe(III) than strain MR-1. The authors identified siderite or vivianite (in the medium with 9 mM of phosphate) as secondary mineral phases (Figure 15). Analysis revealed aggregation/attachment of magnetite crystals on the bacterial cells, suggesting binding via an extracellular polymer, possibly EPS. The extent of bioreduction can be limited by the saturation of magnetite surface with the secondary mineral phases.

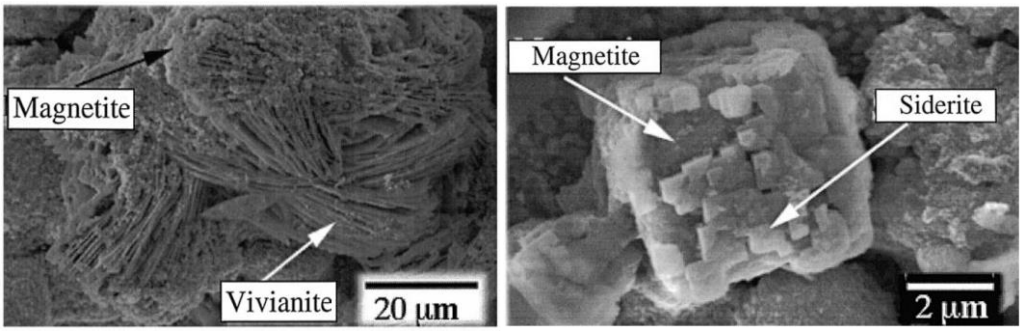

Figure 15: Secondary mineral phases of magnetite bioreduction (Dong et al., 2000).

The influence of biogenic Fe(II) removal from the system was examined by Roden *et al.* (2000) in the presence of *Shewanella putrefaciens* strain CN32 (lactate as electron donor). They performed experiments in batch reactors and in column reactors where biogenic Fe(II) could be removed via aqueous phase flushing. The results pointed out that Fe(II) production quickly reaches an asymptote in the batch reactors, with only 13% of the Fe(III) content reduced. In the column reactors, continuous dissolution of goethite was observed, leading to 95% of Fe(III) reduction (Figure 16). It was shown that removal of biogenic Fe(II) decreases the "passive" influence of surface-bound Fe(II), allowing an increase on the extent of goethite bioreduction and associated cells growth.

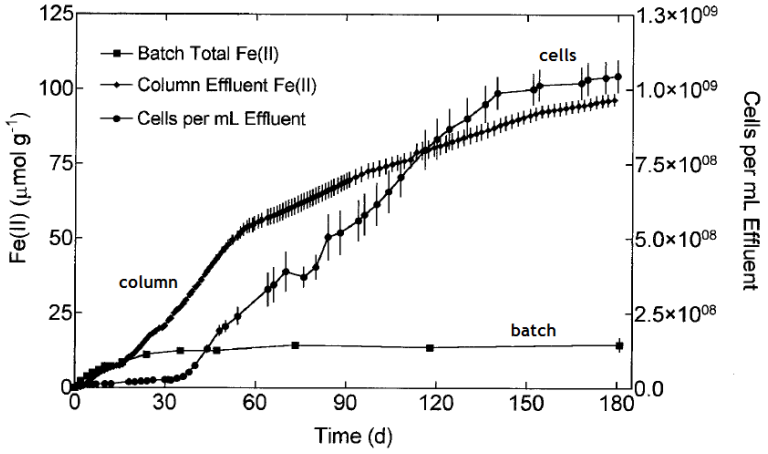

Figure 16: Bioreduction of synthetic goethite in continuous-flow column versus batch reactors (Roden et al., 2000).

Taillefert *et al.* (2007) investigated the effect of mineral species on the Fe(III) bioreduction in the presence of *Shewanella putrefaciens* strain 200 (lactate as electron donor). They pointed out that higher Fe(II) concentrations are reached with poorly crystalline minerals (e.g. 2,6-line ferrihydrite and lepidocrocite) than with well crystalline minerals (e.g. goethite and hematite), as shown in Figure 17.

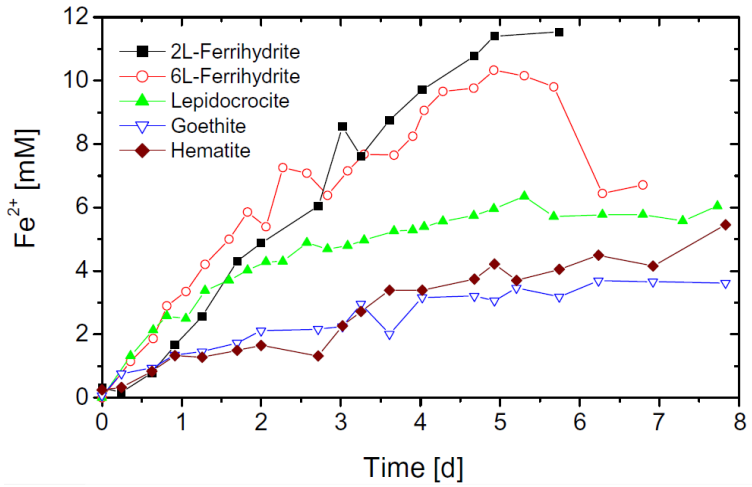

Figure 17: Fe(III) bioreduction according to mineral species (Taillefert et al., 2007).

The authors explain these results by differences in the mineral reactivity and specific surface area. Minerals with higher number of active surface sites will readily be dissolved. For example, amorphous Fe(III) (hydr)oxides that present a higher number of reactive hydroxyl groups will dissolve much faster than well crystallized goethite and hematite. According to Kostka *et al.* (2002), the rate of Fe(III) bioreduction from smectite clay minerals is similar to that for poorly crystalline or amorphous minerals.

Bonneville *et al.* (2004) report that the rates of bioreduction typically show saturation behavior with respect to Fe(III) substrate. When bacterial cell surfaces are saturated by the Fe(III) substrate, the rate of Fe(III) reduction reaches a maximum value (active sites at the outer membrane become saturated). Therefore, further increasing on the concentration of Fe(III) substrate has no effect anymore on the rate of bioreduction.

1.5 Objectives of the study

The currently design for nuclear waste management relies on different metallic materials that are susceptible to corrosion processes. The impact of abiotic parameters on corrosion has already been integrated in the safety assessments of geological disposal. However, the impact of microbial processes is still an open issue and must be further investigated in order to provide biological parameters for predictive reactive transport models.

The main objective of this study is to evaluate the bacterial impact on corrosion processes under anoxic conditions, which will prevail in most of the lifetime of nuclear waste repository. Specific objectives are as follow:

- evaluate the impact of **hydrogenotrophic iron-reducing bacteria** on the corrosion process because the corrosion products expected under anoxic conditions (particularly, H_2 and magnetite) can potentially promote these bacterial metabolisms and activities;
- evaluate the influence of **metallic substrate** (iron powder and carbon steel coupon) on the corrosion process;
- evaluate the role of **H_2 as potential energetic substrate** for bacterial development;
- evaluate the **Fe(III) bioavailability** in magnetite in the presence of H_2 as electron donor.

1.6 Scientific approach

The scientific approach proposed in this study relies on two main setups of experiments which were evaluated by means of geochemical methods.

First setup: experiments with H_2 (as electron donor) at different initial concentrations and magnetite (as electron acceptor) aiming at evaluating Fe(III) bioavailability and hence magnetite stability. Here, it is assumed that the passivating layer is magnetite and that it can be destabilized by bacterial reaction using H_2.

Second setup: experiments with metallic iron samples (iron powder or carbon steel coupon) aiming at analyzing *(i)* mainly dissolved Fe and H_2 production (or consumption by bacteria), and *(ii)* solid corrosion products formed during the corrosion process.

The bacterium chosen for this study was *Shewanella oneidensis* strain MR-1 which is considered as model organism for studying dissimilatory processes in the presence of H_2 as electron donor.

In this study two experimental solutions differing in chemical composition were used: a minimal medium favorable for IRB metabolism (called as M1 solution) and a simplified medium (called as control solution).

CHAPTER 2: MATERIALS AND METHODS

All experiments were monitored using geochemical indicators, which consist mainly in the concentration of dissolved Fe and gaseous H_2 as a function of time, and in the characterization of solid products at the end of the experiments.

2.1 Experimental device

The experiments were performed in batch reactors (Figure 18) at 30°C under abiotic and biotic conditions. Three phases coexist in the experimental system: *(i)* a liquid phase made of the experimental solution (50% v/v); *(ii)* a solid phase, i.e. carbon steel coupon, metallic iron or magnetite powders; and *(iii)* a gas phase containing H_2 — produced by corrosion reaction or injected into the reactor, and other gases from the anaerobic atmosphere (N_2, CO_2) (50% v/v).

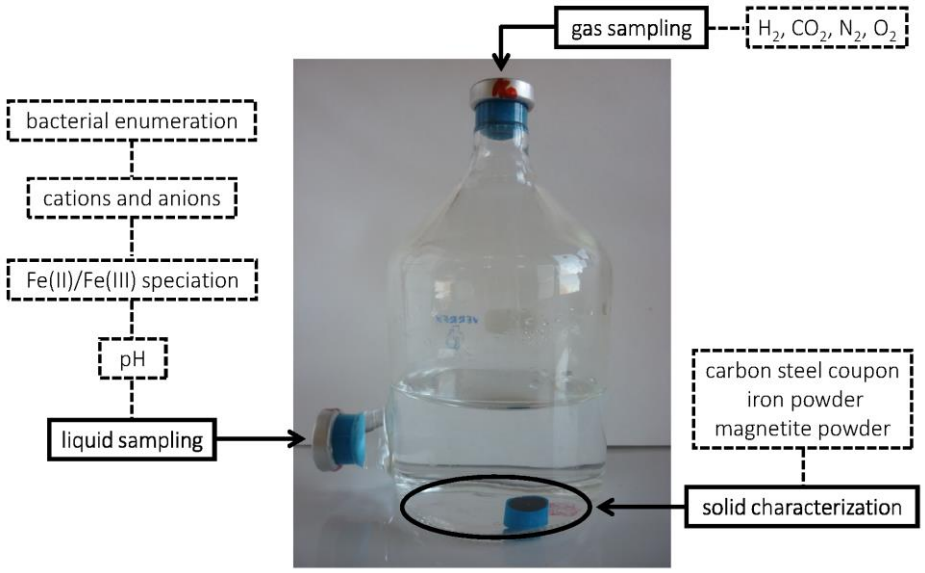

Figure 18: Scheme of the experimental device.

The reactors were filled with 140 mL of experimental solution and with one coupon sample or 1 g of powder. Biotic conditions were achieved by adding into the experimental solution 1 mL of bacterial inoculum. Then, they were sealed with rubber plugs and aluminum caps and flushed with an anaerobic gas flux which is sterilized by passing through a 0.22 µm filter.

The reaction progress was monitored by sampling the gaseous and liquid phases at selected time points. It is noteworthy that O_2 was also monitored during the experiments in order to verify the anaerobic conditions. The solid phase was analyzed only at the end of the experiments. In order to prevent sample oxidation, all reactors were opened inside an anaerobic glovebox and the samples kept in anaerobic atmosphere until analysis.

2.2 Experimental solutions

Two experimental solutions with different chemical composition were used in this study, as shown in Table 6. In some experiments, sodium lactate (22 mM) was also added into the experimental solutions as organic carbon source.

Table 6: Chemical composition of the experimental solutions.

Compound	Concentration	
	M1	Control
Na_2SO_4	-	10 mM
$(NH_4)_2SO_4$	9 mM	-
Na_2SeO_4	11 µM	-
HEPES buffer	17 mM	-
$NaHCO_3$	2 mM	2 mM
Phosphate buffer solution		
K_2HPO_4	0.5 mM	-
KH_2PO_4	0.3 mM	-
Metals supplement solution		
$CoSO_4.7H_2O$	5 µM	-
$NiSO_4.6H_2O$	5 µM	-
NaCl	10 µM	-
Basal salts solution		
H_3BO_3	45 µM	-
$ZnSO_4.7H_2O$	0.8 µM	-
$Na_2MoO_4.2H_2O$	3 µM	-
$CuSO_4.5H_2O$	0.2 µM	-
$MnSO_4.H_2O$	1 µM	-
$MgSO_4.7H_2O$	0.8 mM	-
$CaCl_2.2H_2O$	0.4 mM	-
$FeSO_4.7H_2O$	4 µM	-
Amino acids solution		
arginine	0.11 mM	-
glutamate	0.13 mM	-
serine	0.19 mM	-
Vitamins solution		
nicotinic acid	0.08 mM	0.08 mM
thiamine-HCl	0.01 mM	0.01 mM
biotine	0.40 µM	0.40 µM

The M1 solution is a minimal medium commonly used to cultivate IRB species (Kostka and Nealson, 1998). The original recipe was adapted by Esnault (2010) in order to be representative of the argillite interstitial water from Tournemire or Bure sites in France.

The Na_2SO_4 solution was chosen as control medium in order to facilitate the comparison with results from corrosion studies by means of electrochemical methods. Moreover, the sulfate concentration (10 mM) is similar to that measured in the porewater of the COx clay (Vinsot *et al.*, 2008).

The final pH was adjusted to approximately 7 with NaOH. Both experimental solutions were sterilized by autoclaving (120°C for 20 min), except for the thermolabile components (i.e. amino acids, vitamins) which were filter-sterilized (0.22 µm pore-size) and added to the autoclaved solution under a laminar airflow workstation.

Depending on the goal of the experiment, either Fe(II,III) oxide (insoluble substrate, 7 $g.L^{-1}$) or Fe(III) citrate (soluble substrate, 20 mM) were used as electron acceptors and sodium lactate (organic substrate, 22 mM) or H_2 (inorganic substrate) as electron donors. Biotic conditions were achieved by adding into the experimental solution a bacterial inoculum prepared as described below.

2.3 Bacteria

2.3.1 Bacterial culture

Shewanella oneidensis strain MR-1 (ATCC 700550™) was chosen as model of iron-reducing and hydrogenotrophic bacteria for all experiments. Optimal growth is observed at 30ºC and pH 7-8. Bacterial cells range from 2-3 µm in length and 0.5-0.6 µm in diameter (Venkateswaran *et al.*, 1999).

Pre-cultures were obtained aerobically at the beginning of the stationary growth phase in 200 mL of Luria Bertani Broth (LB) medium (5 $g.L^{-1}$ NaCl, 10 $g.L^{-1}$ tryptone, 5 $g.L^{-1}$ yeast extract) after 24 h at 30°C.

Bacterial inoculum was obtained from the pre-cultures, which were harvested by centrifugation (4000 rpm at 20 min) and washed once with sterile minimal medium (M1 solution). Then, 1 mL of the cell suspension was added to 140 mL of the experimental solution.

2.3.2 Bacterial counting

Planktonic cell counting was performed by epifluorescence microscopy using the LIVE/DEAD® *Bac*Light™ L7012 Bacterial Viability kit (Invitrogen).

In the epifluorescence microscopy, the light is directed through the objective onto the sample by a dichromatic mirror that is placed at an inclination of 45° to the optical axis of incident light. The light passes through an exciter filter which selects the desired excitation wavelength. The excitation light excites the fluorochrome in the sample, and then the excitation light is filtered away from the emitted light by an emission filter between the objective and the detector, which results in a clear fluorescent image.

The LIVE/DEAD® *Bac*Light™ kit is composed of a mixture of two nucleic acid-binding stains: SYTO 9 (3.34 mM) and propidium iodide (20 mM). These stains differ in their ability to penetrate healthy bacterial cells. When used alone, SYTO 9 stains both live and dead bacteria. In contrast, propidium iodide penetrates only bacteria with damaged membranes, reducing SYTO 9 fluorescence. Thus, live bacteria with intact membranes fluoresce green, while dead bacteria with damaged membranes fluoresce orange.

The total bacterial cells were counted with a BH-2 microscope (Olympus) equipped with a universal condenser, a mercury lamp (Olympus BH2-RFL-T2) and a 40x objective lens. The procedure was the following: 20 µL of sample was stained with 20 µL of fluorochromes mixture (SYTO 9 and propidium iodide, 50:50% v/v) for 15 minutes in the dark at room temperature. Then, 20 µL of the sample was placed between a slide (~ 76 x 26 x 1 mm) and a coverslip (22 x 22 mm) and observed directly with the microscope. Only cell-shaped fluorescent particles were taken into account to the counting and at least 10 fields per sample were counted.

2.4 Solid samples

2.4.1 Carbon steel coupons

Carbon steels are corrosion-allowance materials that are expected to have a relatively low corrosion rate in a reducing environment. Therefore, they have been considered as candidate materials for packages used in the nuclear waste geological disposal. In this study, samples of carbon steel A37 were chosen to have the similar properties needed for HLNW disposal. Table 7 shows its chemical composition:

Table 7: Chemical composition of the carbon steel sample.

Element	C	Si	Mn	S	P	Ni	Cr	Ti	Co	Al	Cu
Composition (%)	0.12	0.22	0.62	0.012	0.012	0.02	0.03	<0.005	0.005	0.008	0.04

Iron is the base element.

Cylindrical A37 coupons were laterally insulated from the solution by a diallyl phthalate glass-fiber resin (Presi) in order to expose only an active surface of 0.8 cm^2 (Figure 19). They were polished up to 600 grit SiC abrasive paper, cleaned and weighted for future weight loss analysis. The coupons were sterilized with ethanol by sonication for 15 min, and then dried in a laminar airflow workstation before being introduced into the reactors. Figure 19 shows SEM image of the surface initial state of an uncorroded polished sample. The surface is smooth and homogeneous showing only polishing streaks.

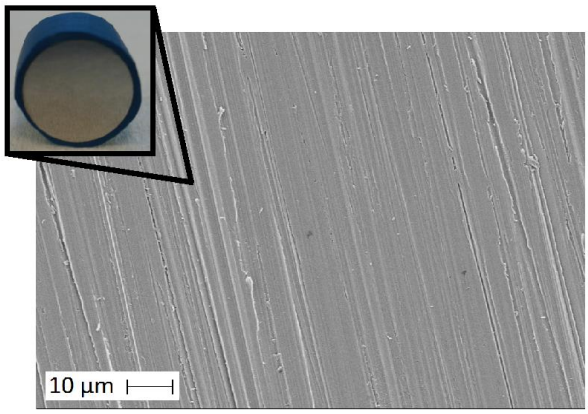

Figure 19: Carbon steel coupon laterally insulated by the resin and SEM micrograph of the surface after polishing (600 grit SiC paper).

2.4.2 Metallic iron powder

The main purpose of working with metallic iron powder is to accelerate the corrosion kinetics in the experiments by increasing the reactive surface. In this study, iron powder was purchased from Merck. SEM image (Figure 20) showed that the powder was made of round spheres of diameters ranging between 2 and 4 µm. A specific surface area of 0.32 ± 0.02 $m^2.g^{-1}$ for particles smaller than 10 µm on average was measured by the N_2-BET method. The sample was sterilised by UV irradiation for 30 min and then added into the reactors to a final solid content of 7 $g.L^{-1}$.

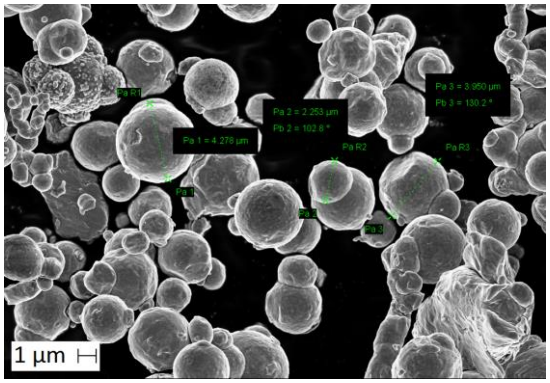

Figure 20: SEM micrograph of the metallic iron powder. Black rectangles indicate the particles size: Pa1= 4 µm; Pa2= 2 µm; and Pa3= 4 µm.

2.4.3 Magnetite powder

In this study, magnetite samples were prepared using the synthesis method described by Schwertmann and Cornell (1991), which consists in the oxidation of ferrous sulfate by potassium nitrate at alkaline conditions. Therefore, a solution of 0.3 M $FeSO_4.7H_2O$ (560 mL) was heated to 90°C and then a mixture (240 mL) of 0.27 M KNO_3 and 3.33 M KOH was added dropwise. The suspension was maintained at 90°C for 1 h with continuous stirring and cooled overnight. All synthesis was carried out under N_2 atmosphere. At the end, a black precipitate was obtained which was washed several times with degassed Milli-Q water followed by freeze-drying. The dried powder (Figure 21) was kept in a desiccator in order to prevent further oxidation.

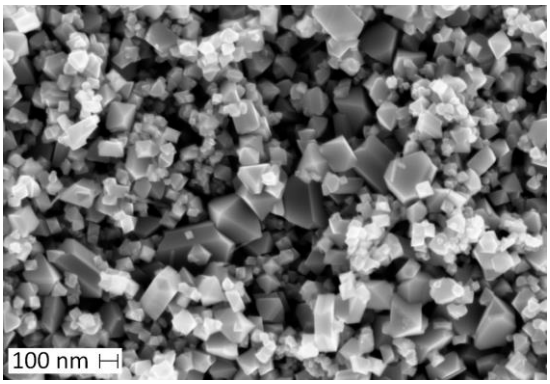

Figure 21: SEM micrograph of the synthesized magnetite powder.

A specific surface area of 11.74 ± 0.03 $m^2.g^{-1}$ for particles smaller than 100 nm on average was measured by the N_2-BET method. X-ray diffraction (XRD) analysis was performed in order to evaluate the purity of the synthesized magnetite (Figure 22). Only

traces of arcanite (K_2SO_4) as residual product of the synthesis were detected, confirming that there is no other forms of Fe(III) in the solid (e.g. no hematite, Fe_2O_3 was found).

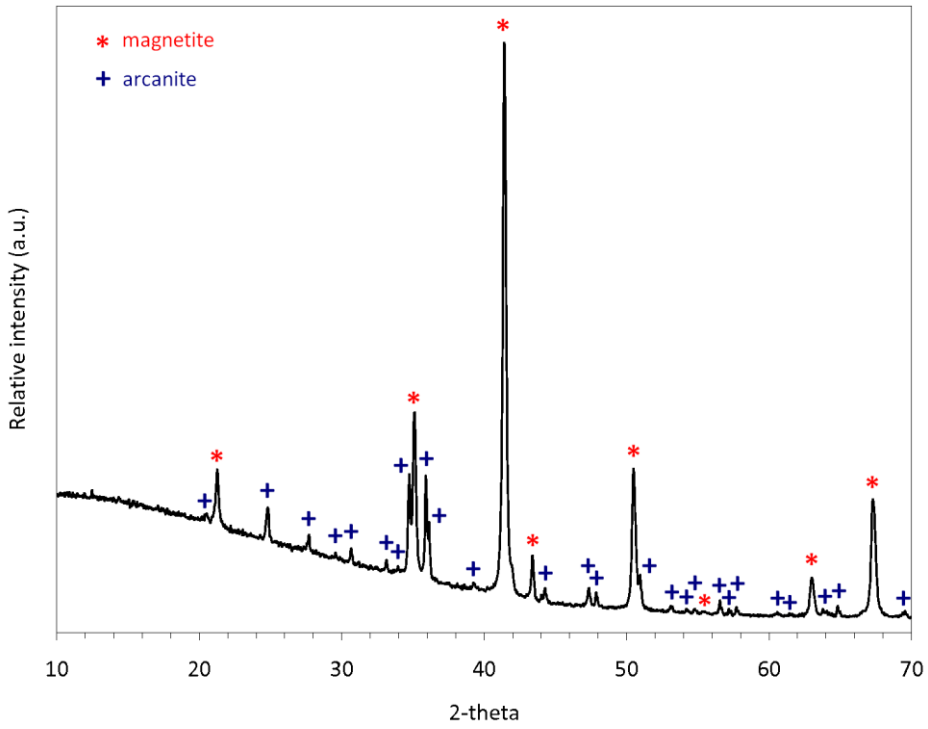

Figure 22: XRD pattern of the synthesized magnetite.

The magnetite powder was sterilised by UV irradiation for 30 min under anaerobic conditions (N_2 100%) and then added into the reactors to a final solid content of 7 $g.L^{-1}$.

2.5 Analytical methods

2.5.1 Solution chemistry

Aliquots from the experimental solution were collected for chemical analysis at selected time points using sterile needles and syringes under a laminar airflow workstation. Concentrations of major cations and anions were measured in order to evaluate, for example, the formation of secondary mineral phases.

Cationic species (Fe, Na, Ca and Mg) were analyzed after 2% (v/v) HNO_3 acidification by inductively coupled plasma optical emission spectrometry (ICP-OES — VISTA-MPX, Varian). This technique is based upon the emission of photons from atoms and ions of the sample excited by argon plasma. The sample is converted to an aerosol by nebulization

process, and then is vaporized and energized by the plasma at a temperature of approximately 8000°C. Once the photons are emitted, their characteristic radiation is sorted by wavelength, which is thus used to identify the elements in the sample. The total number of photons is directly proportional to the element concentration in the sample considering a calibration curve.

Anionic species (Cl, SO_4 and PO_4) were analyzed by ion chromatography (IC — Dionex IonPack AS11-HC) with a conductivity detector, and using a KOH solution as eluent (gradient 1 to 40 mM). The technique is based upon ion exchange reactions between a stationary phase (polymeric resins) and the ions of the sample dissolved in a mobile phase (eluent). The stationary phase exhibits functional groups that retain ions of opposite charge by electrostatic interactions, as described in the general reaction:

$$n\mathrm{R^+A^-} + \mathrm{B^-} \rightleftharpoons n\mathrm{R^+B^-} + \mathrm{A^-} \qquad \textbf{(2.1)}$$

where R^+ are the cationic groups attached to the ion exchange resin and B^- are the anions of the sample.

The Fe(II)/Fe(III) speciation was analyzed colorimetrically by ferrozine assay (Stookey, 1970; Viollier *et al.*, 2000). Ferrozine (monosodium salt hydrate of 3-(2-pyridyl)-5,6-diphenyl-1,2,4-triazine-p,p'-disulfonic acid) is a specific complexing reagent for Fe(II) which forms a colored stable complex in the pH range of 4-9. The procedure used in this study is similar to that described by Viollier *et al.* (2000) which consists of measuring the absorbance of the Fe(II) complex before and after a Fe(III) reduction step (with hydroxylamine as reducing agent). The reduction step aims at determining the total Fe concentration in the sample. Thus, Fe(III) concentration is obtained by the difference between the concentrations of total Fe and Fe(II). The absorbance was measured at 562 nm on an UV-Vis Infinite M1000 microplate spectrophotometer (Tecan). The samples were acidified with 0.5 N HCl (50:50 v/v) prior ferrozine assay in order to analyse the soluble fraction.

All liquid samples collected from the reactors were filtered through a 0.02 µm filter and conserved at -20ºC until analysis to prevent chemical evolution. Such filter pore-size was chosen in order to avoid the effects of fine-grained particulates and colloids on the analysis of dissolved iron.

pH measurements were performed immediately after sampling by using a digital microelectrode coupled to a pH meter previously calibrated at pH 7 (neutral) and pH 4 (acidic). Redox potential (Eh_{SCE}) was also measured in some experiments with the pH.

2.5.2 Dihydrogen production and consumption

Analysis of gases in the headspace of the reactors was performed by micro gas chromatography (GC) on CP-4900 Micro-GC apparatus (Varian) equipped with a thermal conductivity detector and three parallel columns according to Table 8. The gaseous samples were withdrawn by using a needle sterilized with ethanol prior each sampling. As for the IC technique described above, GC is based upon the interaction of a stationary phase (usually packed columns contained in an oven) with the gaseous compounds carried by a gas mobile phase (inert gas).

Table 8: Instrument parameters for gases analysis by micro-GC.

	Column 1	Column 2	Column 3
	10m MS5	10m PPQ Heated In.	10m MS5
Detection	O_2 and N_2	CO_2	H_2
Carrier gas	He	He	N_2
Column pressure (kPa)	200	150	200
Column temperature (°C)	100	100	100
Injection time (ms)	30	30	30
Sampling time (s)	30	30	30
Run time (min)	2	2	2

Total H_2 concentration was obtained as the sum of the concentrations in the gaseous and aqueous phases. The dissolved gas was calculated according to Henry's law:

$$[H_2]_{aq} = \frac{P_{H_2}}{K} \qquad \textbf{(2.2)}$$

where $[H_2]_{aq}$ is the H_2 concentration in solution (mol.L^{-1}), K= 1333.33 L.atm.mol^{-1} is the Henry's constant for H_2 and PH_2 is the H_2 partial pressure (atm) determined by the GC analysis.

2.5.3 Evolution of the solid phases

Steel coupons, metallic iron and magnetite powders were analyzed at the end of the experiments by different techniques which are complementary to each other. Before analysis, all steel coupons were dried inside an M-Braun LABstar MB10 anaerobic glovebox

(O_2 concentration less than 0.5 ppm), and powders were freeze-dried. All samples (massive and powder) were kept under anoxic conditions until analysis.

Steel coupons were analyzed by XRD, Raman microspectroscopy (RM) and Scanning electron microscopy (SEM) with energy dispersive X-ray (EDX) analysis in order to identify corrosion products formed on the surface. Metallic iron and magnetite powders were analyzed by XRD, Fourier-transform infrared spectroscopy (FTIR) and SEM/EDX aiming to identify corrosion products or biogenic minerals resulting from magnetite bioreduction. They were ground in an agate mortar before XRD and FTIR analyses.

2.5.3.1 X-ray diffraction (XRD)

X-ray diffraction (XRD) is a powerful non-destructive technique for identification of crystalline mineral phases and their chemical structure. The interaction of a crystalline sample with a X-rays beam creates scattered X-rays related to the lattice distances in the sample according to Bragg's law:

$$n\lambda = 2d\sin\theta \qquad \textbf{(2.3)}$$

where λ is the wavelength of the X-rays (in angstroms), θ is the scattering angle, *n* is the integer representing the diffraction order and *d* is the lattice distance (in angstroms). Bragg's law describes the condition for constructive interference, where the path difference between two scattered X-rays is equal to an integer multiple of the wavelength. The angles and intensities of scattered X-rays are recorded by a detector, and the resulting diffractogram obtained by plotting the diffracted intensity (vertical axis) as a function of 2θ (horizontal axis).

All solid samples were analyzed with a Panalytical X'Pert Pro MPD (θ-θ) powder diffractometer operating at a power of 1.6 kW (or 40 kV and 40 mA) with a cobalt anticathode ($K\alpha$= 1.79 Å) and a X'Celerator detector at CEREGE laboratory (Aix en Provence, France). Mineral phases were identified by using X'Pert HighScore Plus software (Panalytical) and ICDD-PDF2 2006 database.

Steel coupon samples were positioned at the goniometer center by a motorized x-y-z positioning sample holder in order to analyze accurately only the metal surface. The diffraction patterns (sum of 3 scans) were recorded in the angular range of 10°-$70^\circ(2\theta)$ with step size $0.033^\circ(2\theta)$ and counting time 2.5 s. Powder samples were filled into glass capillaries (300 µm in diameter) sealed with paraffin in order to prevent oxidation during analysis. A W/Si mirror was used to create a monochromatic parallel X-rays beam and to

collimate on the capillary (driven by rotary motion) placed in the goniometer. The diffraction patterns (sum of 6 scans) were recorded at the same conditions for coupon samples but with counting time 0.4 s.

2.5.3.2 Raman microspectroscopy (RM)

Raman spectroscopy is a typically non-destructive technique for identification of mineral phases and their chemical structure by measuring the changes in the polarizability of molecular bonds induced by bond vibrations. The technique is based on the inelastic scattering of a monochromatic light (usually from a laser beam) upon interaction with the sample. The photons of the laser light are absorbed by the sample and subsequently reemitted with different energy (frequency, wavelength). Therefore, Raman scattering corresponds to photons reemitted with a frequency shifted up or down in comparison with the original incident. Raman interaction can lead to two possible scatterings: *(i) Stokes Raman scattering* when molecules absorb energy and the emitted photons have a lower energy than the absorbed photons; and *(ii) anti-Stokes Raman scattering* when molecules lose energy and the emitted photons have higher energy than the absorbed photons. The Raman spectrum results in a plot of intensity of the Raman scattering (vertical axis) versus Raman shift (horizontal axis) presented in units of wavenumbers (cm^{-1}). The coupling of Raman spectroscopy with microscopy (Raman microspectroscopy, RM) enables high spatial resolution and sensitivity.

Steel coupons were analyzed with a Horiba Jobin Yvon LabRam HR800 spectrometer equipped with a Nd-YAG laser at 532 nm, a local length of 800 mm and a Peltier-cooled CCD detector at CEA Saclay/LISL laboratory (Gif-sur-Yvette, France). The samples were kept in anoxic conditions in small confining boxes and measurements were performed through a glass window (500 µm thick). The laser power at the sample was between 0.5 and 5 mW. Microanalysis was achieved through an Olympus BX41 microscope fitted with a 50x long range objective lens. The probed area was about 10 x 10 µm with spectral resolution of 1 and 4 cm^{-1}. The acquisition time ranged from 60 to 600 s depending on the spectral quality. Spectra acquisition was managed by LabSpec 5 software (Horiba Jobin Yvon) and their analysis was performed by comparing the significant bands with literature studies (Bellot-Gurlet *et al.*, 2009; Faria *et al.*, 1997; Frost *et al.*, 2002; Frost and Weier, 2004; Hanesch, 2009; Oh *et al.*, 1998) and RRUFF database (Downs, 2006).

2.5.3.3 Scanning electron microscopy (SEM) with energy dispersive X-ray (EDX) analysis

Scanning electron microscopy (SEM) provides high-resolution images with topographical and morphological information by scanning the sample with an electron beam. When coupled to an energy dispersive X-ray (EDX) detector can also offer information about the chemical composition of the sample. The interaction of atoms in the sample with the electron beam produces distinct signals which can be displayed as an image, such as: secondary electrons (SE) obtained by inelastic scattering with very low energy (< 50 eV), and backscattered electrons (BSE) obtained by elastic scattering with high energy. The electron beam interacts with the sample to a depth of ~ 1 µm.

All solid samples were analyzed at UPMC/LISE laboratory (Paris, France) with a Leica Stereoscan 440 microscope at 20 keV and 5.3 nA coupled to a PGT SPIRIT EDX (Princeton Gamma-Tech) for elemental semi-quantitative analysis (copper calibration, accelerating voltage of 15 kV and working distance of 8 mm). In this study, EDX analysis is only shown as qualitative information since for an accurately quantitative analysis the samples have to be polished and flat. Steel coupons were carbon-coated prior to SEM analysis. Powder samples were not metal coated.

2.5.3.4 Fourier-transform infrared spectroscopy (FTIR)

Fourier-transform infrared spectroscopy (FTIR) is a typically non-destructive technique for identification of chemical bonds and molecular functional groups. FTIR is similar to Raman spectroscopy in that it also uses molecular bond vibration for chemical identification. The FTIR technique is based on the interaction between molecules present in the sample and infrared (IR) light. The molecules absorb IR light at specific wavelengths, known as resonance frequencies that are related to the type of bond or molecular group. Absorption of IR light can occur only if the movement generated by the bond vibration is associated with a change in the dipole moment of the molecule. An IR spectrum results in a plot of absorbed (or transmitted) IR intensity (vertical axis) versus IR frequency (horizontal axis), usually in units of wavenumbers (cm^{-1}).

Powder samples were analyzed with a Bruker IFS28 spectrometer equipped with a DTGS detector and a KBr beam splitter in attenuated total reflection (ATR) mode. The ATR device (*SensIR* Technologies, CT) is fitted with a 9 bounce diamond microprism with a 4.3 mm surface diameter and ZnSe optics. Each single beam spectrum corresponded to 300 co-added scans at 4 cm^{-1} resolution. All frequencies reported have an accuracy of ± 1 cm^{-1}.

The samples were directly placed onto ATR device in an amount enough to cover the crystal area. They were slightly clamped against the ATR crystal. Spectra acquisition was managed by OPUS software (BrukerOptics) and their analysis was performed by comparing the significant bands with literature studies (Frost *et al.*, 2002; Huang and Kerr, 1960; Li *et al.*, 2012; Liu *et al.*, 2011; Namduri and Nasrazadani, 2008; Pekov *et al.*, 2007; Remazeilles and Refait, 2009; Russell, 1979) and RRUFF database (Downs, 2006).

2.5.3.5 Weight loss analysis

Weight loss analysis of the steel coupon samples was performed following the American Society for Testing and Materials (ASTM) standard G1-03 (ASTM, 2011). All coupons were weighted before introduction into the reactors in order to obtain the initial weight. At the end of the experiments, the coupons were dried in a desiccator and weighted. Afterwards, they were cleaned in a solution 50% (v/v) HCl plus 5 $g.L^{-1}$ of hexamethylenetetramine for 30 s for removal of corrosion products, rinsed with deionized water and acetone, and then dried in a desiccator and reweighted. Two uncorroded coupons were cleaned by the same procedure in order to evaluate the extent of metal loss resulting from cleaning, which was determined to be ± 0.4 mg (± 2 $\mu m.y^{-1}$). The weight loss was converted to corrosion rate by using the following equation:

$$v(corr) = \frac{3650 \times x}{d \times t \times A} \qquad \textbf{(2.4)}$$

where:

$v\ (corr)$ is the corrosion rate in $\mu m.y^{-1}$

x is the mass loss in mg determined by subtracting the weight after cleaning from the initial weight of the coupons

d is the density for low carbon steel (7.85 $g.cm^{-3}$)

t is the exposure time in days

A is the total area of the coupon in cm^2

The amount of corrosion products attached to the metal surface can be evaluated by the difference of weights before cleaning the coupon (weight at the end of the experiment) and corrosion reaction (initial weight).

2.6 Summary of the main experiments

Table 9 summarizes the reactional conditions of the main experiments performed in this study, which are discussed in the chapters 4 and 5.

Table 9: Summary of the reactional conditions of the main geochemical experiments.

Objective	Solid sample	Solution	Conditions	Time (months)	Analysis of the solid phases
evaluation of the dissimilatory Fe(III) reduction	synthesized magnetite ($7\ g.L^{-1}$)	M1 + control (Na_2SO_4) (140 mL)	anaerobic (3 conditions): 4% H_2 (H_2:N_2 / 4:96%) pH_i ~ 7.3 (M1 + control) 10% H_2 (H_2:CO_2:N_2 / 10:20:70%) pH_i ~ 6.3 (M1); 6.0 (control) 60% H_2 (H_2:CO_2:N_2 / 60:10:30%) pH_i ~ 6.6 (M1); 6.3 (control) 30°C abiotic + biotic without lactate	0-1	XRD FTIR SEM/EDX
evaluation of the corrosion process	iron powder ($7\ g.L^{-1}$)	M1 + control (Na_2SO_4) (140 mL)	anaerobic (N_2:CO_2 / 90:10%) pH_i ~ 6.4 (M1); 6.2 (control) 30°C abiotic + biotic without lactate	0-1	XRD FTIR SEM/EDX
	carbon steel coupon ($1;\ 0.8\ cm^2$)	M1 + control (Na_2SO_4) (140 mL)	anaerobic (N_2:CO_2 / 90:10%) pH_i ~ 6.4 (M1); 6.2 (control) 30°C abiotic + biotic without lactate	0-1 0-5	XRD RM SEM/EDX weight loss

CHAPTER 3: INFLUENCE OF REACTIONAL PARAMETERS ON THE BACTERIAL ACTIVITY

The objective of this chapter is to assess some reactional parameters that could influence on the activity of *Shewanella oneidensis* strain MR-1 and consequently Fe(III) reduction. These experiments were exploratory studies aiming at determining the best reactional conditions to be applied on the upcoming experiments.

The experiments were carried out with the M1 solution (initial pH= 7) using soluble Fe(III) citrate (20 mM) as the sole electron acceptor. A qualitative analysis was performed by accompanying colour variation of the medium. The colour variation is attributed to the change in the nature and/or concentration of the ferric citrate complex which in turn can be associated to a Fe(III) bioreduction. At the beginning, the solution is yellow due to the high Fe(III) concentration. It changes to colourless when Fe(III) concentration becomes low, indicating reduction of Fe(III) to Fe(II). The influence of incubation temperature, headspace gas composition, electron donor substrate and bacterial cell density were evaluated on the rate of Fe(III) bioreduction.

3.1 Incubation temperature

The temperature changes within nuclear waste repository with time. It is expected to reach 90°C in the first 10 years and then to decrease to 40°C after 1,000 years and 27°C after 10,000 years (Andra, 2005a). Therefore, the assessment of the bacterial activity in different temperature conditions and its impact on the Fe(III) bioreduction is required.

Two temperatures (30°C and 37°C) that are in the range for optimal growth of mesophilic bacteria (e.g. *Shewanella* sp.) were examined. The objective of these experiments was to evaluate if *Shewanella oneidensis* strain MR-1 can tolerate a higher temperature than the optimal temperature (30°C according to Venkateswaran *et al.* (1999)). This ability could potentially accelerate the rate of Fe(III) bioreduction. These experiments were performed with 22 mM lactate as electron donor, N_2:CO_2 (90:10%) as anaerobic gas and an initial bacterial concentration of 10^7 cells.mL^{-1}.

The results showed that the solution became colourless, after 2 days of reaction, only at 30°C (Figure 23). The solution colour did not change at 37°C, suggesting a limitation of the bacterial activity on the Fe(III) reduction at this temperature. In fact, the bacterial cells cultured at 37°C were examined with an optical microscope. They were observed to be as long filaments, instead of being rod-shaped under normal conditions (i.e.

30°C). This confirms that the cells undergo an environmental stress at 37°C affecting their activity.

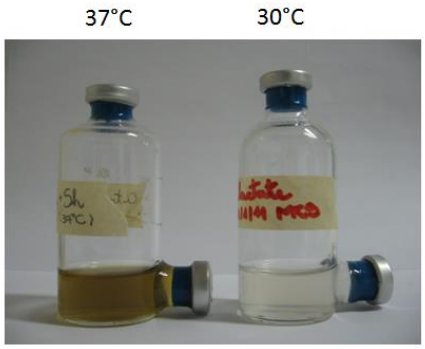

Figure 23: Influence of temperature (30°C and 37°C) on the Fe(III) bioreduction after 2 days of reaction with the M1 solution (45 mL), lactate (22 mM)/Fe(III) citrate (20 mM) and 10^7 cells.mL^{-1} under N_2:CO_2 (90:10%) atmosphere.

3.2 Headspace gas composition for anaerobic conditions

Two anaerobic gas compositions were evaluated: 100% N_2 and N_2:CO_2 (90:10%). An evaluation on the presence of CO_2 in the gas composition is justified because this compound is expected within nuclear waste repository due to the degradation of disposal materials and as metabolic end-products of biological processes. Besides that, *Shewanella oneidensis* is also an autotrophic bacterium, and thus an evaluation in the autotrophic behavior is required. These experiments were performed at 30°C with 22 mM lactate as electron donor and an initial bacterial concentration of 10^7 cells.mL^{-1}.

The solution became colourless after 6 days of reaction in the presence of N_2:CO_2 gas, showing that the rate of Fe(III) bioreduction was faster with this anaerobic gas compared to 100% N_2 gas (Figure 24).

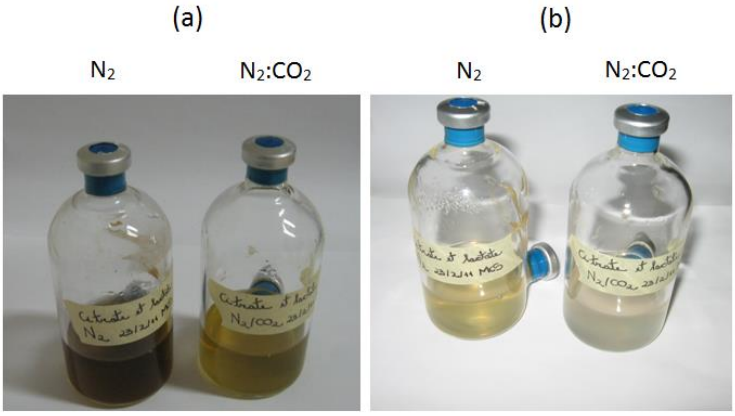

Figure 24: Influence of anaerobic gas composition (N_2 and N_2:CO_2) on the Fe(III) bioreduction at 30°C with the M1 solution (45 mL), lactate (22 mM)/Fe(III) citrate (20 mM) and 10^7 cells.mL^{-1}: (a) 2nd day; and (b) 6th day of reaction.

The results confirm that CO_2 in the anaerobic gas can serve as mineral carbon source for bacterial development, which results in a higher bacterial activity on the Fe(III) reduction.

3.3 Electron donor substrates

Three electron donor substrates were evaluated: 22 mM lactate (N_2:CO_2 / 90:10%), 10% H_2 (H_2:CO_2:N_2 / 10:20:70%) and 60% H_2 (H_2:CO_2:N_2 / 60:10:30%). The objective of these experiments was to evaluate the potential use of H_2 as energetic substrate and its impact on the rate of Fe(III) bioreduction. A comparison with lactate was performed since most of the studies in the literature use lactate as electron donor. These experiments were performed at 30°C with an initial bacterial concentration of 10^7 cells.mL^{-1}.

The results showed that the solution became colourless after 2 days of reaction with lactate (organic electron donor), showing that the rate of Fe(III) bioreduction is much faster with lactate than with H_2 (inorganic electron donor). However, H_2 also promotes bioreduction, and the solution becomes colourless more rapidly with 60% H_2 (6 days) than with 10% H_2 (13 days), as shown in Figure 25. Thus, the higher the H_2 concentration, the faster the rate.

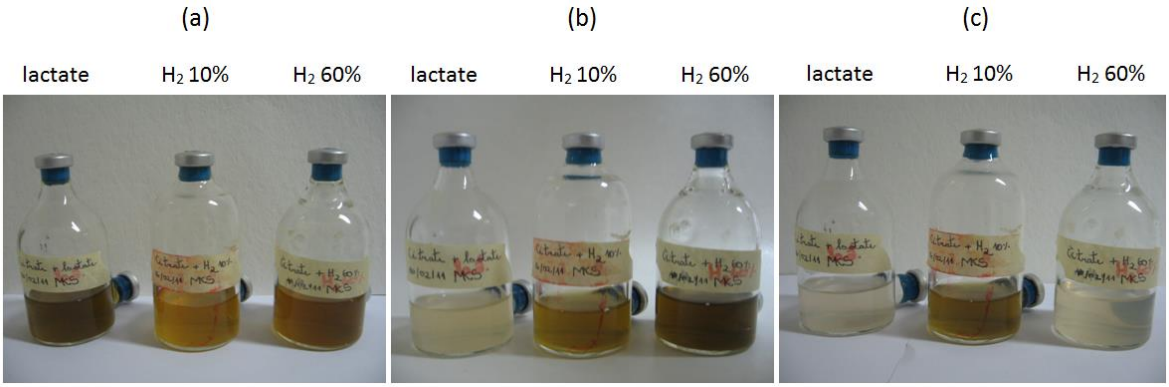

Figure 25: Influence of electron donor (lactate, H_2 10% and 60%) on the Fe(III) bioreduction at 30°C with the M1 solution (45 mL), Fe(III) citrate (20 mM) and 10^7 cells.mL^{-1}: (a) 1st day; (b) 2nd day; and (c) 6th day of reaction.

There is no significant difference in the thermodynamic free energy for Fe(III) bioreduction between lactate and H_2 as electron donors (Amend and Shock, 2001; Lovley *et al.*, 1989; Thauer *et al.*, 1977), as shown in the equations 3.1 and 3.2 respectively:

$$4\ Fe^{+3} + CH_3CHOHCOO^- + 2\ H_2O \rightarrow 4\ Fe^{+2} + CH_3COO^- + HCO_3^- + 5\ H^+ \qquad \textbf{(3.1)}$$

$$\Delta G^0 = -115\ kJ/mol\ electron$$

$$2\ Fe^{+3} + H_2 \rightarrow 2\ Fe^{+2} + 2\ H^{+} \quad \textbf{(3.2)}$$
$$\Delta G^0 = -114\ kJ/mol\ electron$$

Therefore, it can be suggested that the bioreduction reaction is faster with lactate because lactate can be readily used as organic carbon source for bacterial metabolism in addition to the CO_2 (mineral carbon source) present in the anaerobic gas composition (N_2:CO_2 / 90:10%). In the experiments with H_2 gas, only CO_2 is available as carbon source.

These experiments confirmed that *Shewanella oneidensis* strain MR-1 can use H_2 as an electron donor coupled to Fe(III) reduction in the absence of an organic electron donor. This ability will be important especially in the disposal environment containing low amounts of organic matter but with high availability of H_2 resulting from corrosion processes. Moreover, the bacterial activity and consequently the rate of Fe(III) bioreduction is dependent on the H_2 concentration — when its concentration increases, the kinetics of Fe(III) reduction also increases. It is noteworthy that the citrate anions concentration (20 mM) remains constant during each experiment, which assures that there is no other source of organic substrate for bacterial development in the reactions with H_2. The experiments pointed out to a hierarchical order on the rate of Fe(III) bioreduction: lactate > 60% H_2 > 10% H_2.

3.4 Bacterial cell density

Three initial bacterial cell concentrations were evaluated: high (H: $5x10^7$ cells.mL^{-1}), intermediate (I: $8x10^6$ cells.mL^{-1}) and low (L: $2x10^6$ cells.mL^{-1}). These experiments were performed at 30°C with 60% H_2 (H_2:CO_2:N_2 / 60:10:30%) as electron donor as well as anaerobic gas.

As shown in Figure 26, the colour of the solution begins to change after 2 days of reaction only with a high cell density (10^7 cells.mL^{-1}), becoming colourless after 26 days. These results pointed out that Fe(III) reduction is significant only when cell densities are equal or higher than 10^7 cells.mL^{-1}, at least over a period of almost 30 days.

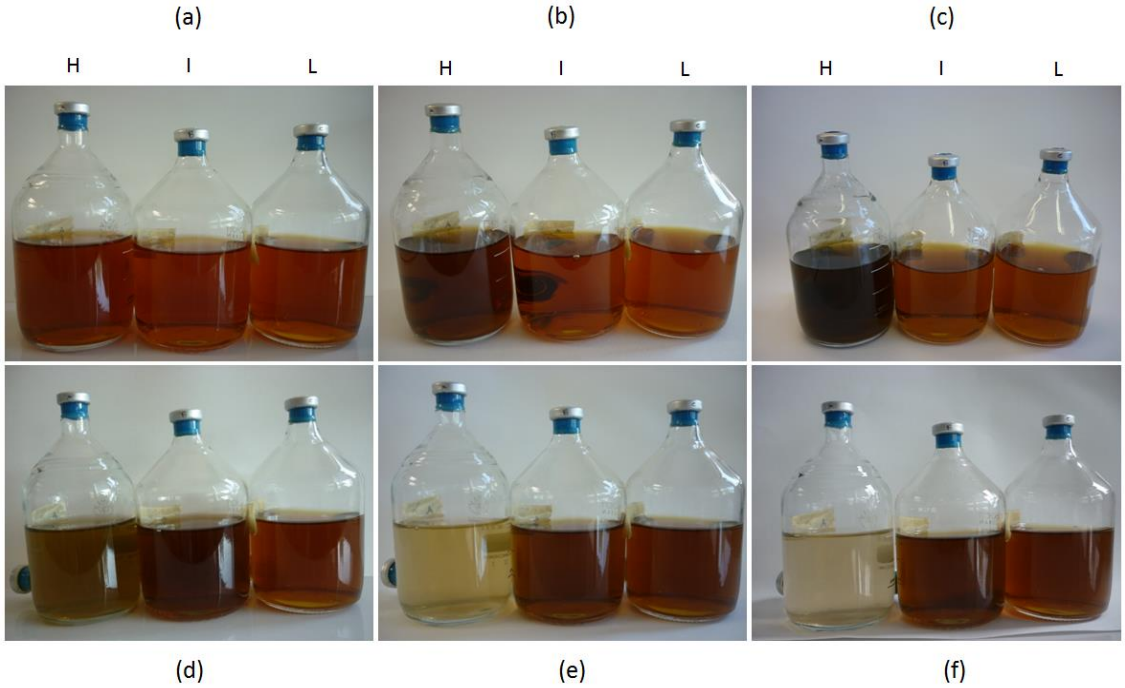

Figure 26: Influence of bacterial cell density (H for high; I for intermediate; L for low) on the Fe(III) bioreduction at 30°C with the M1 solution (180 mL) and H_2 (60%)/Fe(III) citrate (20 mM): (a) 0 day; (b) 2nd day; (c) 7th day; (d) 15th day; (e) 19th day; and (f) 26th day of reaction.

In order to evaluate the Fe(III) reduction from an insoluble substrate, magnetite powder was added into the reactor with high bacterial cell density that had changed to colourless (Figure 27a).

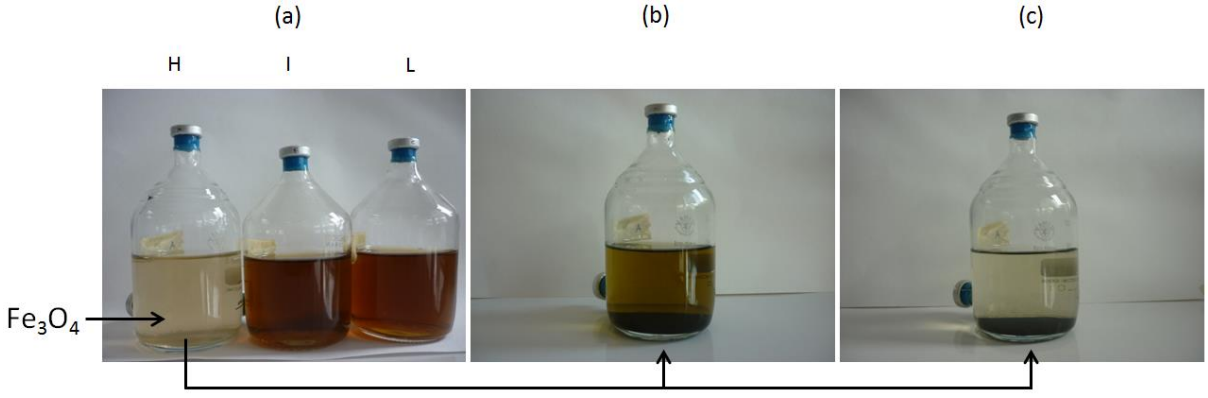

Figure 27: Fe(III) bioreduction from magnetite in the presence of high bacterial cell density (10^7 cells.mL^{-1}) at 30°C with the M1 solution (180 mL) and 60% H_2: (a) addition of magnetite powder; (b) 5th day; and (c) 20th day of reaction.

It is observed that the solution becomes green after 5 days of reaction with magnetite (Figure 27b). This shows that a portion of magnetite is dissolved releasing Fe(III) in solution. Then, the solution becomes again colourless after 15 days of reaction in the presence of bacteria, indicating that soluble Fe(III) is bioreduced to Fe(II) (Figure 27c).

Regarding the influence of bacterial cell density, the results pointed out that cell concentrations lower than 10^7 cell.mL^{-1} may be not high enough to promote significant Fe(III) reduction. They also show that Fe(III) contained in magnetite, a crystalline iron oxide of mixed oxidation state (Fe_3O_4 : $Fe^{2+}Fe^{3+}{}_2O_4$), is available for bioreduction as already demonstrated by Esnault *et al.* (2011). The reduction process seems to involve initially a mechanism of dissolution and posterior Fe(III) reduction.

3.5 Partial conclusions

These exploratory studies about the influence of reactional parameters on the Fe(III) bioreduction allowed us to gain insights on this complex process. It was confirmed that the model organism of this study (*Shewanella oneidensis* strain MR-1) is capable to use H_2, an inorganic substrate, for anaerobic respiration. The H_2 concentration seems to be directly proportional to the rate of Fe(III) bioreduction. Structural Fe(III) from magnetite, an insoluble substrate, is bioavailable.

From these preliminary results, some reactional parameters were identified for the upcoming experiments, since they showed to be more suitable for bacterial activity, such as: incubation temperature at 30°C, CO_2 in the anaerobic gas composition and initial bacterial cell densities equal or higher than 10^7 cells.mL^{-1}. Thus, taking into account that Fe(III) and H_2 can be an important driver for bacterial activity, a study regarding the H_2 consumption associated to Fe(III) bioreduction from an insoluble substrate (magnetite) is discussed in the chapter 4.

CHAPTER 4: DISSIMILATORY FE(III) REDUCTION OF MAGNETITE

The objective of this chapter is to assess the structural Fe(III) bioavailability in magnetite samples in the presence of H_2 as the sole electron donor for bacterial anaerobic respiration (Fe(III)/H_2 as redox couple). Such Fe(III) bioavailability can potentially alter the magnetite stability, affecting therefore the passivating properties of layers made of this corrosion product commonly identified under geological conditions. To this end, three initial concentrations of H_2 gas (4%, 10% and 60%) were tested with synthetic magnetite in the presence and absence of *Shewanella oneidensis* strain MR-1. The initial bacterial concentration was 10^8 cells.mL^{-1} for the biotic experiments, and 0 cells.mL^{-1} for the abiotic experiments in all reactional conditions.

The experiments were carried out at 30°C and the anaerobic conditions were achieved by flushing the system with H_2 gas: 4% H_2 (H_2:N_2 / 4:96%), 10% H_2 (H_2:CO_2:N_2 / 10:20:70%) and 60% H_2 (H_2:CO_2:N_2 / 60:10:30%). The experiments were accompanied mainly by measuring the concentration of dissolved Fe(II) (ferrozine assay) and total H_2 (GC) in the M1 and control (Na_2SO_4) solutions. At the end of each experiment, the magnetite samples were analyzed by XRD, FTIR and SEM/EDX in order to evaluate the formation of biogenic minerals.

4.1 Fe(III) (bio)reduction and Fe(II) production

Monitoring of pH and redox potential (Eh_{SCE}) values shows that changing the H_2 and CO_2 gas concentrations impacts these reactional parameters, as shown in Figure 28 and Figure 29 for the M1 and control solutions, respectively.

The pH remains more basic with 4% H_2 than with 10% and 60% H_2 for both experimental solutions. This is because the presence of CO_2 in the composition of 10% and 60% H_2 gas decreases the initial pH (around 7.4). Consequently, the decrease was higher with 10% H_2 (20% CO_2) than with 60% H_2 (10% CO_2): the initial pH decreases to 6.3 (10% H_2) and 6.6 (60% H_2) in the M1 solution and to 6.0 (10% H_2) and 6.3 (60% H_2) in the control solution. As shown in Figure 29, the pH varies significantly with 4% H_2 in the control solution due to the absence of a buffer (M1 solution has phosphate and HEPES buffers). In contrast, the pH remains more stable with 10% and 60% H_2 probably because of the formation of carbonic acid-bicarbonate buffer system by dissolved CO_2. A slight difference (0.2 pH unit) between abiotic and biotic conditions was observed in the pH with 60% H_2 (Figure 28e and Figure 29e): the pH is increased at the end of the experiments in the presence of bacteria. For the other conditions, no significant difference was observed in

the pH and Eh_{SCE} between abiotic and biotic conditions. In brief, the initial pH depends on the CO_2 concentration and the control solution seems to be more reductive than the M1 solution (effect more pronounced with 4% H_2) when comparing the Eh_{SCE} values measured in the experiments.

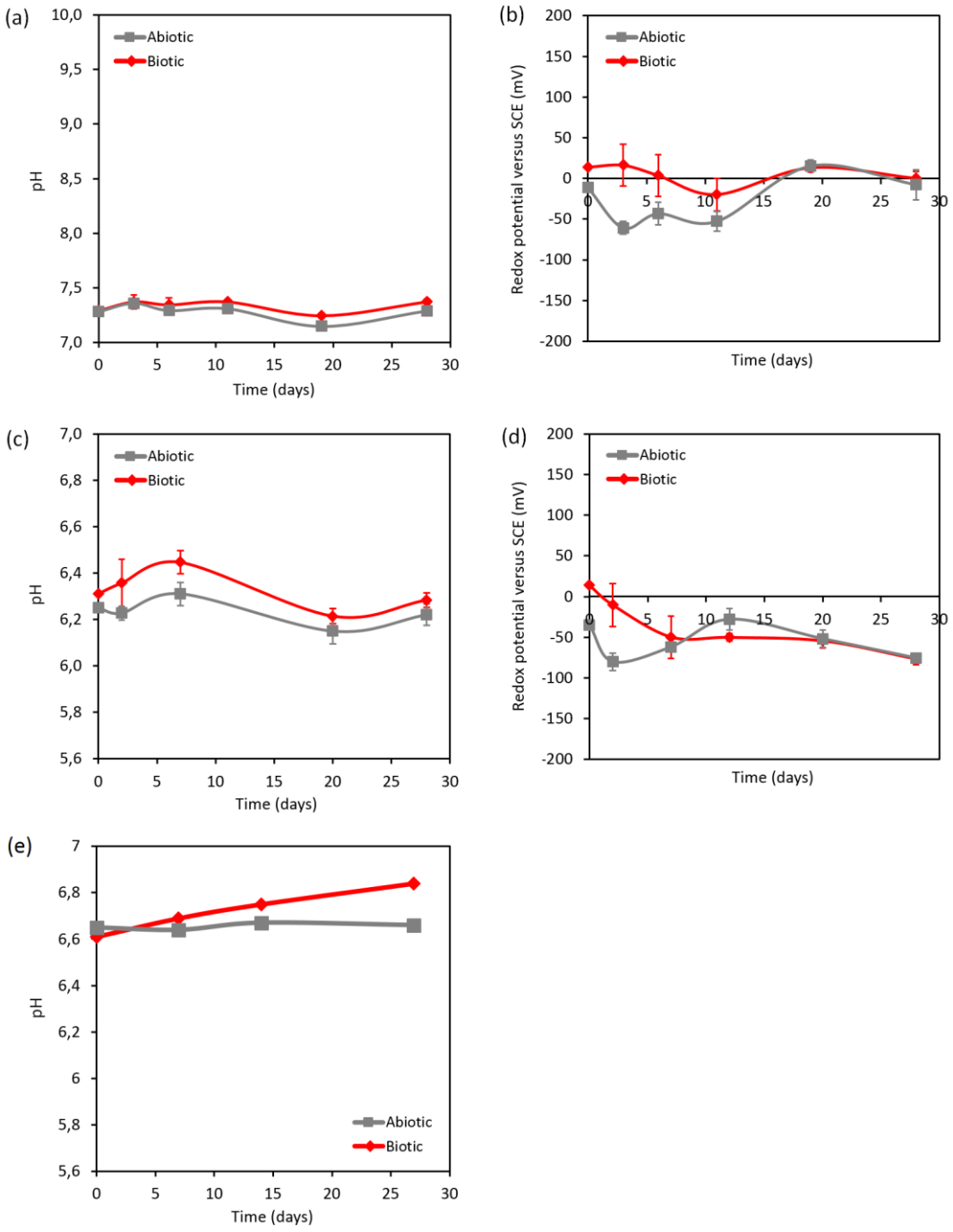

* redox potential was not measured in the experiments with 60% H_2.

Figure 28: Evolution of pH (a, c, e) and Eh_{SCE} (b, d) during Fe(III) (bio)reduction in the M1 solution and with magnetite powder: (a, b) 4% H_2; (c, d) 10% H_2; and (e) 60% H_2. Biotic conditions are indicated by red curves and abiotic conditions by grey curves. Values are the mean and the standard deviation (n=3).

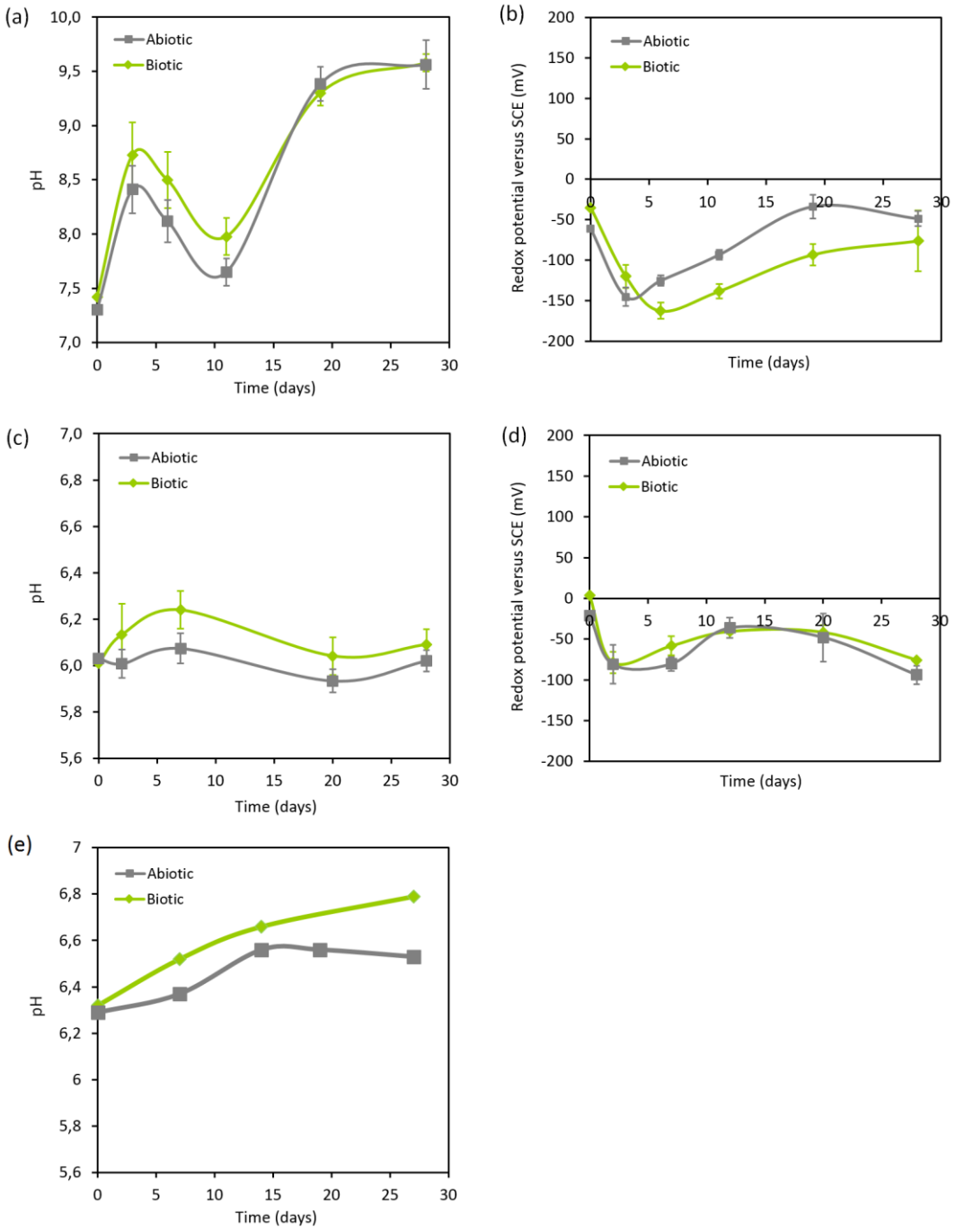

* redox potential was not measured in the experiments with 60% H_2.

Figure 29: Evolution of pH (a, c, e) and Eh_{SCE} (b, d) during Fe(III) (bio)reduction in the control (Na_2SO_4) solution and with magnetite powder: (a, b) 4% H_2; (c, d) 10% H_2; and (e) 60% H_2. Biotic conditions are indicated by green curves and abiotic conditions by grey curves. Values are the mean and the standard deviation (n=3).

Furthermore, the bacterial concentration was monitored in the biotic experiments for each reactional condition, as shown in Figure 30.

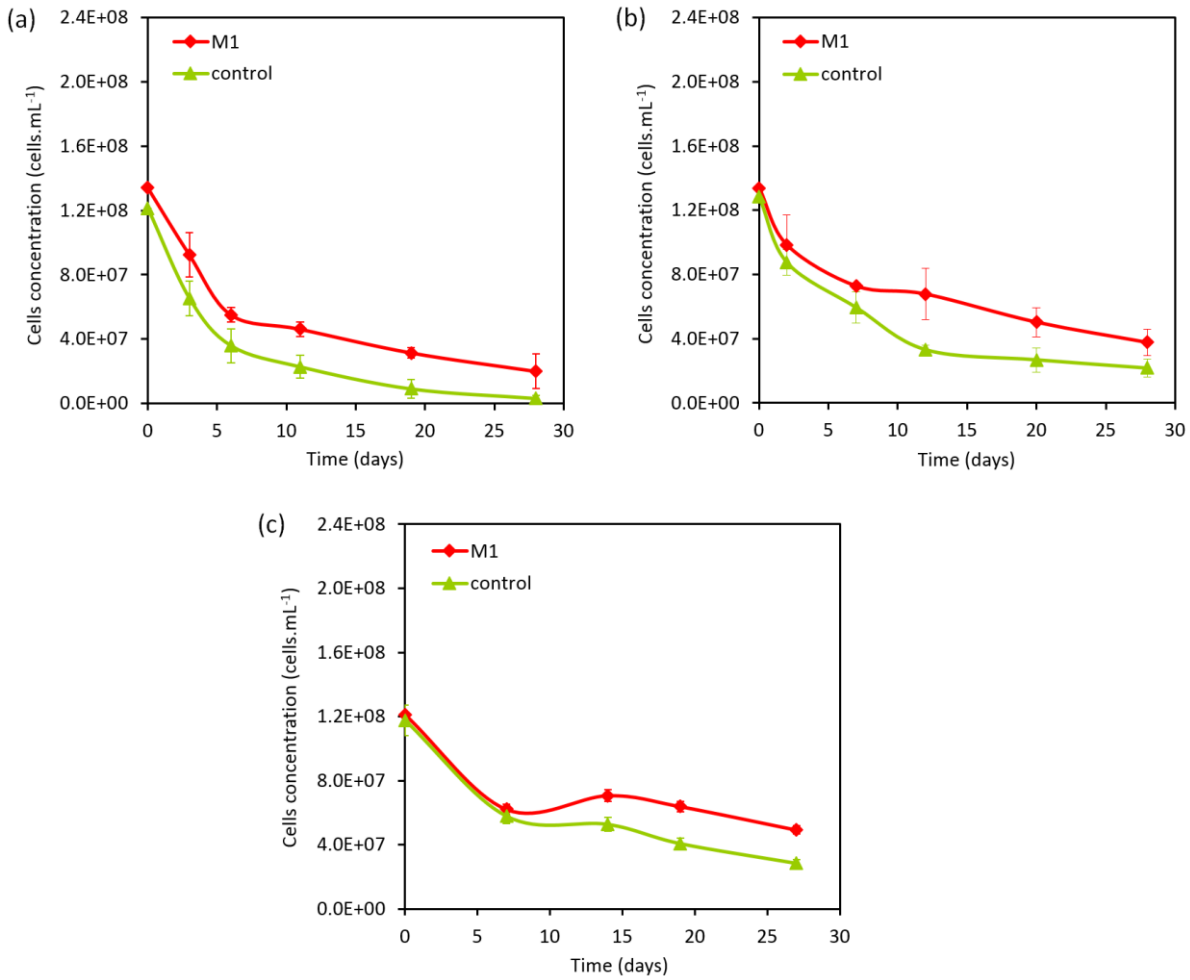

Figure 30: Evolution of bacterial cells: (a) 4% H_2; (b) 10% H_2; and (c) 60% H_2. M1 solution is indicated by red curves and control (Na_2SO_4) solution by green curves. Values are the mean and the standard deviation (n=3).

A decrease in the cells concentration was observed with time for all conditions, being higher in the control solution than the M1 solution. This decrease can result from four potential phenomena: *(i)* bacterial aggregate on the solid surface (bacterial counting considers only planktonic cells); *(ii)* nutrient sorption on the solid surface leading to a limitation of bacterial growth; *(iii)* absence of organic matter in the experiments; and/or *(iv)* depletion of nutrients because of experimental conditions (i.e. batch reactors). It is noteworthy that the control solution is poorer in terms of essential nutrients compared to the M1 solution, which can explain the larger decrease in the cells concentration. A test experiment with magnetite and 4% H_2 was performed by using the Luria Bertani Broth (LB) medium, which provides a broad base of nutrients for bacterial growth, in order to evaluate the effect of the solution composition on the evolution of bacterial cells. A three-fold increase in the cells concentration was observed after 2 days of reaction ($7x10^7$ cells.mL^{-1} at 0 day and $2x10^8$ cells.mL^{-1} at 2nd day), and this increase continued until the end of the experiment (30 days). These results indicate that the composition of the

experimental solutions (M1 and control) is the parameter most likely to influence bacterial growth.

However, despite the decrease in the bacterial concentration, microbial impact on the Fe(III) reduction in magnetite suspensions could be demonstrated. The bacterial activity was evaluated by monitoring the Fe(II) production in solution ($[Fe(II)]_{aq}$) with time, as shown in Figure 31 and Figure 32 for the control and M1 solutions, respectively.

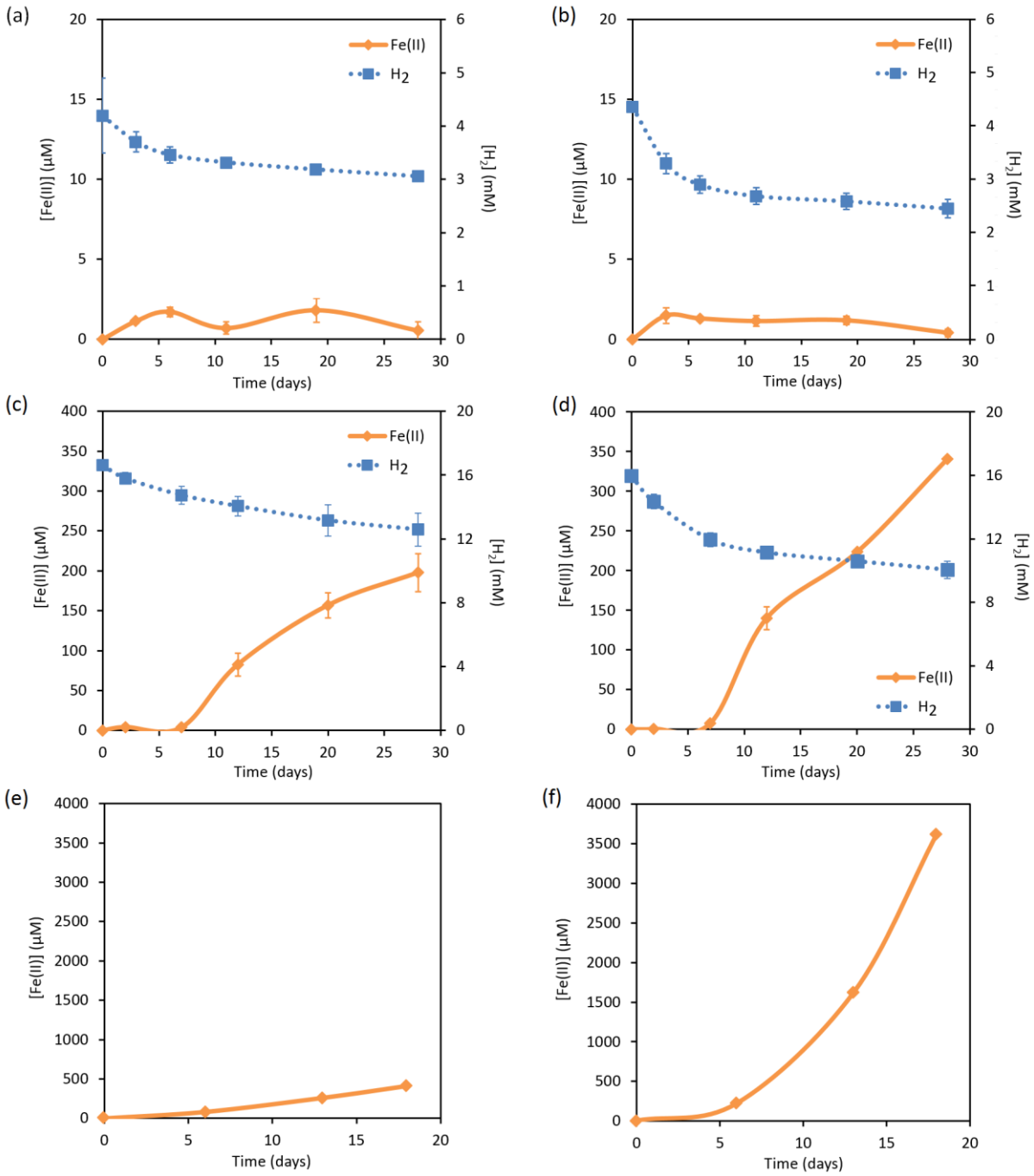

Figure 31: H_2-consumption and Fe(II)-production by Fe(III) reduction from magnetite powder in the control (Na_2SO_4) solution: (a, b) 4% H_2; (c, d) 10% H_2; and (e, f) 60% H_2. (a, c, e) abiotic; and (b, d, f) biotic conditions. Values are the mean and the standard deviation (n=3).

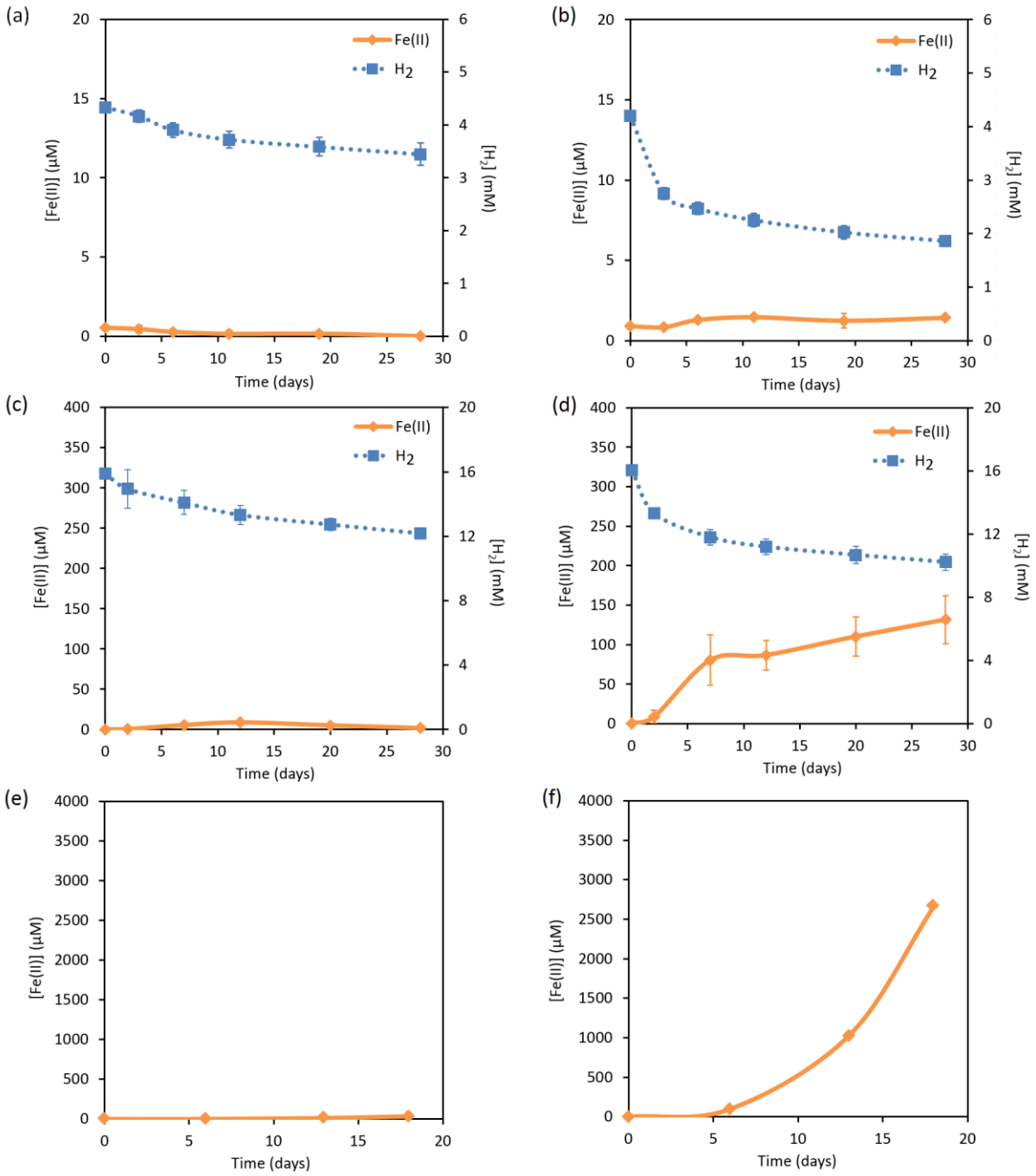

Figure 32: H_2-consumption and Fe(II)-production by Fe(III) reduction from magnetite powder in the M1 solution: (a, b) 4% H_2; (c, d) 10% H_2; and (e, f) 60% H_2. (a, c, e) abiotic; and (b, d, f) biotic conditions. Values are the mean and the standard deviation (n=3).

For the control (Na_2SO_4) solution, $[Fe(II)]_{aq}$ increases with the H_2 concentration in the system, as shown in Figure 31. High amounts of Fe(II) were observed at the end of the experiments in abiotic conditions with 10% (198 µM) and 60% H_2 (409 µM) (Figure 31c, e). This Fe(II) production in the absence of bacteria can be attributed to the chemical reduction by H_2 of Fe(III) released by magnetite; indeed, a slight decrease in the H_2 concentration was observed in these experiments. Nevertheless, $[Fe(II)]_{aq}$ still remains

higher in biotic than abiotic conditions, demonstrating the bacterial impact on the Fe(III) reduction in the control solution. In the presence of bacteria, dissolved Fe(II) concentrations of 1 µM, 340 µM and 3600 µM were measured with 4%, 10% and 60% H_2, respectively (Figure 31b, d, f). The results clearly show that the increase in the $[Fe(II)]_{aq}$ is concomitantly followed by a decrease in the H_2 concentration (H_2 consumption by bacteria could not be detected in the experiments with 60% H_2 for both control and M1 solutions due to the limit of detection of the GC analysis).

For the M1 solution, the results are different from those obtained in the control solution especially with respect to the abiotic conditions. $[Fe(II)]_{aq}$ remains roughly constant in these experiments: 0 µM, 2 µM and 34 µM with 4%, 10% and 60% H_2, respectively (Figure 32a, c, e). Such low detection of Fe(II) in solution can be explained, for example, by a complexation of Fe(II) with elements present in the M1 composition (i.e. HEPES, phosphate, sulfate). Moreover, we cannot exclude that elements of the M1 solution can be also adsorbed on the magnetite surface, which could block mineral reactive sites and thus prevent dissolution. Note that the M1 solution has a complex chemical composition compared to the control solution (see Table 6 in the chapter 2). Nevertheless, a significant impact in the Fe(II) production was shown in the presence of bacteria. The Fe(III) bioreduction becomes effective after 5 days of reaction, showing an increase in the $[Fe(II)]_{aq}$ that reaches a maximum of 1 µM and 132 µM with 4% and 10% H_2, respectively (Figure 32b, d). $[Fe(II)]_{aq}$ keeps increasing with 60% H_2 at least until the end of the experiments; 2700 µM at 18 days (Figure 32f). As for the control solution, the increase in the $[Fe(II)]_{aq}$ is concomitantly followed by a decrease in the H_2 concentration. It is noteworthy that the decrease in the bacterial cells concentration (Figure 30) is slowed down after 5 days, which can emphasize bacterial development by Fe(III) reduction coupled to H_2 oxidation. In both reactional conditions (control and M1 solutions), the H_2 concentration in the system seems to influence the bacterial activity and hence the dissolution of magnetite.

Note that the magnetite particle size is very small (~ 100 nanometers), i.e. very high surface area, which can result in rapid dissolution rates and can explain the high $[Fe(II)]_{aq}$ measured in the experiments, particularly in abiotic conditions.

Figure 33 shows another presentation form of the results indicated in the Figure 31 and Figure 32 regarding the effect of the H_2 concentration on bacterial dissolution of magnetite. It is clearly observed that the Fe(II) production increases 3 orders of magnitude by changing the H_2 concentration of 4% to 60%. It is noteworthy that $[Fe(II)]_{aq}$ remains high in the control solution probably because of the cumulative effects of chemical and biological Fe(III) reduction. The extent of Fe(III) bioreduction (Figure 33e) was estimated assuming that 1 mole of Fe(II) is produced for each mole of Fe(III) reduced, with an initial

Fe(III) amount of 62 mM in magnetite samples. The results show a greater dissolution of magnetite with 60% H_2, reaching 4.3% in the M1 solution and 5.9% in the control solution over 1 month of reaction.

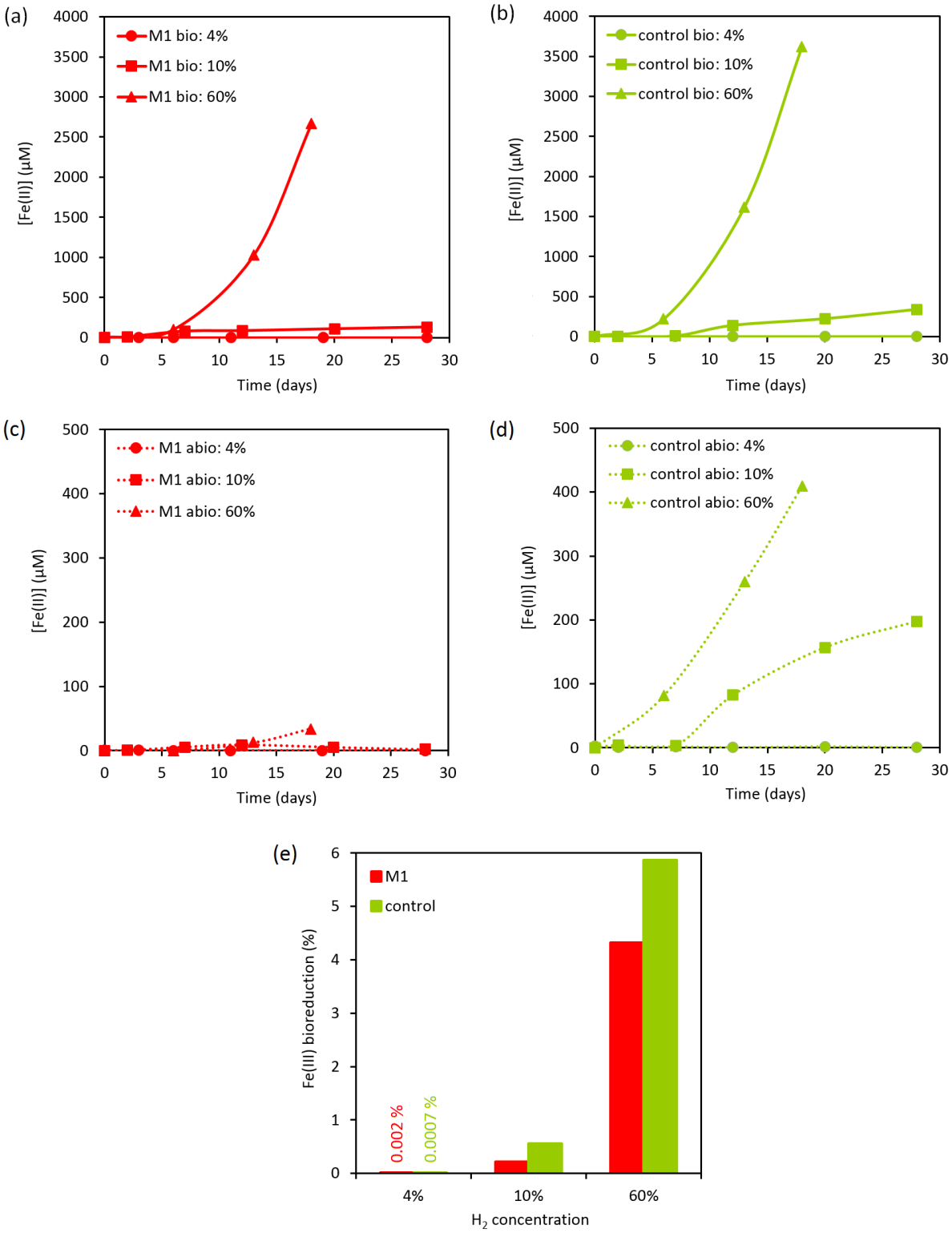

Figure 33: (a-d) Fe(II)-production by Fe(III) reduction from magnetite powder in the M1 (a, c) and control (Na_2SO_4) (b, d) solutions: (a, b) biotic and (c, d) abiotic conditions. (e) Extent of Fe(III) bioreduction over 1 month of reaction.

4.2 Fe(II) secondary mineral phases

Figure 34 shows diffractograms of the magnetite samples at the end of each experiment.

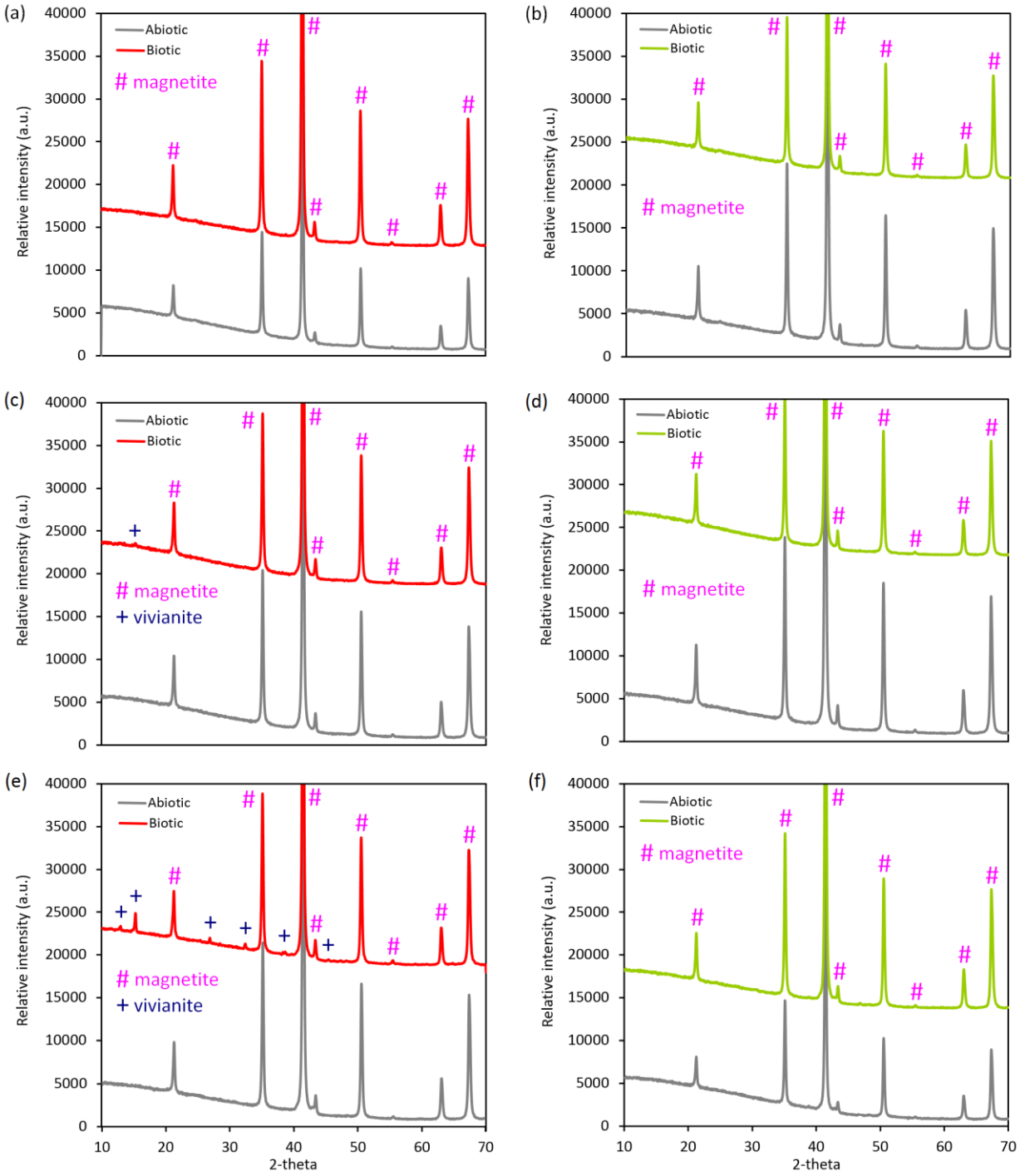

Figure 34: XRD patterns of the secondary mineral phases formed in the M1 (a, c, e) and control (Na_2SO_4) (b, d, f) solutions for 1 month of reaction: (a, b) 4% H_2; (c, d) 10% H_2; and (e, f) 60% H_2. Biotic conditions are indicated by red or green diffractograms and abiotic conditions by grey diffractograms.

As shown in Figure 34, vivianite was identified with 10% and 60% H_2 only in biotic conditions in the M1 solution. With increased H_2 concentration, vivianite became more abundant. This could be expected because the formation of this biogenic mineral is a direct consequence of the increase in the concentration of Fe(II) in solution. In contrast, no secondary mineral phases were identified in the control medium for both abiotic and biotic conditions.

In Figure 35 SEM observations reveal no significant difference in the magnetite morphology after 1 month of reaction with 4%, 10% and 60% H_2 for both biotic and abiotic conditions in the M1 and control solutions (SEM results not shown for the control solution).

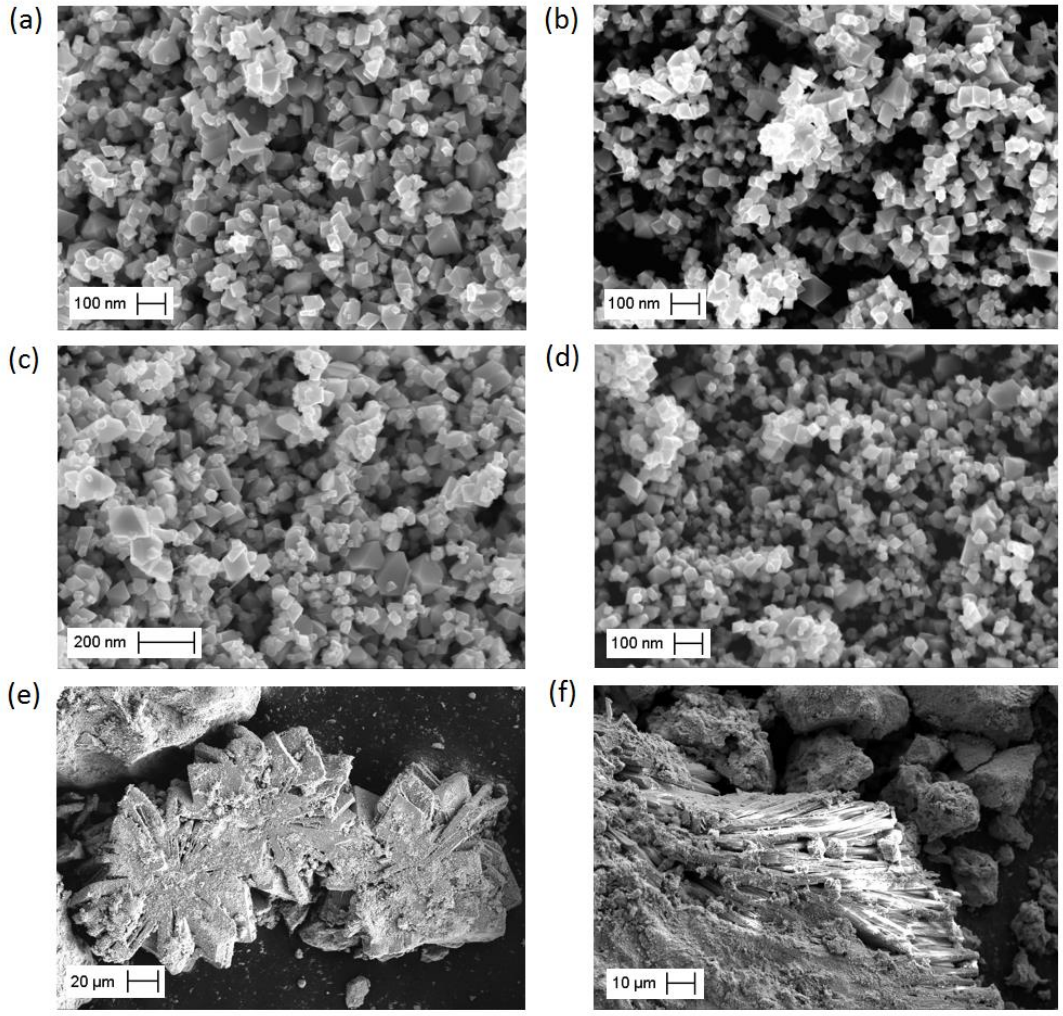

Figure 35: SEM micrographs of the magnetite powder and secondary mineral phases formed in the M1 solution for 1 month of reaction: (a, c, e) 10% H_2; and (b, d, f) 60% H_2. (a-b) abiotic; and (c-f) biotic conditions.

The formation of vivianite was confirmed in the M1 medium in the presence of bacteria with 10% and 60% H_2 (EDX analysis shows Fe, O and P in the chemical composition). This biogenic mineral appears as large isolated crystals (Figure 35e, f), being

larger with 60% H_2 than with 10% H_2. No secondary mineral phases were identified in the control solution, corroborating XRD results.

Characterization of all magnetite samples by FTIR failed to reveal additional evidence about secondary mineral phases, even in the samples in which vivianite was identified by XRD and SEM/EDX analyses. Figure 36 shows an example of FTIR spectra obtained with samples reacted in the M1 and control solutions in the presence of 10% H_2 (all samples show the same pattern regardless of the reactional condition). The sole significant feature is the band at 560 cm^{-1} which is assigned to Fe-O stretching mode of the tetrahedral and octahedral sites in the magnetite samples.

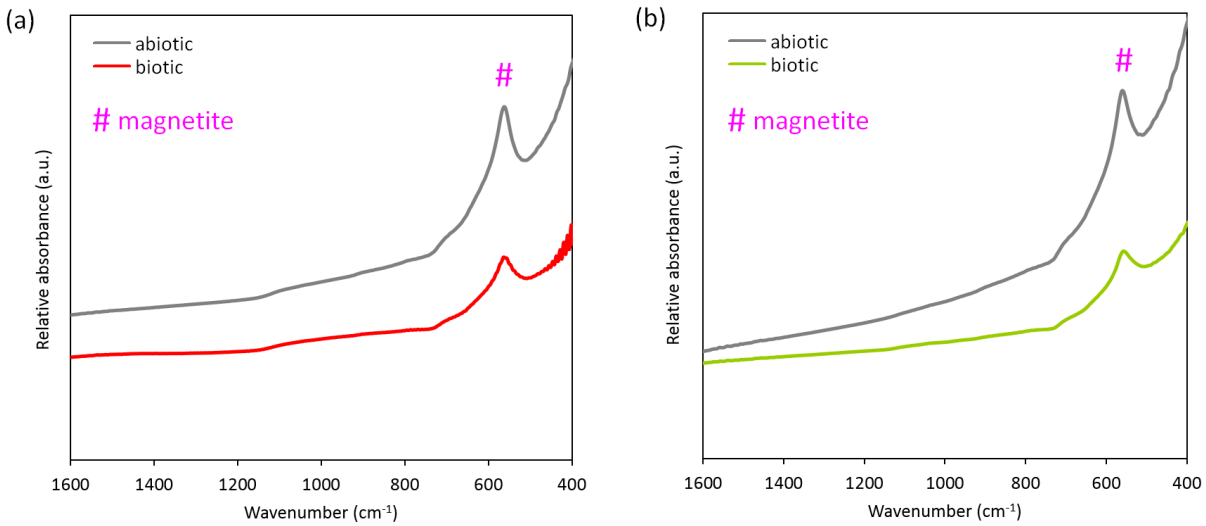

Figure 36: FTIR spectra of the magnetite powder in the M1 (a) and control (Na_2SO_4) (b) solutions for 1 month of reaction in the presence of 10% H_2. Biotic conditions are indicated by red or green spectra and abiotic conditions by grey spectra.

4.3 Partial conclusions

Our results clearly demonstrated that a hydrogenotrophic iron-reducing bacteria (*Shewanella oneidensis* strain MR-1) was capable of reducing structural Fe(III) in magnetite suspensions (Kerber-Schütz *et al.*, 2013a). This capability was notably enhanced with the increase in the H_2 concentration: 4% H_2 < 10% H_2 < 60% H_2. In the M1 solution, for example, the increase from 0.002% to 4.3% in the bioreduction extent with 4% and 60% H_2 respectively, emphasizes the important role of H_2 as energetic substrate for anaerobic respiration, especially in the disposal environment containing low amounts of organic matter. Vivianite was the sole biogenic mineral identified in the M1 medium with 10% and 60% H_2, and no secondary mineral phases were observed in the control medium. In spite of

an abiotic effect on the dissolution of magnetite, the impact of the bacterial activity was still observed with respect to the Fe(III) reduction in magnetite.

The findings emphasize that the Fe(III) bioavailability in the presence of H_2 gas can potentially alter the stability of magnetite, which in turn can affect its passivating properties in corrosion processes. Note that the H_2 gas pressure used in the experiments (~ 0.6 bar) is much lower than the maximum H_2 gas pressure expected in the repository at Bure site (~ 50 bar). Thus, a higher destabilization of magnetite can still be expected. An evaluation dedicated to the impact of HOB and IRB activities on anoxic corrosion process is discussed in the chapter 5.

CHAPTER 5: BACTERIAL IMPACT ON THE CORROSION PROCESS

The objective of this chapter is to assess the impact of hydrogenotrophic iron-reducing bacteria (*Shewanella oneidensis* strain MR-1) on the corrosion process under anoxic conditions. To this end, iron powder and carbon steel coupons were used as metallic samples to evaluate the corrosion kinetics and corrosion products in both cases. Experiments with iron powder aimed to enhance the surface area and hence the iron corrosion and H_2 production; and experiments with carbon steel aimed to simulate the corrosion process in more "realistic conditions" in terms of the type of material and reactive surface area.

The experiments were carried out at 30°C with no electron donor/acceptor added to the reactor. Here, the objective was to supply bacterial metabolism only with corrosion products (iron oxides and H_2) formed during the corrosion reaction. Anaerobic conditions were achieved by flushing the system with N_2:CO_2 (90:10%) gas. The experiments were accompanied mainly by measuring the concentration of dissolved Fe (ICP-OES) and total H_2 (GC) in the M1 and control (Na_2SO_4) solutions followed by solid characterization at the end of the experiments.

5.1 Metallic iron powder

The experiments with metallic iron powder were performed over a period of 1 month. At the end of each experiment, the samples were analyzed by XRD, FTIR and SEM/EDX in order to identify the corrosion products formed upon the corrosion reaction.

5.1.1 Evolution of Fe and H_2

Figure 37 shows the evolution of dissolved Fe and H_2 produced by iron powder corrosion over 1 month in the M1 and control solutions. The initial bacterial concentration was 10^8 cells.mL^{-1} for the biotic experiments, and 0 cells.mL^{-1} for the abiotic experiments for both reactional media.

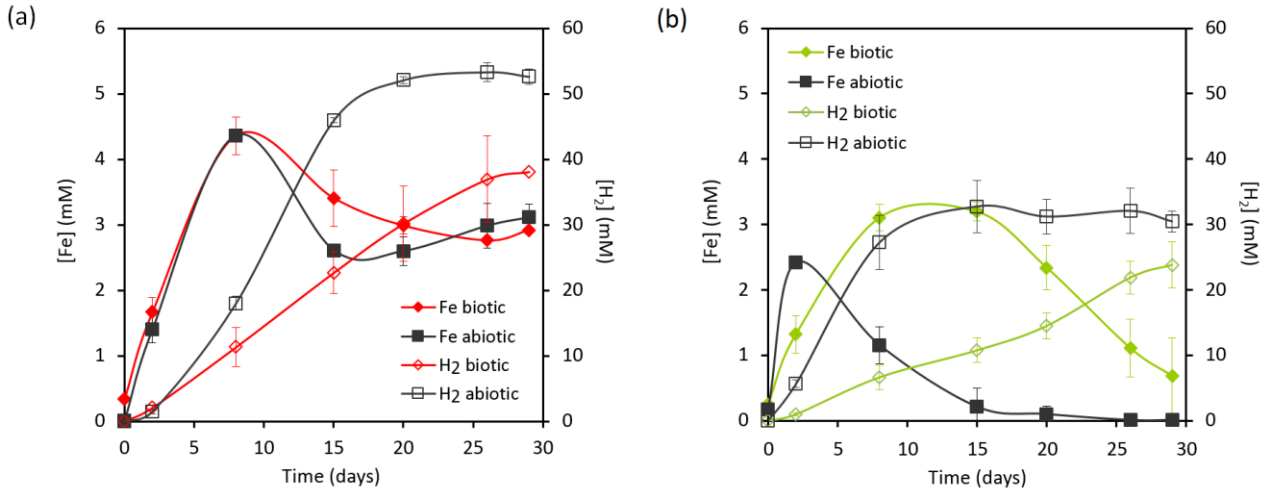

Figure 37: Production of dissolved Fe and H_2 by iron powder corrosion: (a) M1 and (b) control (Na_2SO_4) solutions for 1 month of reaction. Biotic conditions are indicated by red or green curves and abiotic conditions by black curves. Values are the mean and the standard deviation (n=3).

In the case of the M1 solution (Figure 37a), dissolved Fe ($[Fe]_{aq}$) increases significantly during 8 days (4.5 mM at 8 days) and then decreases (3 mM at 29 days), indicating precipitation of solid corrosion products in the system. There is no significant difference in the evolution of dissolved Fe between biotic and abiotic conditions. On the other hand, the net production of H_2 reaches a plateau in abiotic conditions after 20 days (53 mM), indicating decreasing corrosion kinetics. Its concentration remains much lower in the presence of bacteria (38 mM at 29 days) when compared to abiotic conditions (53 mM at 29 days), which suggests that *Shewanella oneidensis* use a portion of the H_2 produced by corrosion for redox reactions (i.e. Fe(III) reduction coupled to H_2 oxidation).

In the case of the control solution (Figure 37b), almost all aqueous Fe is precipitated in solid corrosion products. The kinetics behavior of H_2 production is similar to that for the M1 solution in both biotic and abiotic conditions.

Comparing all the results shown in Figure 37, the corrosion extent changes according to the reactional medium with or without bacteria — the production of dissolved Fe and H_2 was much lower (about 2 times) in the control solution than in the M1 solution. This indicates that the reactional medium can govern the corrosion reaction and consequently the corrosion rate, becoming an important parameter on the assessment of corrosion processes.

Figure 38 shows the concentration in solution of major elements measured at the beginning (T_i= 0 day) and the end (T_f= 30th day) of the corrosion reaction. For almost all compounds, no change in concentration is observed, even in the presence of bacteria. As an exception, phosphate concentration decreases significantly at the end of the reactions

(0.8 mM to 0 mM) in both biotic and abiotic conditions, suggesting incorporation into solid corrosion products formed in the M1 solution.

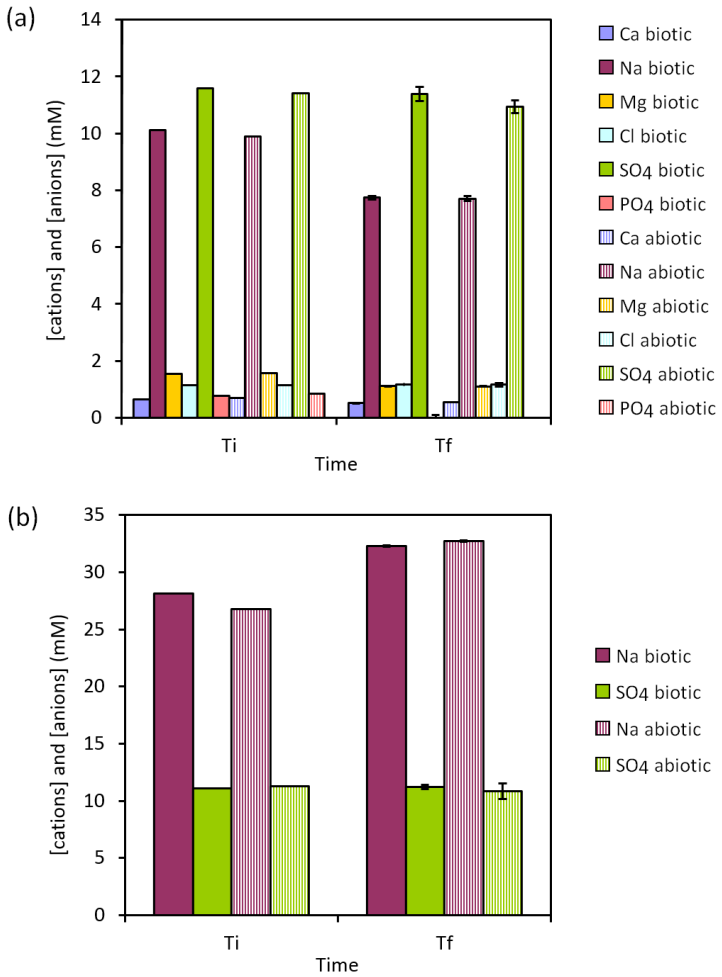

Figure 38: Evolution of major cations and anions in solution during iron powder corrosion: (a) M1 and (b) control (Na_2SO_4) solutions for 1 month of reaction. Biotic conditions are indicated by solid columns and abiotic conditions by dashed columns. Values are the mean and the standard deviation (n=3).

Furthermore, Figure 39 shows the pH and redox potential (Eh_{SCE}) measured during the experiments. It is noteworthy that both experimental solutions were adjusted to pH 7 before reaction. After flushing the system with N_2:CO_2 (90:10%) gas for anaerobic conditions, the initial pH decreases due to the presence of CO_2 in the gas composition — a higher decrease is observed in the control medium (pH_i= 6.2) because of the absence of buffer in this solution, unlike the M1 medium (pH_i= 6.5). On the one hand, the pH increases significantly along the experiments reaching a final pH around 7.9 and 7.6 in the M1 solution and 7.7 and 7.2 in the control solution for abiotic and biotic conditions, respectively (Figure 39a, c). This increase is related to the release of hydroxyl ions (OH^-) by corrosion reaction (eq. 1.6). On the other hand, the Eh_{SCE} decreases along the

experiments because the reactional medium becomes more reductive due to the H_2 production and diffusion. Thus, the system with the M1 solution is more reductive than the control solution probably as a consequence of the higher H_2 concentration (Figure 39b, d).

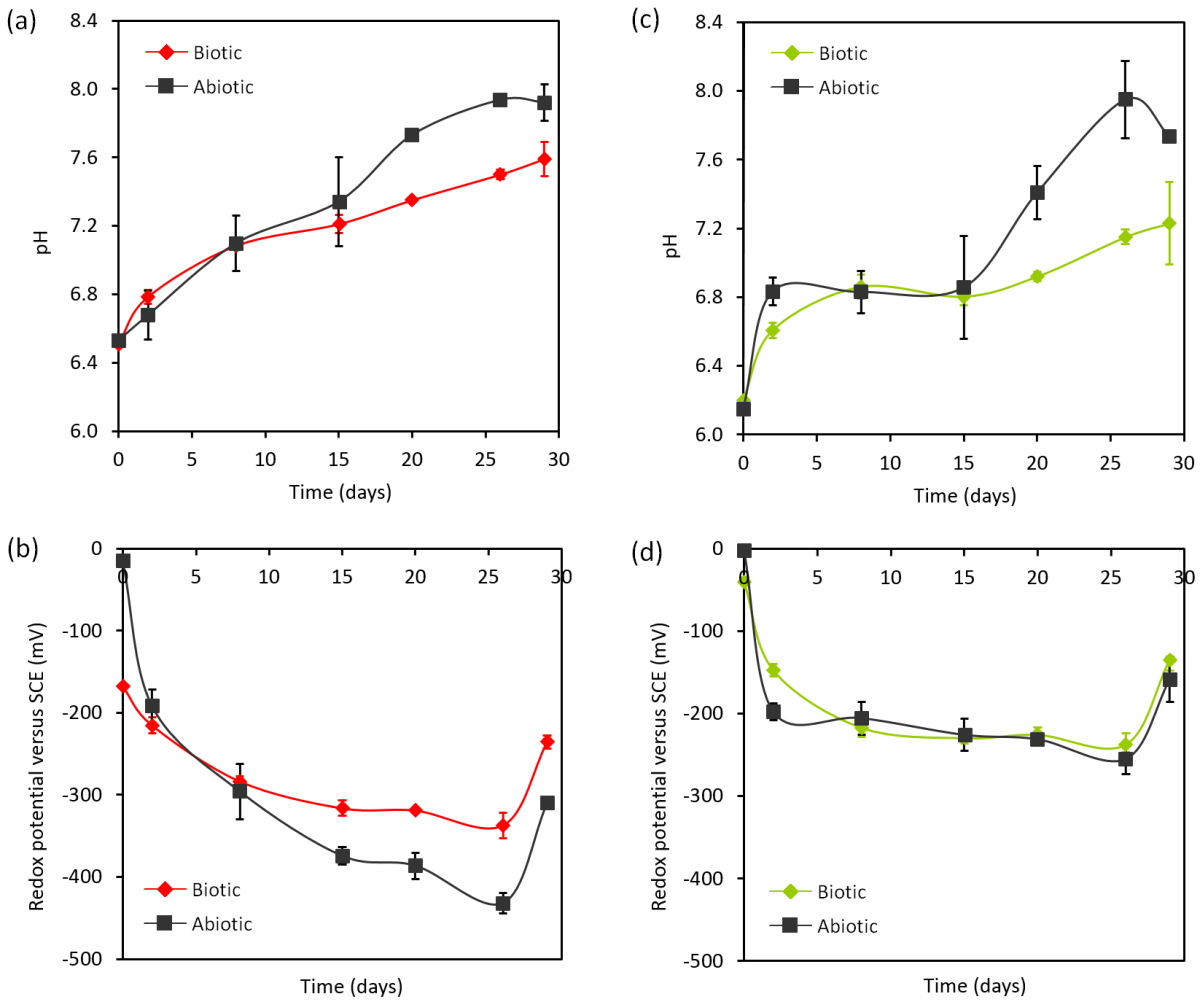

Figure 39: Evolution of pH (a, c) and Eh_{SCE} (b, d) during iron powder corrosion for 1 month of reaction: (a, b) M1 and (c, d) control (Na_2SO_4) solutions. Biotic conditions are indicated by red or green curves and abiotic conditions by black curves. Values are the mean and the standard deviation (n=3).

The bacterial concentration was monitored in the biotic experiments, as shown in Figure 40. The population decreases with time for the M1 and control solutions. Here, again, we can argue the limitation of batch reactor systems which do not allow to continual recycling of nutrients for bacterial growth. Moreover, as previously mentioned in the chapter 4, the experimental solutions (especially the control, Na_2SO_4) are poor in nutriments compared to other growth media and there is no organic carbon source for bacterial growth, which can lead to a decrease in the bacterial population.

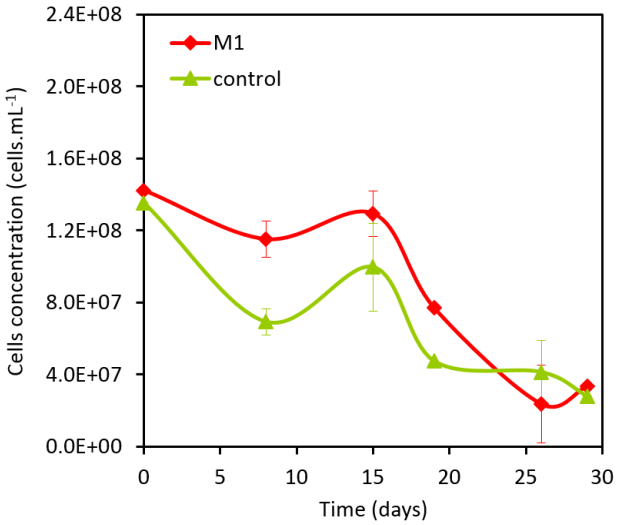

Figure 40: Evolution of bacterial cells in the experiments with iron powder samples. M1 solution is indicated by red curve and control (Na_2SO_4) solution by green curve. Values are the mean and the standard deviation (n=3).

5.1.2 Solid corrosion products

Figure 41 shows diffractograms of the iron powder samples at the end of each experiment.

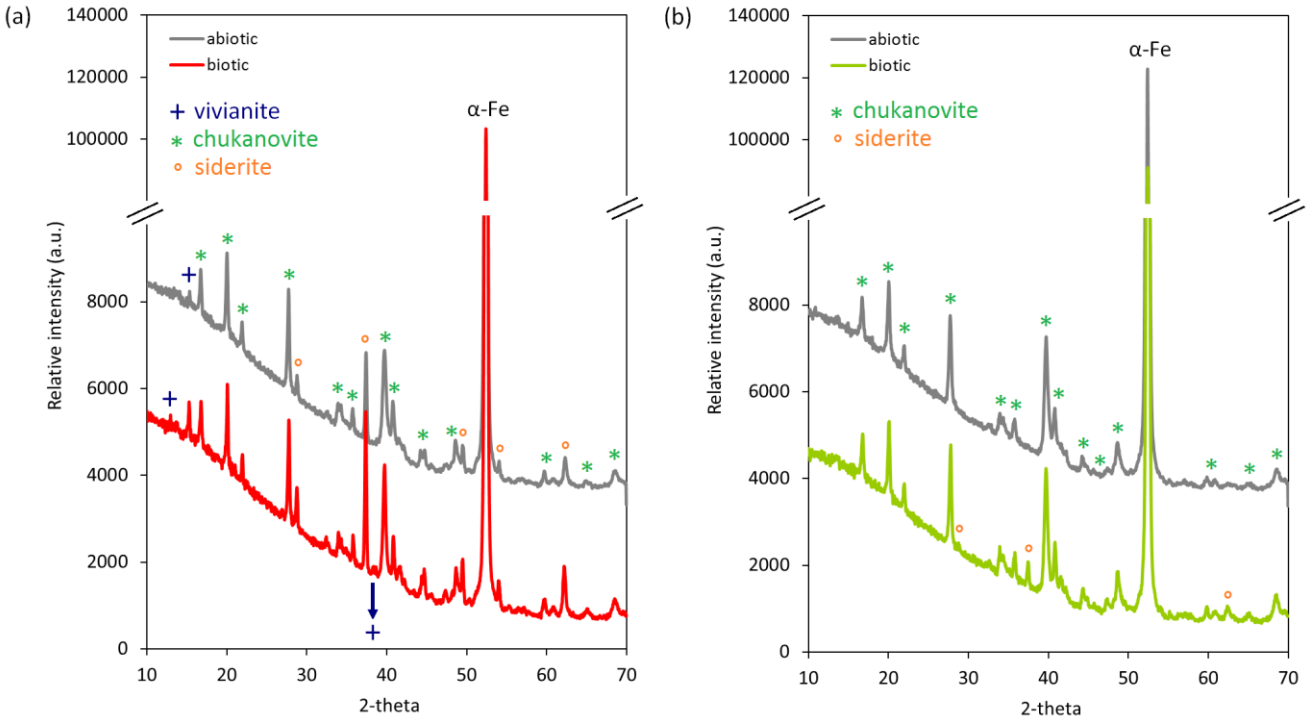

Figure 41: XRD patterns of the corrosion products formed in the M1 (a) and control (Na_2SO_4) (b) solutions for 1 month of reaction in the presence of iron powder sample. Biotic conditions are indicated by red or green diffractograms and abiotic conditions by grey diffractograms.

XRD analysis reveals that vivianite, siderite and chukanovite are the main corrosion products for abiotic and biotic conditions in the M1 solution (Figure 41a). Formation of vivianite is also supported by the decrease in the phosphate concentration at the end of the experiments, as shown in Figure 38. In the control solution, chukanovite is observed for abiotic and biotic conditions, while siderite is only identified in the biotic experiments (Figure 41b).

Figure 42 shows FTIR analysis of the solid corrosion products. Two shoulder bands at 1520 cm^{-1} and 1360 cm^{-1} are evidenced for both M1 and control solutions, which are assigned to carbonate C–O stretching mode in the chukanovite. In addition, the sharp band at 835 cm^{-1} can be assigned to CO_3^{-2} out-of-plane bending mode and the band at 955 cm^{-1} to O-H bending mode. Siderite was identified for the M1 solution by a weak shoulder band at 866 cm^{-1} assigned to CO_3^{-2} group. Bands at 1055 cm^{-1} and 775 cm^{-1} can be attributed to CO_3^{-2} groups weakly bound to the solid corrosion products. Siderite was not observed in the control solution probably due to its low abundance in the samples (XRD peaks in low intensity), and that could also be the reason why vivianite was not detected in the experiments with M1 solution (typical bands for vivianite are found at 1040 cm^{-1} and 990 cm^{-1} due to the P-O stretching mode).

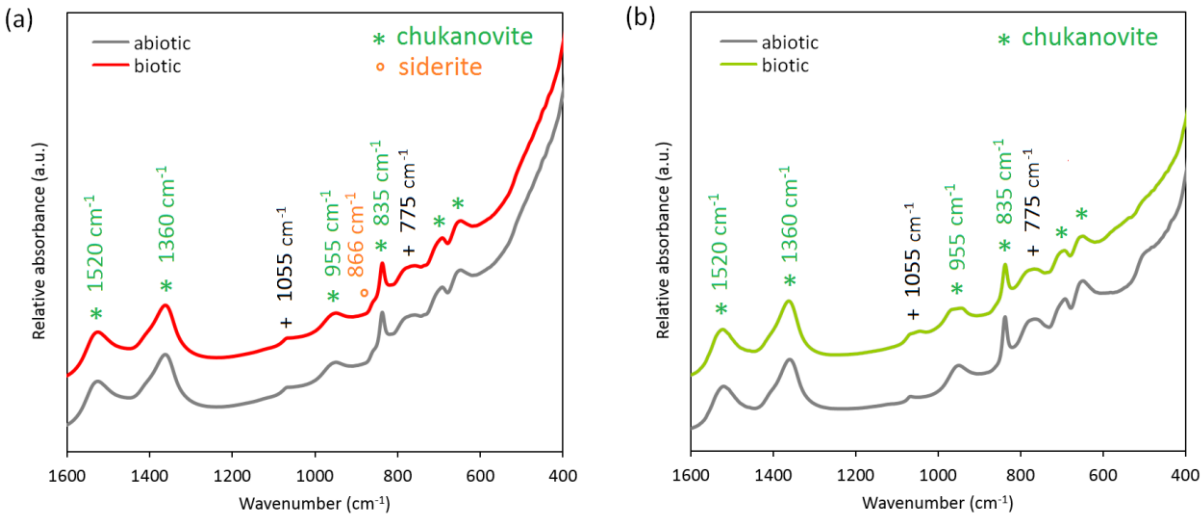

Figure 42: FTIR spectra of the corrosion products formed in the M1 (a) and control (Na_2SO_4) (b) solutions for 1 month of reaction in the presence of iron powder sample. Biotic conditions are indicated by red or green spectra and abiotic conditions by grey spectra.

Figure 43 and Figure 44 show SEM analysis of the solid corrosion products formed in the M1 and control solutions, respectively. On the one hand, the presence of siderite was revealed by structures with rhombohedral shape (indicated by 2 in the Figure 43 and Figure 44), with a chemical composition determined by EDX of 53 wt % Fe and 46 wt % O (C could not be quantified by this technique). On the other hand, chukanovite was observed as

acicular aggregates (indicated by 3 in the Figure 43 and Figure 44) with around 63 wt % Fe and 37 wt % O. The formation of vivianite was confirmed by SEM/EDX analysis in the M1 solution in both abiotic and biotic conditions (Figure 43b, d). This mineral phase appears as blade shaped crystals which are larger than siderite and chukanovite.

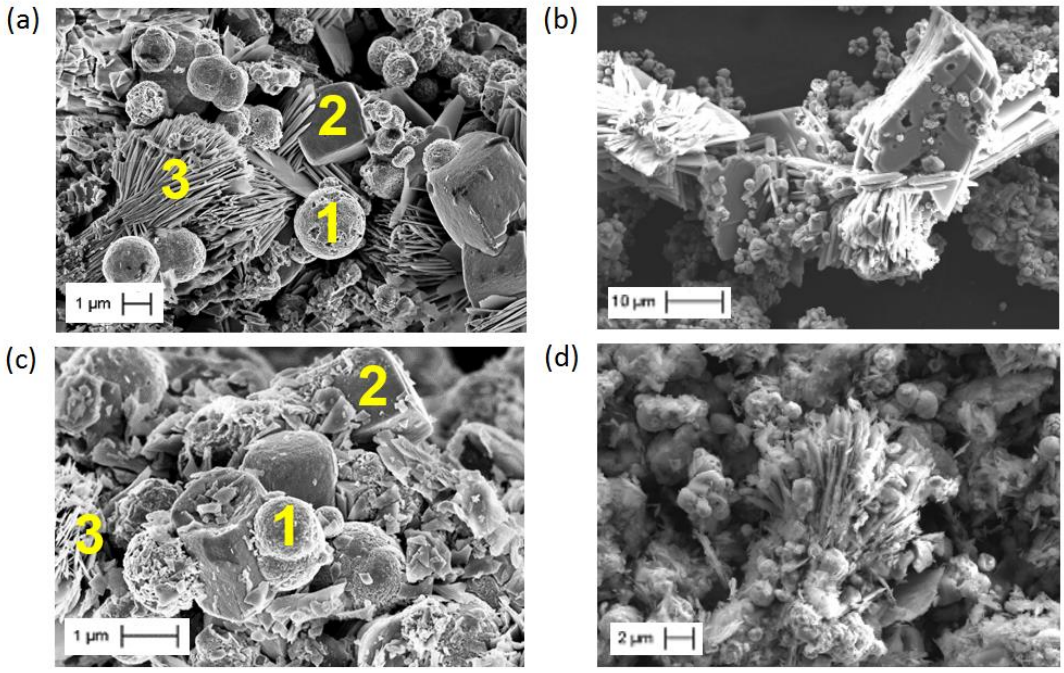

Figure 43: SEM micrographs of the corrosion products formed in the M1 solution for 1 month of reaction in the presence of iron powder sample: (a, b) biotic; and (c, d) abiotic conditions. (1) iron powder; (2) siderite; (3) chukanovite; and (b, d) vivianite.

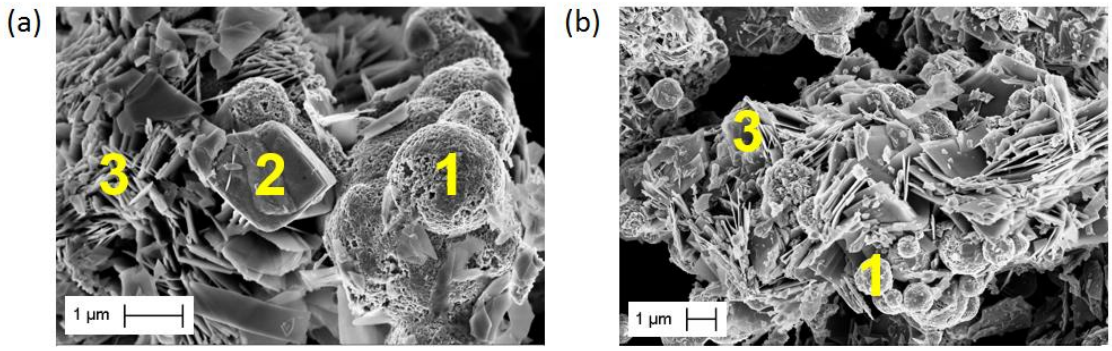

Figure 44: SEM micrographs of the corrosion products formed in the control (Na_2SO_4) solution for 1 month of reaction in the presence of iron powder sample: (a) biotic; and (b) abiotic conditions. (1) iron powder; (2) siderite; and (3) chukanovite.

It is noteworthy that magnetite was not identified as a corrosion product in the experiments with iron powder over 1 month of reaction. We can discuss that the reaction time may not have been sufficient for the formation of this mineral phase. As instance, Combarieu *et al.* (2007) carried out laboratory experiments with iron powder in contact

with COx argillite at 90°C and under anoxic conditions, yet they could not observe magnetite in their experiments before 3 months of reaction. Another hypothesis is that the magnetite layer formed in our experiments might be very small (10-100 nm) and may go undetected under several layers of external corrosion products (e.g. siderite, chukanovite, vivianite) (Michelin *et al.*, 2013).

5.2 Carbon steel coupons

The experiments with carbon steel coupons were performed over a period of 1 and 5 months. At the end of each experiment, the samples were analyzed by XRD, RM and SEM/EDX in order to identify the corrosion products formed on the steel surface. Corrosion rates were obtained by weight loss analysis and H_2 concentration measurements for comparison purposes. Note that from the experiments performed in triplicate, one of the coupons was used in the surface analysis and the other two coupons in the weight loss analysis.

5.2.1 Evolution of Fe and H_2

Figure 45 shows the evolution of dissolved Fe and H_2 produced by carbon steel corrosion over 1 month (Figure 45a, b) and 5 months (Figure 45c, d) in the M1 and control solutions. The initial bacterial concentration was 10^8 cells.mL^{-1} and 10^7 cells.mL^{-1} for the biotic experiments of 1 and 5 months, respectively, and 0 cells.mL^{-1} for the abiotic experiments.

For 1 month of reaction in abiotic conditions, equimolar amounts of dissolved Fe ($[Fe]_{aq}$) and H_2 are produced by corrosion in the M1 (0.3 mM at 29 days) and control (0.1 mM at 29 days) solutions. This behavior is in good agreement with the stoichiometry of aqueous corrosion reaction under anoxic conditions (eq. 1.6). The bacterial impact on the corrosion is observed after 2 days, in which larger amounts of Fe and H_2 are produced compared to abiotic conditions. As shown in Figure 45a, a decrease in the $[Fe]_{aq}$ is observed after 15 days in biotic conditions for the M1 solution (0.4 mM to 0.3 mM). In the same conditions, the H_2 concentration remains much lower when compared to $[Fe]_{aq}$. This emphasizes the use of H_2 by bacteria for redox reactions. In contrast, a H_2 consumption was not observed in the control solution (Figure 45b), in which the amounts of Fe and H_2 remain similar until the end of the experiment. Such observation can suggest that bacteria are less active in the control solution due to the low H_2 amounts available in the system — as instance, a H_2 consumption could be observed with iron powder samples where high H_2

amounts are produced by corrosion reaction (Figure 37), which results in a higher bacterial activity and consequently H_2 consumption. This corroborates the results shown in the chapters 3 and 4, demonstrating that the bacterial activity is dependent on the available H_2 concentration.

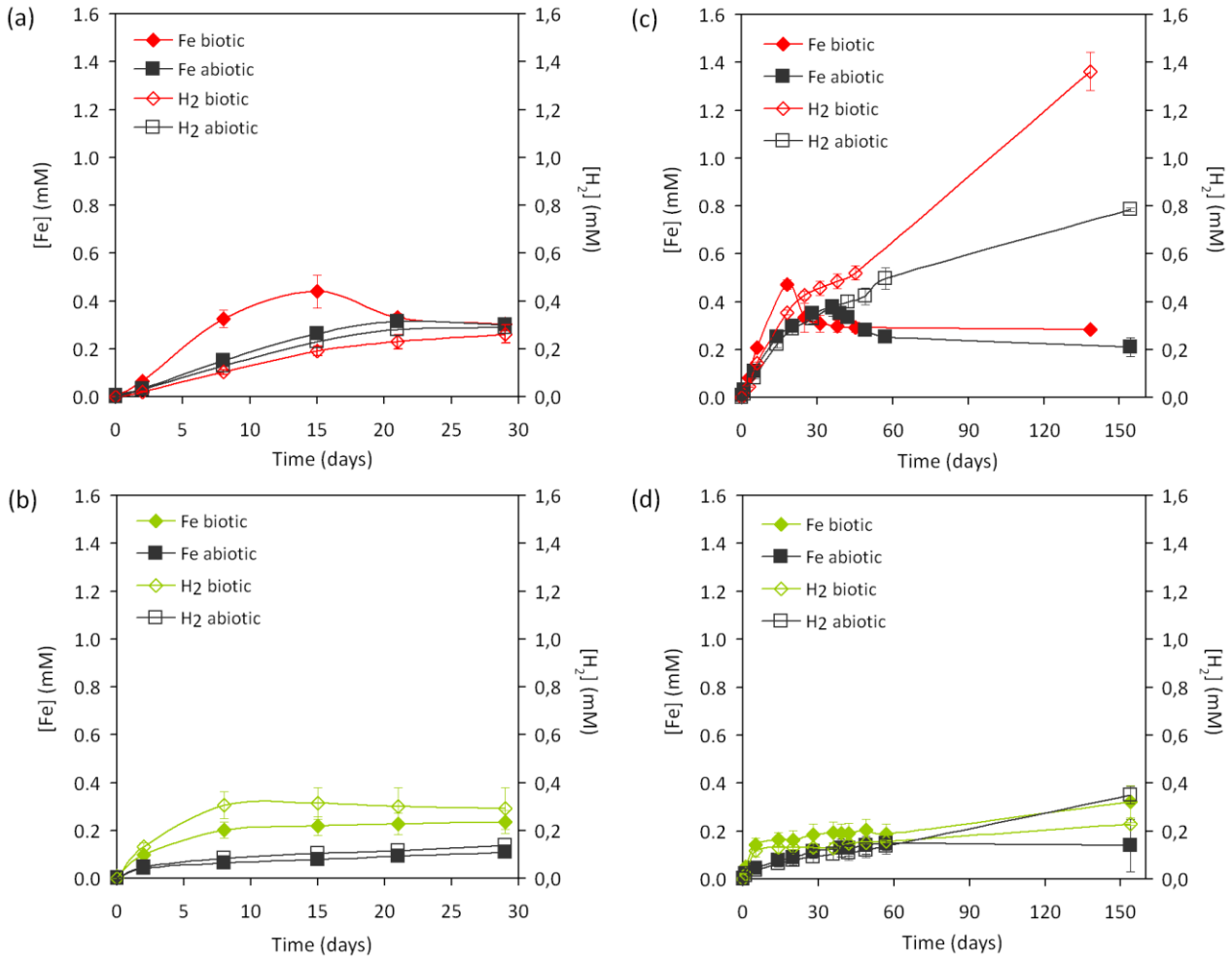

Figure 45: Production of dissolved Fe and H_2 by carbon steel corrosion: (a) M1 and (b) control (Na_2SO_4) solutions for 1 month of reaction; (c) M1 and (d) control solutions for 5 months of reaction. Biotic conditions are indicated by red or green curves and abiotic conditions by black curves. Values are the mean and the standard deviation (n=3), except for abiotic conditions for 1 month (n=1).

Regarding 5 months of reaction, the evolution of Fe and H_2 during the first 30 days has a similar behavior of the 1-month experiments. Figure 45(c) shows for the M1 solution a decrease in the net production of H_2 in abiotic conditions (0.8 mM at 154 days) when compared to biotic conditions (1.4 mM at 138 days), suggesting that corrosion kinetics is slowed down with time due to a passivation process. The $[Fe]_{aq}$ increases in both biotic and abiotic conditions for the M1 solution, and then decreases followed by stabilization (the same was observed after 15 days in biotic conditions for 1-month experiments). A decrease in the $[Fe]_{aq}$ is attributed to the formation of solid corrosion products. The lagging period

before precipitation of solid products is shorter in biotic than abiotic conditions: 18 days against 36 days. In contrast, no $[Fe]_{aq}$ decrease is observed in the control solution during 1 and 5 months (Figure 45b, d) probably due to the low amount of Fe released by corrosion reaction, and resulting undersaturation conditions with respect to secondary mineral phases.

Comparing the samples iron powder and carbon steel coupon (Figure 37 and Figure 45, respectively), we observe that the corrosion extent is significantly lower with steel coupons due to the difference in reactive surface. Again, it was shown in the experiments with steel coupons that the corrosion extent changes as a function of the reactional medium (M1 and control), as for the iron powder samples. However, corrosion in the M1 solution is significantly accelerated in biotic conditions and, despite H_2 consumption by bacteria, larger amounts of dissolved Fe and H_2 are measured in comparison with abiotic conditions.

In addition to the Fe and H_2 concentrations, other major elements were measured in solution at the beginning (T_i= 0 day) and the end (T_f= 30th day) of the reaction in the 1-month experiments (Figure 46). As for the iron powder experiments, the dissolved concentration of most elements remains constant with no significant difference between biotic and abiotic conditions. Again, only phosphate concentration decreases at the end of the reactions (0.8 mM to 0.1 mM), indicating incorporation into solid corrosion products (e.g. vivianite) formed in the M1 solution.

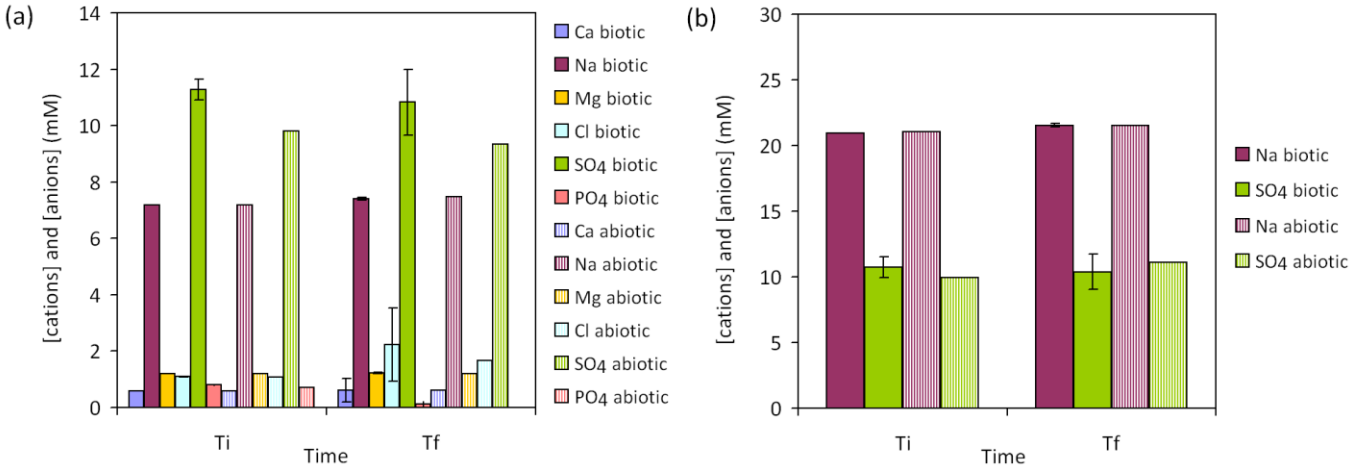

Figure 46: Evolution of major cations and anions in solution during carbon steel corrosion: (a) M1 and (b) control (Na_2SO_4) solutions for 1 month of reaction. Biotic conditions are indicated by solid columns and abiotic conditions by dashed columns. Values are the mean and the standard deviation (n=3), except for abiotic conditions (n=1).

Furthermore, as shown in Figure 47, pH measurements indicate that pH increases slightly during corrosion reaction with no significant difference between abiotic and biotic conditions: final pH around 6.6 in the M1 solution and 6.3 in the control solution.

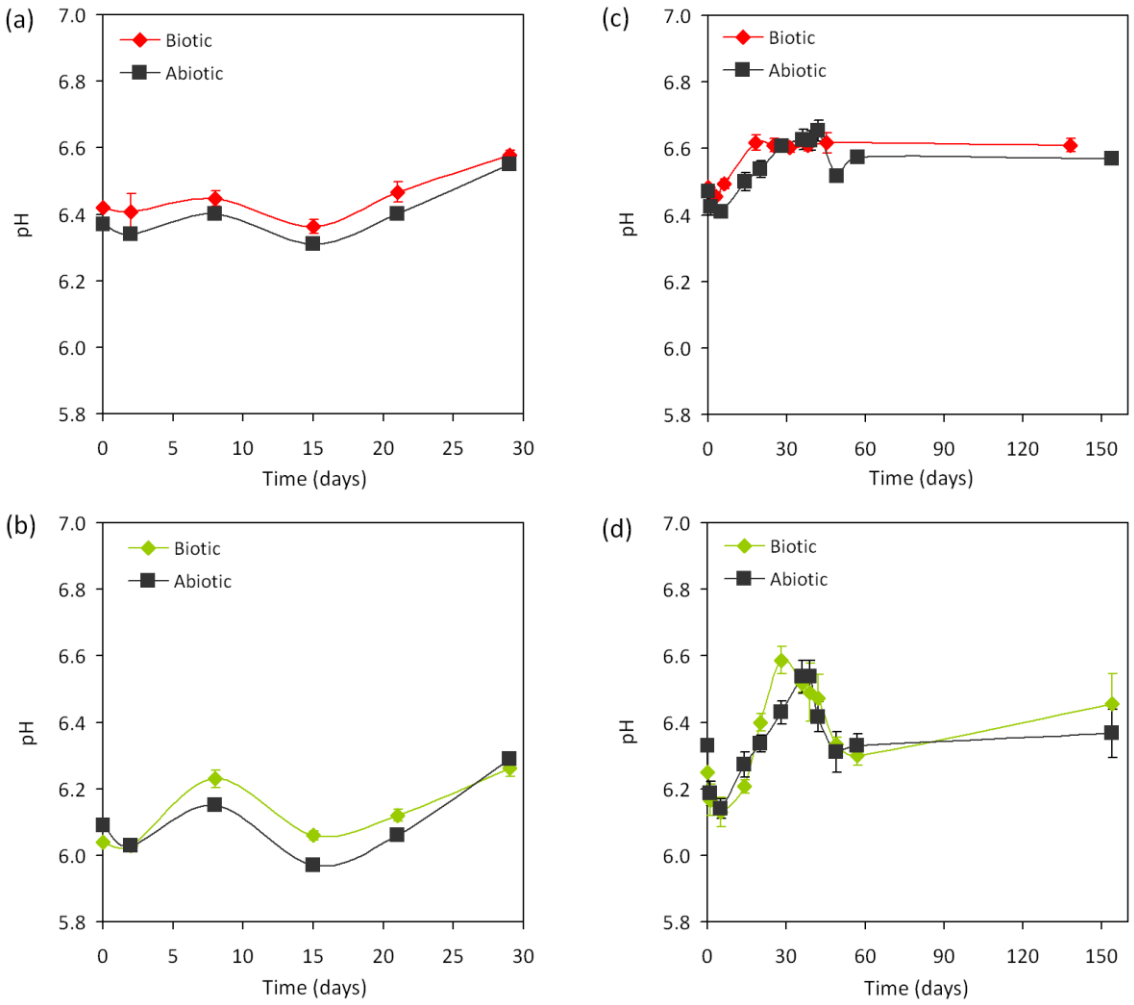

Figure 47: pH evolution during carbon steel corrosion: (a) M1 and (b) control (Na_2SO_4) solutions for 1 month of reaction; (c) M1 and (d) control solutions for 5 months of reaction. Biotic conditions are indicated by red or green curves and abiotic conditions by black curves. Values are the mean and the standard deviation (n=3), except for abiotic conditions for 1 month (n=1).

Figure 48 shows the monitoring of bacterial concentration for the 1-month experiments. Again, a decrease was observed with time probably due to the same reasons discussed previously. However, we cannot exclude that formation of biofilms on the metal surface also leads to a decrease in the number of planktonic cells. Comparing iron powder and carbon steel coupon samples (Figure 40 and Figure 48, respectively), it is observed a higher decrease in the bacterial concentration with iron powder due to the difference in the reactive surface.

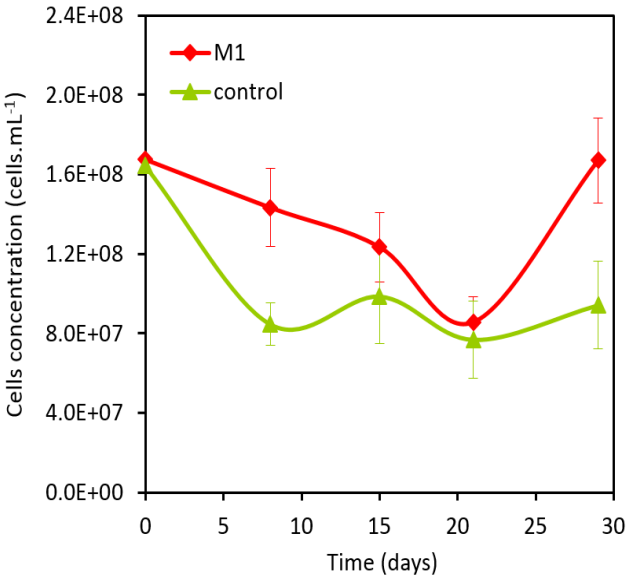

Figure 48: Evolution of bacterial cells in the 1-month experiments with carbon steel samples. M1 solution is indicated by red curve and control (Na_2SO_4) solution by green curve. Values are the mean and the standard deviation (n=3).

5.2.2 Solid corrosion products

All experiments with the M1 solution resulted in the formation of an orange precipitate in solution (in small amounts) for abiotic and biotic conditions over time. The precipitate was characterized as lepidocrocite (γ-FeOOH), appearing as thin plates with "flowery" structures in the SEM analysis (Figure 49) and with O and Fe as the main composition as demonstrated by EDX analysis.

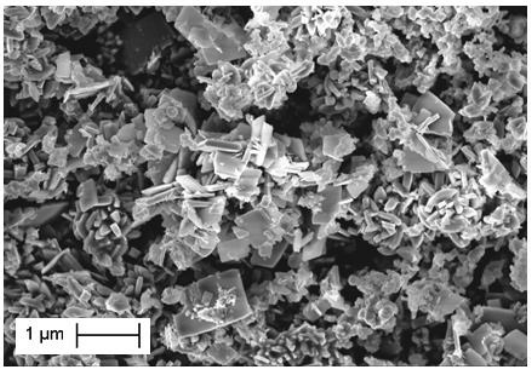

Figure 49: SEM micrograph of the precipitate formed in the M1 solution in abiotic and biotic conditions.

The same precipitate was not formed in the control solution, even after 5 months of reaction. The hypothesis could be raised that the M1 solution contains some oxidizing

species, allowing oxidation of aqueous Fe(II) released by corrosion reaction and posterior precipitation of Fe(III)-containing phases under anaerobic conditions. A test experiment was performed in the same conditions but in the absence of steel coupon sample, so without production of aqueous Fe(II) by corrosion reaction. In this case, the orange precipitate is not observed, corroborating our hypothesis in which the oxidation do not take place in the absence of aqueous Fe(II).

Furthermore, a black layer and a white deposit (over the black layer and noticeably shinier) are progressively formed on the coupon surface in the M1 solution in both abiotic and biotic conditions, indicating reaction between the surface and species in solution, as shown in Figure 50. Almost no alteration is observed macroscopically after 1 and 5 months of reaction in the control medium.

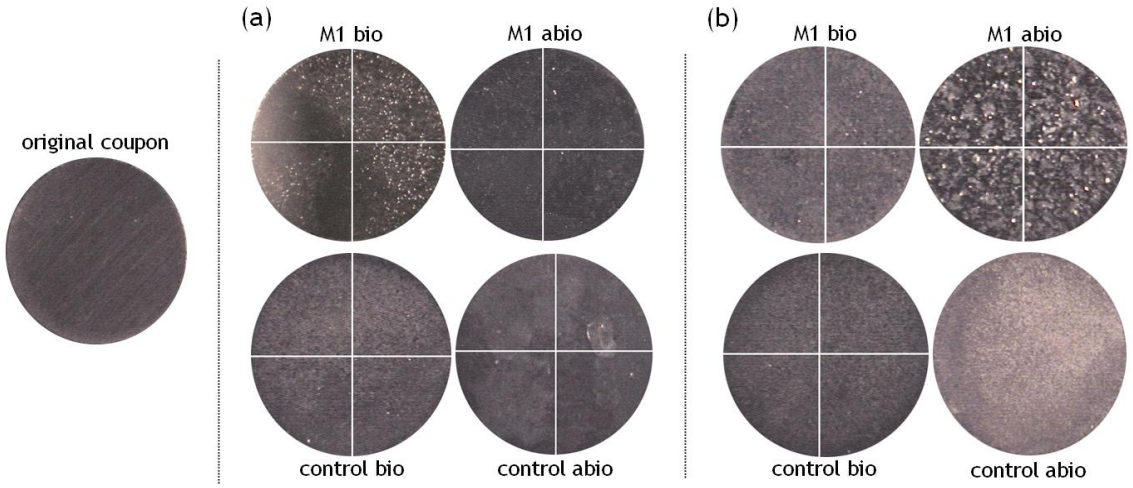

Figure 50: Macroscopic observation of the steel coupons after (a) 1 and (b) 5 months of reaction.

Figure 51 shows diffractograms of the steel surface at the end of each experiment. The formation of vivianite as a corrosion product is observed in the M1 solution in abiotic and biotic conditions after 1 and 5 months of reaction (Figure 51a, c). The intensity of the peak assigned to ferrite ($2\theta = 52^\circ$) decreases significantly over an exposure time of 5 months, suggesting higher mineralization of corrosion products on the metal surface in the M1 medium. Concomitantly, the intensity of the peaks assigned to vivianite (notably at $2\theta = 13^\circ$ and 15°) increases in the presence of bacteria. For the control solution (Figure 51b, d), secondary mineral products were not detected on the steel surface by XRD analysis. The XRD patterns show only the peak assigned to ferrite in abiotic and biotic conditions. We could confirm the absence of solid corrosion products by comparing the samples after reaction with an initial sample of carbon steel (uncorroded coupon). As shown in Figure 52, both diffractograms are very similar corroborating the observed results.

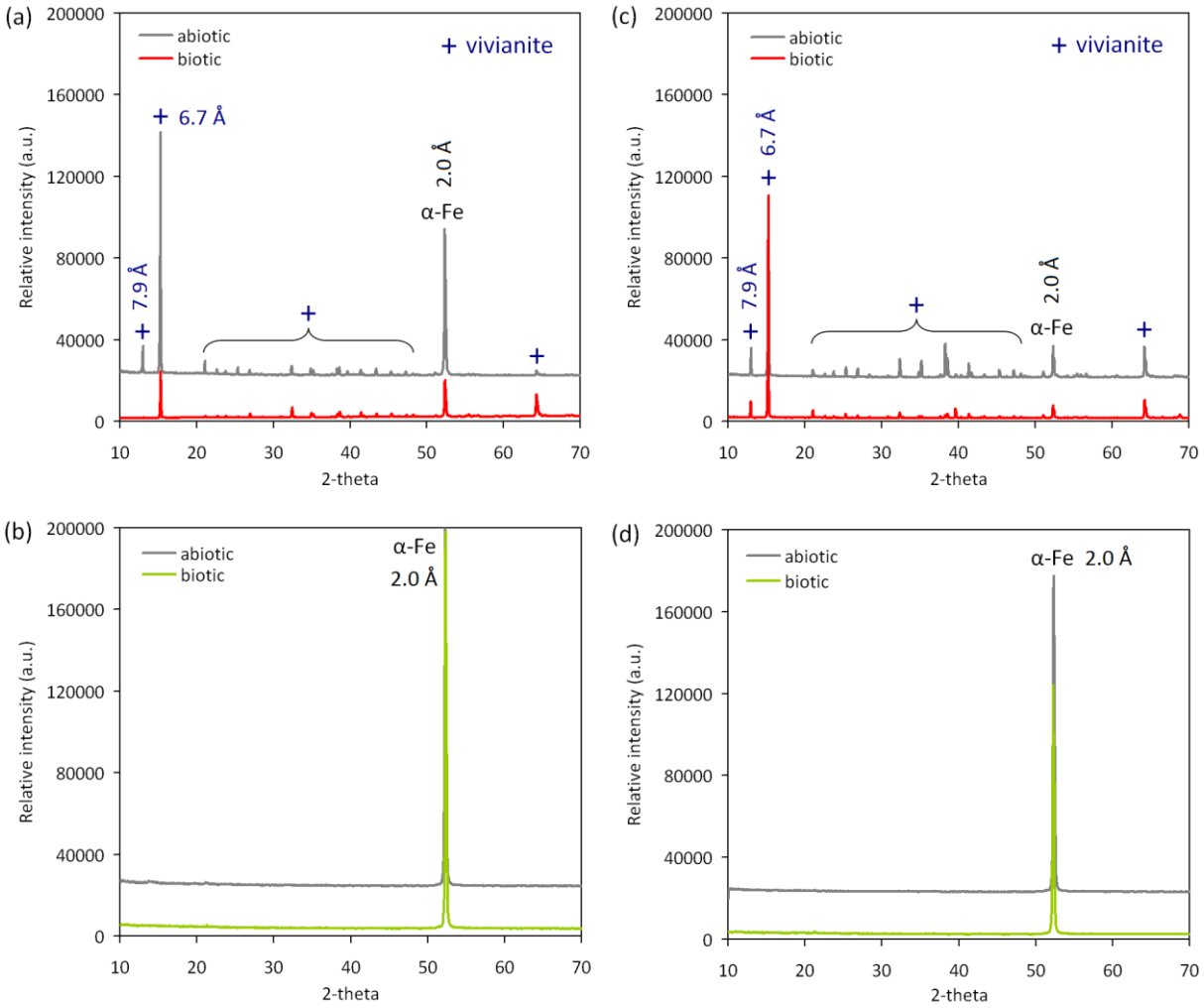

Figure 51: XRD patterns of the corrosion products formed on the carbon steel surface: (a) M1 and (b) control (Na_2SO_4) solutions for 1 month of reaction; (c) M1 and (d) control solutions for 5 months of reaction. Biotic conditions are indicated by red or green diffractograms and abiotic conditions by grey diffractograms.

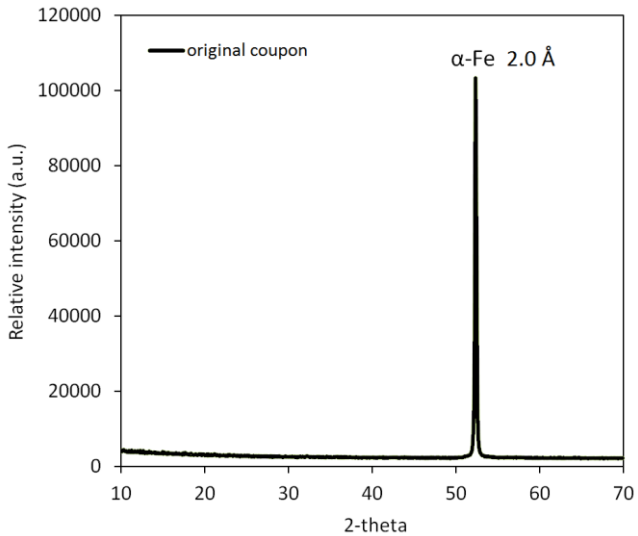

Figure 52: XRD pattern of an initial sample of carbon steel (uncorroded coupon).

Figure 53 shows Raman analysis for the solid corrosion products formed on the steel surface in the M1 solution. The results correspond to the spectral signature of vivianite, confirming the formation of this mineral phase in both abiotic and biotic conditions over exposure time of 1 and 5 months. The intensity of vivianite bands is greater in the presence of bacteria, increasing significantly after 5 months of reaction. This can point out that vivianite formation is favored by bacterial activity with an increase in its abundance with time (Coy, 2013).

Moreover, magnetite could be detected in abiotic conditions after 5 months of reaction (Figure 53b, the inset image highlights the band assigned to magnetite at 670 cm^{-1}). This finding supports the results showed in Figure 45(c), in which the corrosion kinetics decreases in abiotic conditions due to a passivation process (formation of protective corrosion product film). In contrast, in the presence of bacteria, magnetite is no longer observed suggesting that *Shewanella oneidensis* dissolves this corrosion product in order to reduce Fe(III) coupled to H_2 oxidation.

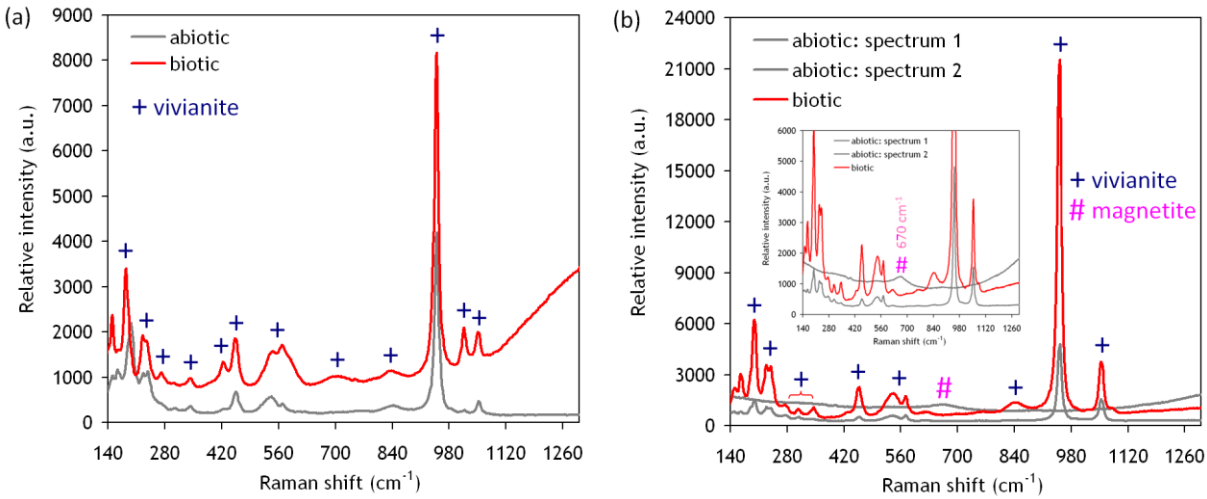

Figure 53: Raman spectra of the corrosion products formed on the carbon steel surface in the M1 solution: (a) 1 month; and (b) 5 months of reaction. Biotic conditions are indicated by red spectra and abiotic conditions by grey spectra.

Figure 54 shows SEM images of the carbon steel surface reacted in the M1 solution. A layer of corrosion product closer to the steel surface and covered by larger deposits is observed for all surfaces (Figure 54a, c, e, g). EDX analysis showed Fe, O and P in the chemical composition for the larger deposits, which is typical to the presence of vivianite. These observations corroborate the XRD and Raman results. Figure 54(b, d, f, h) focus on the layer of corrosion product formed closer to the steel surface. After 1 month of reaction in biotic conditions (Figure 54b), the surface exhibits features of high corrosion. In contrast, in abiotic conditions (Figure 54d), polishing streaks are still visible. EDX analysis

showed in both conditions the presence of Fe and O with trace elements (i.e. Ni, Se), suggesting formation of iron oxides. After 5 months of reaction in biotic conditions (Figure 54f), structures typically attributed to the presence of biofilm are observed, as EPS products appear in a lighter shade at the metal surface. In abiotic conditions (Figure 54h), aggregates with similar morphology to magnetite ("cotton" balls structures) can be noted, and were shown by EDX analysis to contain Fe and O. This observation corroborates the Raman results.

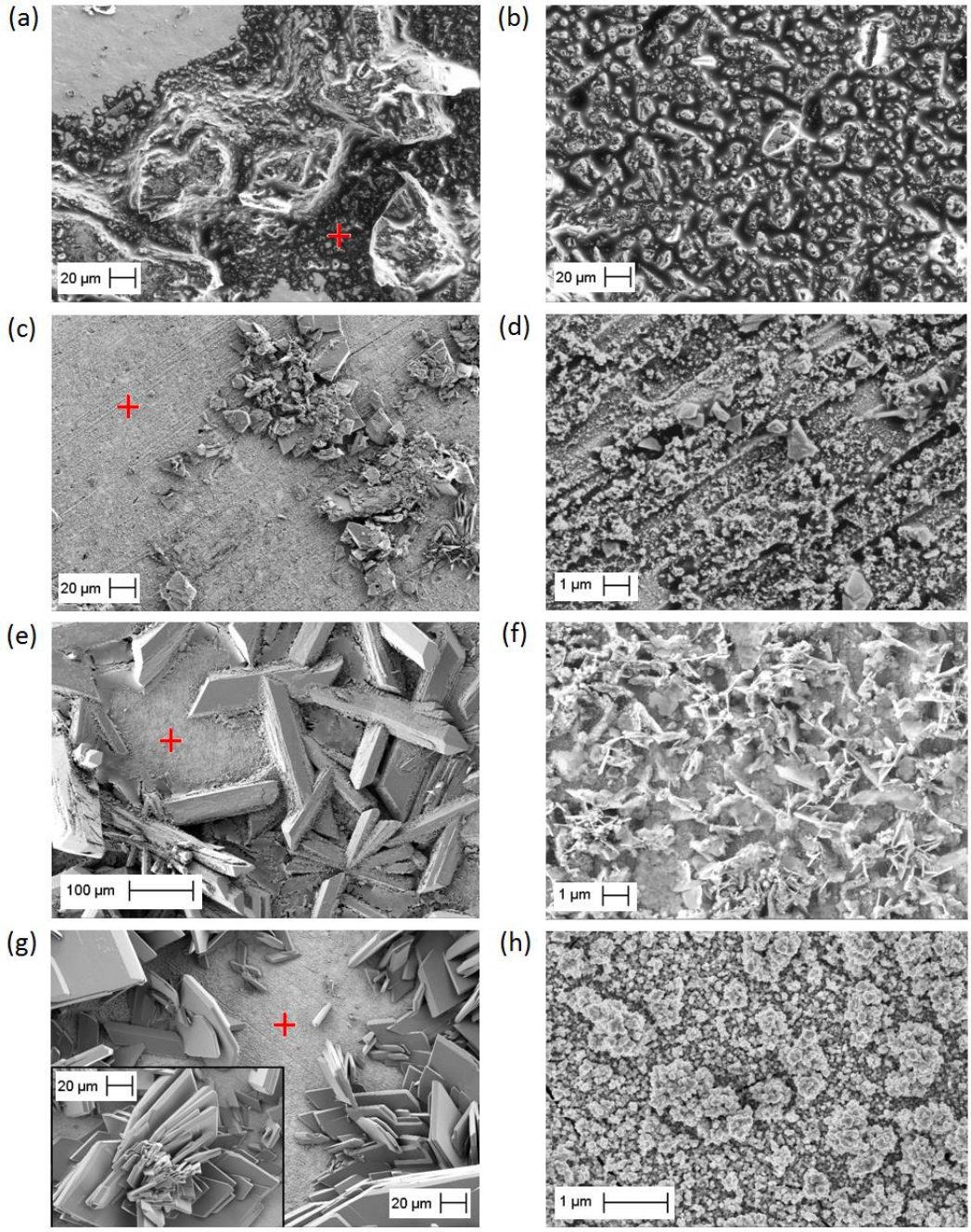

Figure 54: SEM micrographs of the corrosion products formed on the carbon steel surface in the M1 solution: (a-d) 1 month; and (e-h) 5 months of reaction. (a, b, e, f) biotic; and (c, d, g, h) abiotic conditions. All micrographs on the right side correspond to the target areas ("+" symbol) on the left side.

Figure 55 shows SEM analysis of the carbon steel surface reacted in the control solution. Two distinct areas (indicated by 1 and 2 in the Figure 55) are observed for all reactional conditions. For both areas, EDX analysis shows mainly Fe in the chemical composition (e.g. more than 95 wt % for the area 1), suggesting that the steel surface suffers degradation by corrosion but without formation of solid corrosion products. Regular pits of about 14 µm in width could be observed in abiotic conditions after 5 months of reaction (Figure 55d, the inset image). Such distribution of pits over the entire metal surface may be attributed to an increase in the cathodic reaction.

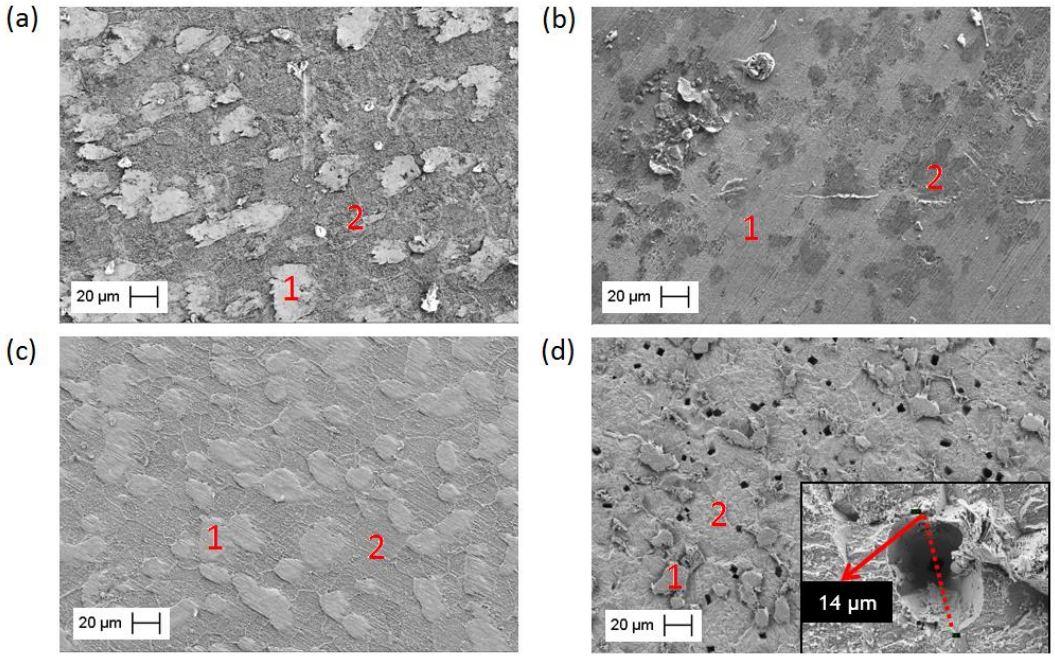

Figure 55: SEM micrographs of the carbon steel surface in the control (Na_2SO_4) solution: (a, b) 1 month; and (c, d) 5 months of reaction. (a, c) biotic; and (b, d) abiotic conditions.

Cross-section analysis was performed for the steel coupons reacted over 5 months (Figure 56). For samples reacted in the M1 solution, Figure 56(a, b) shows that the size of vivianite deposit ranges from 100 µm to 130 µm in height. Moreover, the presence of bacteria seems to influence significantly pitting in the M1 solution, as pits in biotic and abiotic conditions have average depths of 42 µm and 25 µm, respectively. On the other hand, the pits have similar depth in the control solution for abiotic (22 µm) and biotic (27 µm) conditions, showing perhaps a smaller diameter in the presence of bacteria (Figure 56c, d).

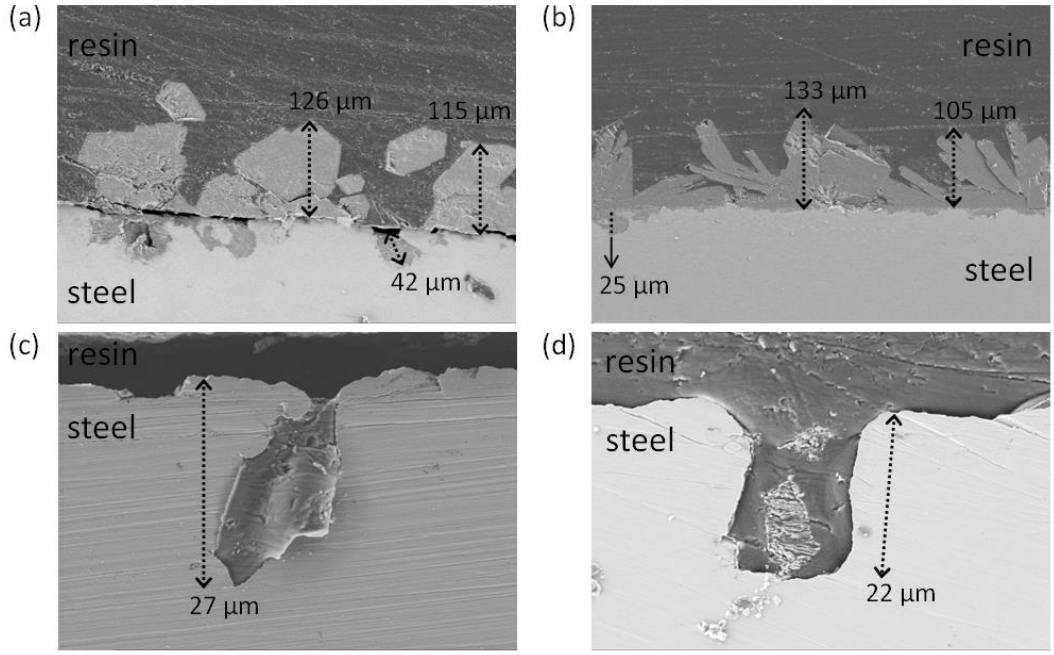

Figure 56: Cross section of the carbon steel coupons reacted 5 months: (a, b) M1; and (c, d) control (Na_2SO_4) solutions. (a, c) biotic; and (b, d) abiotic conditions.

5.2.3 Evolution of corrosion rate

Figure 57 shows the results obtained from weight loss analysis (note that two coupons were used in these analyses). Figure 57(a) illustrates the evolution of weight loss (WL) and corrosion rate (CR) and Figure 57(b) the amount of corrosion products attached to the steel surface.

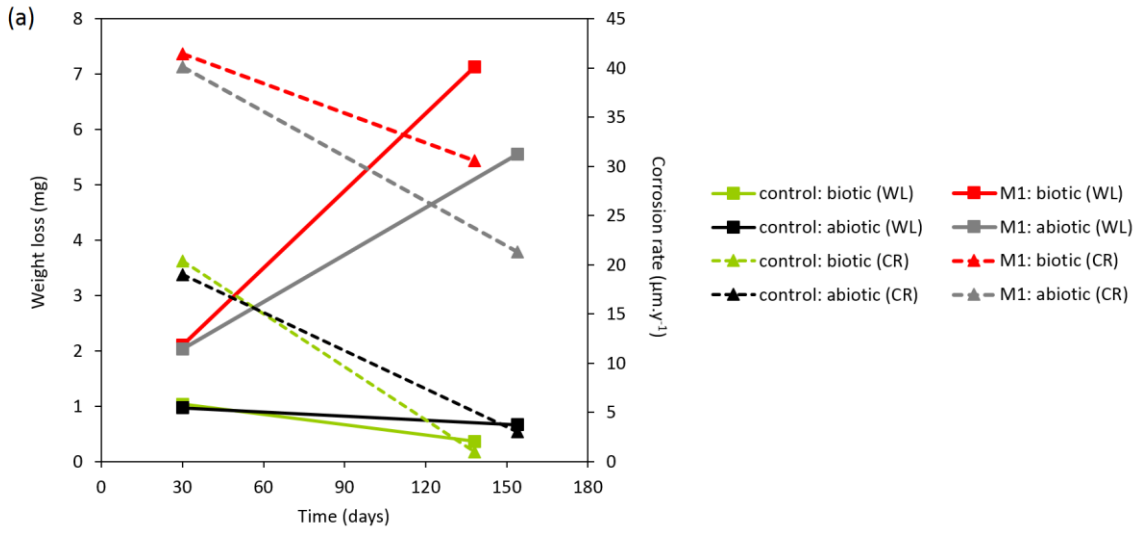

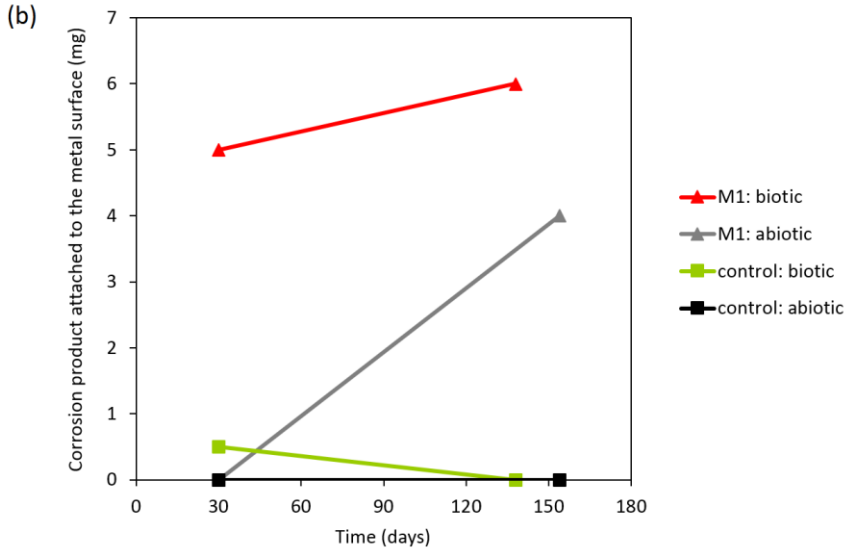

Figure 57: Results from weight loss analysis: (a) weight loss (WL) and corrosion rate (CR); and (b) amount of corrosion product attached to the steel surface. Biotic conditions are indicated by red or green lines and abiotic conditions by black or grey lines.

Both weight loss and amount of corrosion products increase with time for the M1 solution, contrary to the control solution for which constant values were observed. However, the corrosion rate decreases with time for both M1 and control solutions and for abiotic and biotic conditions. No corrosion products attached to the steel surface could be detected in the control medium even after 5 months of reaction (Figure 57b), corroborating the previously results with respect to the non-formation of secondary mineral phases in these conditions.

In this study, corrosion rates obtained by weight loss and H_2 concentration measurements were compared in order to evaluate the correspondence between both techniques. We can find in the literature a number of studies in which corrosion rates are measured by both weight loss and from the rate of H_2 generation (Smart *et al.*, 2001; Smart *et al.*, 2002a; Smart *et al.*, 2002b).

For calculations using H_2, two scenarios were assumed in our study: *(1)* taking into account no formation of magnetite as corrosion product, according to the equation 5.1; and *(2)* taking into account formation of magnetite as corrosion product, according to the equation 5.2.

$$Fe + 2\ H_2O \rightarrow Fe(OH)_2 + H_2 \qquad \textbf{(5.1)}$$

$$3\ Fe + 4\ H_2O \rightarrow Fe_3O_4 + 4\ H_2 \qquad \textbf{(5.2)}$$

In this way, corrosion rates in the 1 month-experiments were estimated considering the scenario (1), and in the 5 months-experiments considering the scenario (2) once the characterization of solid corrosion products pointed out magnetite formation.

Table 10 summarizes the results of the corrosion rates obtained from the weight loss and H_2 concentration measurements. The thickness loss was estimated from the weight loss analysis.

Table 10: Time-averaged corrosion rates obtained from weight loss and H_2 concentration measurements.

Exposure time (month)	Solution	Condition	Thickness loss (µm)	Weight loss ($\mu m.y^{-1}$)	$[H_2]$ without Fe_3O_4 ($\mu m.y^{-1}$)	$[H_2]$ with Fe_3O_4 ($\mu m.y^{-1}$)
0-1	M1	biotic	3 ± 2	41 ± 2	43 ± 7	
	M1	abiotic	3 ± 2	40 ± 2	87*	
	control	biotic	2 ± 2	21 ± 2	37 ± 9	
	control	abiotic	2 ± 2	19 ± 2	20*	
0-5	M1	biotic	12 ± 2	31 ± 2		32 ± 2
	M1	abiotic	9 ± 2	22 ± 2		16 ± 3
	control	biotic	0.4 ± 2	1 ± 2		4 ± 1
	control	abiotic	1 ± 2	3 ± 2		5 ± 2

* value from one reactor (1-month experiments were not performed in triplicate for abiotic conditions); the other values considering $[H_2]$ are the mean and the standard deviation (n=2).

According to Table 10, the time-averaged corrosion rates estimated from both techniques are comparable for short-term experiments, except for the experiment in abiotic condition in the M1 solution at 1 month, in which the value considering the H_2 concentration was much higher compared to weight loss result.

In all conditions, the rate is always high in the M1 solution, confirming that corrosion extent is dependent on the reactional medium. With respect to the control solution, there is no significant difference between abiotic and biotic conditions at 1 and 5 months of reaction, which emphasizes our previous results (e.g. evolution of Fe and H_2, pits depth). With respect to the M1 solution, the bacterial impact is significant at 5 months of reaction, as the corrosion rate is enhanced by a factor of almost 2 compared to abiotic conditions. This endorses that the mechanism likely to influence the corrosion rate is the bioreduction of Fe(III) from magnetite coupled to the H_2 oxidation.

Figure 58 shows the instantaneous corrosion rates estimated from H_2 concentration measurements in the 5-months experiments. It was considered the scenario (1) for the first 30 days and the scenario (2) for the last 124 days of reaction. It is shown a parabolic decrease in the corrosion rate with time, corroborating the data from literature in that

short-term corrosion rate is higher than the long-term one. At longer times, the corrosion rate seems to reach a constant value (< 10 µm.y^{-1} at least in the case where magnetite is not destabilized by bacterial activity).

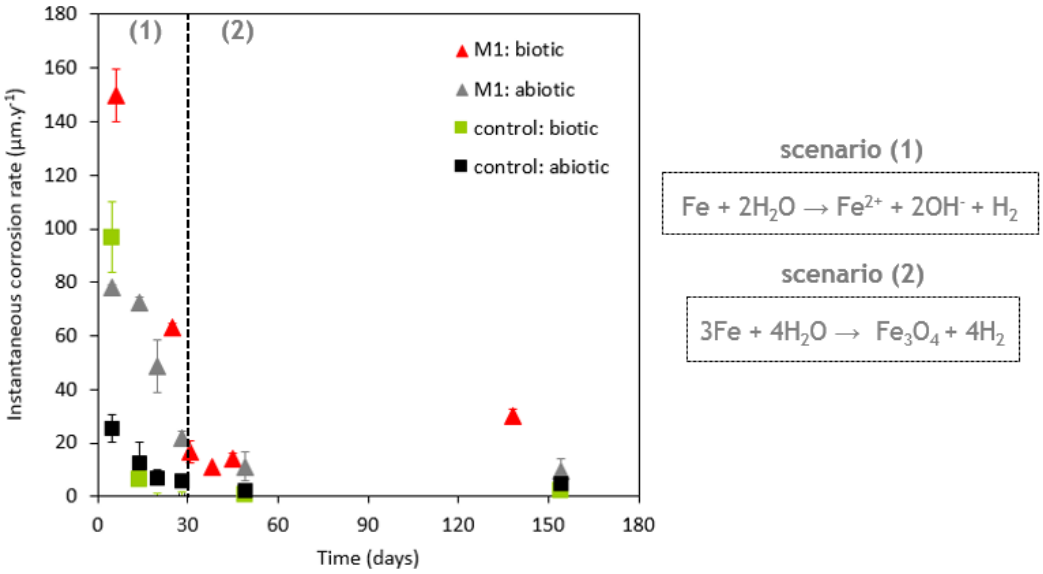

Figure 58: Instantaneous corrosion rates estimated from H_2 concentration measurements in the 5-months experiments: (▲) M1 and (■) control (Na_2SO_4) solutions. Biotic conditions are indicated by red or green symbols and abiotic conditions by black or grey symbols. Values are the mean and the standard deviation (n=2).

5.3 Partial conclusions

Our results pointed out that the reactional medium is an important parameter to be considered for the assessment of corrosion processes. For all metallic samples (carbon steel coupon and iron powder) the corrosion extent was much higher in the M1 solution than in the control (Na_2SO_4) solution for both abiotic and biotic conditions.

The impact of bacterial activity on the corrosion process was clearly evidenced in the M1 solution and carbon steel samples at 5 months of reaction. Magnetite was formed within this time period in abiotic conditions, while in the presence of bacteria this mineral phase was no longer identified. It corroborates the mechanism of bacterial-induced corrosion described in the literature for IRB species: a destabilization/dissolution of passivating oxide layers by structural Fe(III) reduction coupled, in this case, to H_2 oxidation. This depassivation process resulted in a higher corrosion rate (the rate is enhanced by a factor of almost 2 compared to abiotic conditions) (Kerber-Schütz *et al.*, 2013b).

The solid corrosion products were different according to the reactional medium and metallic sample. Magnetite (over 5 months) and vivianite (over 1 and 5 months) were the main mineral phases identified on carbon steel in the M1 solution. In contrast, formation of solid corrosion products could not be observed for the control solution. Vivianite, siderite and chukanovite were the mineral phases identified on iron powder in the M1 solution over the time period of 1 month. In the control solution, siderite and chukanovite were identified. All these mineral phases are typical corrosion products of anaerobic corrosion (Saheb *et al.*, 2008; Schlegel *et al.*, 2010). Regarding the vivianite formation, it is noteworthy that some studies have pointed out that IRB can inhibit corrosion by formation of a protective vivianite layer. However, the same behavior was not observed in our experiments maybe because vivianite was formed as bulk crystals (and not as a layer), covering in a non-homogenous manner the metallic surface. The presence of vivianite crystals can lead to an increase in the cathodic reaction which could favor the formation of deep pits on the metallic surface.

Furthermore, the H_2 availability in the reactional system seems to influence the bacterial activity. This was obvious for the control solution, in which H_2 consumption by bacteria was only observed in the presence of iron powder and not with carbon steel coupon. It means that bacteria are more active when high H_2 amounts are available; as instance, siderite formation as corrosion product was only favored in the presence of bacteria in the experiments with iron powder. These findings corroborate the results discussed in the chapter 4, in which the extent of Fe(III) reduction in magnetite was enhanced in the presence of bacteria when the H_2 concentration was increased.

CHAPTER 6: CONCLUSIONS AND PERSPECTIVES

The survival capability and adaptation of microorganisms is remarkable even in the extreme conditions that will prevail during the lifetime of nuclear waste repository. The impact of microbial activities therefore needs to be further investigated in order to determine if biological parameters should be integrated in safety assessments of geological disposal. Moreover, it is widely accepted that microorganisms can affect the corrosion process due to their influence (directly or indirectly) on the chemical and physical characteristics at the metal/environment interface.

In this context, the main objective of the present study was to evaluate the impact of hydrogenotrophic and IRB activities on anoxic corrosion process. It was assumed that the redox couple Fe(III)/H_2 (electron acceptor/electron donor) is an important driver for microbial activities potentially affecting the corrosion rate by destabilizing the passive layer (magnetite).

Our scientific strategy consisted of laboratory experiments monitored over short periods of time (1 and 5 months) by means of geochemical indicators, such as the concentration of dissolved Fe and gaseous H_2, and the nature of solid products at the end of the experiments. Two experimental solutions differing in chemical composition were adopted: *(i)* a minimal medium (called as M1 solution) commonly used to cultivate IRB species, and *(ii)* a simplified medium (called as control solution). *Shewanella oneidensis* strain MR-1 was chosen as model organism for studying dissimilatory processes in the presence of H_2 as electron donor. The results obtained in this study is divided into two main experimental approaches: *(i)* experiments with H_2 and magnetite aiming at verifying if bacteria can use H_2 to reduce structural Fe(III); and *(ii)* experiments with metallic iron samples (iron powder or carbon steel coupon) aiming at evaluating the impact of microbial activities on the anoxic corrosion process.

Concerning the first experimental approach, the results pointed out a chemical effect on the dissolution of magnetite in addition to the biological effect. Low amounts of aqueous Fe(II) were measured in abiotic conditions as a result of the chemical reduction by H_2 of Fe(III) released by magnetite (a slight decrease in the H_2 concentration was indeed observed in these experiments).

However, in spite of the chemical effect, the impact of the bacterial activity was still demonstrated in our experiments. The results clearly evidenced that magnetite is destabilized in the presence of hydrogenotrophic IRB due to structural Fe(III) reduction coupled to H_2 oxidation, regardless of the experimental solution (M1 and control). The extent of Fe(III) bioreduction was notably enhanced with the increase in the H_2 concentration in the system: 4% H_2 < 10% H_2 < 60% H_2. It confirms the role of H_2 as

energetic substrate for anaerobic respiration, especially in the disposal environment containing low amounts of organic matter.

Comparing both M1 and control solutions and taking into account the abstraction of chemical effect on the dissolution of magnetite, similar amounts of Fe(II) were released in solution by Fe(III) reduction in the presence of bacteria, around 150 µM and 3000 µM with 10% and 60% H_2, respectively. On the one hand, the formation of biogenic minerals was only possible in the M1 solution with 10% and 60% H_2. Vivianite was identified in these conditions as a direct consequence of increase in the aqueous Fe(II) and the presence of phosphate in the composition of the M1 solution. Vivianite appeared as large isolated crystals, being larger with 60% H_2 than with 10% H_2. On the other hand, secondary mineral phases were not identified in the control solution for both abiotic and biotic conditions.

The results obtained in the first experimental approach emphasize that Fe(III) bioconsumption in the presence of H_2 gas potentially alters the stability of magnetite, which in turn can affect the passivating properties of layers made of this corrosion product commonly identified under geological conditions. Moreover, we can conclude that H_2 availability is the parameter likely to control the dissolution of magnetite. A direct correlation between H_2 concentration – bacterial activity – extent of Fe(III) bioreduction was evidenced, even in the control solution that is poorer in terms of essential nutrients for bacterial metabolism compared to the M1 solution. It seems that bacteria are more active, independently of the solution composition, when high H_2 amounts are available.

Concerning the second experimental approach, the results pointed out that the metallic corrosion extent changes according to the experimental solution. The production of dissolved Fe and H_2 gas by corrosion was much higher in the M1 solution than in the control one for all metallic samples tested (iron powder and carbon steel coupon) in abiotic or biotic conditions. As example, the corrosion rate of carbon steel in abiotic conditions was increased twice in the M1 solution over an exposure time of 1 month: 40 $\mu m.y^{-1}$ against 19 $\mu m.y^{-1}$ in the control solution. This emphasizes that the reactional medium must be carefully evaluated for predicting long-term corrosion processes.

Now, comparing the samples iron powder and carbon steel coupon, the corrosion extent was significantly higher with iron powder due to the difference in reactive surface. Moreover, the solid corrosion products were different for each metallic sample, as shown in Table 11. Note that formation of solid corrosion products on the carbon steel surface could not be evidenced in the control solution for all exposure times.

Table 11: Solid corrosion products identified in the corrosion experiments.

Metallic sample	Exposure time (month)	Solution	Condition	Solid corrosion products
iron powder	0-1	M1	biotic	vivianite, siderite, chukanovite
		M1	abiotic	vivianite, siderite, chukanovite
		control	biotic	siderite, chukanovite
		control	abiotic	chukanovite
carbon steel coupon	0-1	M1	biotic	vivianite
		M1	abiotic	vivianite
		control	biotic	-
		control	abiotic	-
	0-5	M1	biotic	vivianite
		M1	abiotic	magnetite, vivianite
		control	biotic	-
		control	abiotic	-

vivianite ($Fe_3(PO_4)_2 \cdot 8H_2O$); siderite ($FeCO_3$); chukanovite ($Fe_2(OH)_2CO_3$); magnetite (Fe_3O_4)

A clear influence of the bacterial activity on the anoxic corrosion process was observed for carbon steel in the M1 solution after 5 months of reaction (note that M1 solution is representative of the argillite interstitial water from Tournemire or Bure sites in France). Formation of magnetite was only observed in abiotic conditions, whereas this mineral phase was no longer identified in the presence of bacteria. These results confirm the mechanism associated to IRB species in which a destabilization/dissolution of passivating oxide layers by structural Fe(III) reduction, in these particular conditions, can enhance corrosion processes. The corrosion rates estimated in this study support these findings, showing an increase of almost 2 times in the presence of bacteria after 5 months of reaction. However, there was no difference on the corrosion rates between abiotic and biotic conditions in the 1-month experiments, probably because there was no formation of magnetite within this time period. At the moment, this process of biocorrosion could not be confirmed for the control (Na_2SO_4) solution where the corrosion rate decreases but no magnetite could be observed (XRD and SEM analyses).

It is noteworthy that in almost all reactional conditions a H_2 consumption by bacteria was observed, emphasizing again the role of H_2 as energetic substrate. Such H_2 consumption was not observed only in the experiments with carbon steel samples in the control solution. This can emphasize that bacteria are less active when low H_2 amounts are available, corroborating the results related to the dissolution of magnetite. Here we can highlight a favorable effect of the presence of hydrogenotrophic bacteria, that is: H_2 consumption could decrease the eventual risks of H_2 embrittlement of metallic materials and potentially the build-up of H_2 gas into the repository.

Moreover, in all experiments a decrease in the planktonic bacterial population was observed with time, but nevertheless an effect of the bacterial activity could still be noted. These results raise the question that the bacterial activity is not directly related to the bacterial concentration in the solution. This fact becomes relevant in the experiments where biofilms can be formed (i.e steel coupon surface).

This study gives new insights regarding the understanding of biocorrosion phenomena, identification of physicochemical mechanisms, and determination of key parameters controlling the corrosion rate. A geochemical study allowed obtaining an integration of the evolution of the aqueous, gas and solid components improving the knowledge of the mechanisms involved in the biocorrosion processes. Although electrochemical methods were not employed in this study, it is noteworthy that geochemical and electrochemical approaches can be complementary to each other for investigations of biocorrosion, especially when long-term measurements are not possible with electrochemical methods.

The interaction between microorganisms, disposal materials and geological medium is a complex system to be handled using just one scientific approach. An integrative approach, including modelling, becomes necessary for long-term prediction in the framework of HLNW disposal. Unfortunately, modelling could not be conducted in this study. However, our work brings useful data allowing future modelling, such as values of corrosion rate, concentrations of chemical elements (Fe, H_2,…) and identification of mineral phases. Our results point out that bacterial activity can induce a slight increase in the corrosion rates (a factor lower than 2 in the conditions of the experiments). Nevertheless, we must place these findings in the context of geological disposal where the maximum H_2 gas pressure expected is much higher (~ 50 bars in the Bure site in France) with respect to the H_2 gas pressure used in our experiments (~ 0.6 bar).

Some questions still remain, especially with respect to the dynamics of microbial activity throughout the corrosion process on long-term.

A few further research topics could be proposed aiming to complement the results presented in this study and to address the gaps:

- experiments with carbon steel in the control (Na_2SO_4) solution and in the presence of high H_2 amounts in order to evaluate if H_2 can promote a better microbial activity and hence corrosion extent;
- experiments with continuous flow reactors in order to avoid limitations of microbial growth (e.g. depletion of nutrients) and to investigate specific parameters (maintaining all the other parameters constant). This type of experiment could also allow acquisition of data on longer period of time;

- implementation of a global microbial activity model representing the main biological reactions in predictive reactive transport models.

PRESENTATION DU TRAVAIL EN FRANÇAIS

7.1 Introduction

La production d'énergie nucléaire, le cycle du combustible nucléaire et l'utilisation de matières radioactives dans l'industrie et la médecine produisent des déchets radioactifs classés selon leur activité et la "période radioactive" des radionucléides qu'ils contiennent. Contrairement à d'autres types de déchets industriels, la toxicité des déchets radioactifs décroît au cours du temps en raison de la décroissance radioactive des radioéléments. Par ailleurs, le volume de ces déchets reste faible et donc une stratégie de confinement est à mettre en œuvre pour les isoler de l'environnement. Ainsi les déchets radioactifs sont différents des déchets de combustibles fossiles (gaz de combustion) qui sont généralement rejetés directement dans l'atmosphère. Le plus grand défi en matière de gestion de déchets radioactifs est donc d'assurer la sûreté de leur confinement à long terme.

Parmi les types de déchets radioactifs, les déchets de haute activité et à vie longue (HAVL) sont considérés comme les plus dangereux car ils sont composés essentiellement de combustibles usés ou de résidus de retraitement (produits de fission et d'activation). Leur processus de décroissance radioactive peut durer des centaines de milliers d'années, ils doivent donc être isolés et stockés de manière à assurer une protection de l'homme et des écosystèmes contre les risques associés à ces déchets.

Le stockage en couche géologique profonde et stable (e.g. les dômes de sel, les structures de granit et certains types de formations argileuses) est la solution envisagée pour la gestion de déchets HAVL dans de nombreux pays (Allemagne, États-Unis, Finlande, France, Japon, Royaume-Uni, Russie et Suède). Cette stratégie est basée sur un système multi-barrières avec différents matériaux naturels et/ou artificiels destinés à assurer le confinement de la radioactivité à long terme.

En France, par exemple, les déchets de type HAVL sont fixés dans une matrice de verre (processus de vitrification), isolés dans des colis en acier inoxydable, puis stockés dans des sur-conteneurs en acier au carbone qui seront placés dans un chemisage métallique situé dans une formation argileuse profonde. Le chemisage permet la mise en place et la récupération éventuelle des colis garantissant ainsi la réversibilité du stockage. Le sur-conteneur constitue une barrière hermétique ayant pour fonction de garantir l'intégrité mécanique du colis et son étanchéité de façon à limiter l'arrivée d'eau du site qui conduira à la corrosion du fer et donc à la dégradation des déchets (Andra, 2005a). L'eau du site est considérée comme le principal vecteur d'altération des colis de déchets.

En raison de l'impact économique et environnemental des déchets radioactifs, l'évaluation de leur comportement à long terme est nécessaire pour assurer la performance du stockage géologique. L'impact des paramètres abiotiques (e.g. température, pression) sur la corrosion est déjà pris en compte dans les évaluations de sûreté (Andra, 2005a). En revanche, des études sur l'impact des activités microbiennes restent nécessaires pour fournir des paramètres biologiques pour la prédiction à long terme des phénomènes de biocorrosion.

Il est bien connu que les micro-organismes peuvent s'adapter et survivre même à des conditions extrêmes, telles que celles qui vont régner dans l'environnement des colis de déchets radioactifs (i.e. rayonnement, température élevée) (Meike and Stroes-Gascoyne, 2000; Pedersen, 2002). Par ailleurs, dans des conditions anoxiques, le processus de corrosion produit du dihydrogène (H_2) et des minéraux Fe(II,III) tels que la magnétite (Fe_3O_4). Ces produits de corrosion peuvent donc fournir des substrats énergétiques pour les réactions d'oxydo-réduction catalysées par le développement microbien anaérobie: l'H_2 comme donneur d'électrons et le Fe(III) en tant qu'accepteur d'électrons. Il est à noter que l'H_2 peut être un substrat important en particulier dans les environnements pauvres en matières organiques biodégradables. Des conditions saturées en eau et la disponibilité de tels produits de corrosion peuvent ainsi favoriser les activités de bactéries hydrogénotrophes et ferri-réductrices dans le site de stockage. Toutefois, le rôle de bactéries ferri-réductrices sur le processus de corrosion est encore sujet à débat. Plusieurs études ont montré des effets inhibiteurs ou accélérateurs sur la corrosion en fonction des conditions environnementales (Dubiel *et al.*, 2002; Herrera and Videla, 2009; Lee and Newman, 2003; Mehanna *et al.*, 2008; Potekhina *et al.*, 1999). Généralement, l'accélération de la corrosion par ces bactéries est associée à la déstabilisation/dissolution des couches d'oxydes de passivation (i.e. la magnétite) par la réduction du Fe(III) structural conduisant à une reprise du processus de corrosion (Esnault *et al.*, 2011).

La problématique de recherche de cette étude se définit par ces questions ouvertes sur les impacts potentiels des activités de bactéries hydrogénotrophes et ferri-réductrices sur le stockage géologique des déchets radioactifs:

- les bactéries hydrogénotrophes et ferri-réductrices peuvent-elles influencer les vitesses de corrosion et modifier la nature et la quantité des produits de corrosion?
- les bactéries hydrogénotrophes et ferri-réductrices peuvent-elles influencer les propriétés protectrices de la magnétite par la réduction du Fe(III) structural?
- l'H_2 résultant de la corrosion peut-il servir de substrat énergétique?

Dans le cadre du stockage géologique des déchets radioactifs, l'échelle de temps est de l'ordre de plusieurs milliers à plusieurs centaines de milliers d'années. Par conséquent, la prédiction des phénomènes de biocorrosion à long terme et dans des conditions de stockage géologique nécessite une approche intégrative avec des expériences *in situ* ainsi qu'en laboratoire, des études d'analogues archéologiques et de la modélisation (Libert *et al.*, 2013). Notre approche scientifique est basée sur des expériences en laboratoire afin de comprendre les phénomènes, d'en identifier les mécanismes physico-chimiques et de déterminer les paramètres contrôlant la vitesse de corrosion (sur de courtes périodes de temps).

L'objectif principal de cette étude est d'évaluer le rôle des activités de bactéries hydrogénotrophes et ferri-réductrices sur le processus de corrosion anoxique en utilisant des indicateurs géochimiques. *Shewanella oneidensis* strain MR-1 a été choisi comme micro-organisme modèle et des conditions abiotiques et biotiques ont été mises en œuvre. L'approche expérimentale se décline en trois types d'expériences:

(i) en présence de magnétite et de l'H_2 visant à vérifier si les bactéries peuvent utiliser l'H_2 pour réduire le Fe(III) structural de la magnétite;
(ii) en présence de poudre de fer métallique afin d'augmenter la surface spécifique et par conséquent la corrosion du fer et la production d'H_2;
(iii) en présence de coupons d'acier au carbone (type A37) visant à évaluer le processus de corrosion dans des conditions plus "réalistes" en termes de type de matériau et de surface réactive.

Cette étude se divise en six chapitres. Le **chapitre 1** est fourni des informations générales sur le stockage géologique des déchets radioactifs, sur les activités microbiennes dans des formations géologiques profondes et sur la corrosion métallique aqueuse et les phénomènes de biocorrosion. Le **chapitre 2** présente une description des méthodes et des procédures expérimentales utilisées dans cette étude. Le **chapitre 3** est dédié à une étude préliminaire sur les paramètres réactionnels pouvant influer sur l'activité de *Shewanella oneidensis* et par conséquent sur la réduction du Fe(III). Le **chapitre 4** présente les résultats concernant la biodisponibilité du Fe(III) de la magnétite et l'influence de la concentration d'H_2 sur sa réduction. Le **chapitre 5** montre les résultats de l'impact des activités des bactéries hydrogénotrophes et ferri-réductrices sur le processus de corrosion anoxique avec de la poudre de fer et des coupons en acier au carbone. Enfin, un résumé des principales conclusions de cette étude et de ses perspectives est présenté dans le **chapitre 6**.

7.2 Résumé du contexte de l'étude

Démontrer la sûreté du stockage géologique de déchets HAVL sera une avancée majeure permettant l'acceptation sociale du développement de l'énergie nucléaire dans les prochaines décennies. La stratégie généralement acceptée pour assurer le confinement à long terme des radionucléides est le stockage dans des formations géologiques stables et profondes grâce à un système multi-barrières impliquant plusieurs matériaux métalliques. La corrosion de ces matériaux est inévitable dans des conditions saturées en eau et donc une meilleure compréhension des processus de corrosion à long terme est nécessaire pour démontrer la sûreté du stockage géologique et d'en assurer l'avenir.

Plusieurs études ont démontré que les micro-organismes (e.g. bactéries et archaebactéries) sont présents dans la plupart des formations géologiques profondes déjà étudiées (Boivin-Jahns *et al.*, 1996; Mauclaire *et al.*, 2007; Poulain *et al.*, 2008; Stroes-Gascoyne *et al.*, 2011; Urios *et al.*, 2012). Par ailleurs, l'introduction de micro-organismes non indigènes due aux activités humaines au sein du site de stockage des déchets radioactifs est inévitable pendant les phases de construction et d'exploitation du stockage.

Les micro-organismes ont des capacités surprenantes à survivre dans des conditions extrêmes telles que celles rencontrées dans le champ proche des colis HAVL, comme la présence de rayonnement, la chaleur ou encore des conditions de pH élevé (Meike and Stroes-Gascoyne, 2000; Pedersen, 2002). Il est donc nécessaire de conclure sur l'impact des activités microbiennes afin de déterminer si des paramètres biologiques doivent être intégrés dans les modèles d'évaluation de sûreté du stockage géologique.

Il est important de noter que même si la croissance et l'activité des micro-organismes dans un milieu géologique compact restent hypothétiques en raison d'un problème de disponibilité de l'espace poral des argiles, cette croissance reste possible dans la zone de fracture connectée (présence d'hétérogénéités, fissures) et dans les vides technologiques entre les matériaux du stockage du système multi-barrière. De plus, la corrosion est le principal processus modifiant significativement l'inventaire des éléments nutritifs et énergétiques au sein du site de stockage des déchets radioactifs en fournissant de nouveaux substrats pour la croissance microbienne. Cette étude s'intéresse aux produits de corrosion l'H_2 et la magnétite (un solide couramment associé aux propriétés de passivation des métaux) pouvant être utilisés comme substrats énergétiques par les bactéries hydrogénotrophes et ferri-réductrices pour leur métabolisme (Figure 59). En effet, l'H_2 est un substrat important dans les environnements profonds souvent pauvres en matière organique biodégradable.

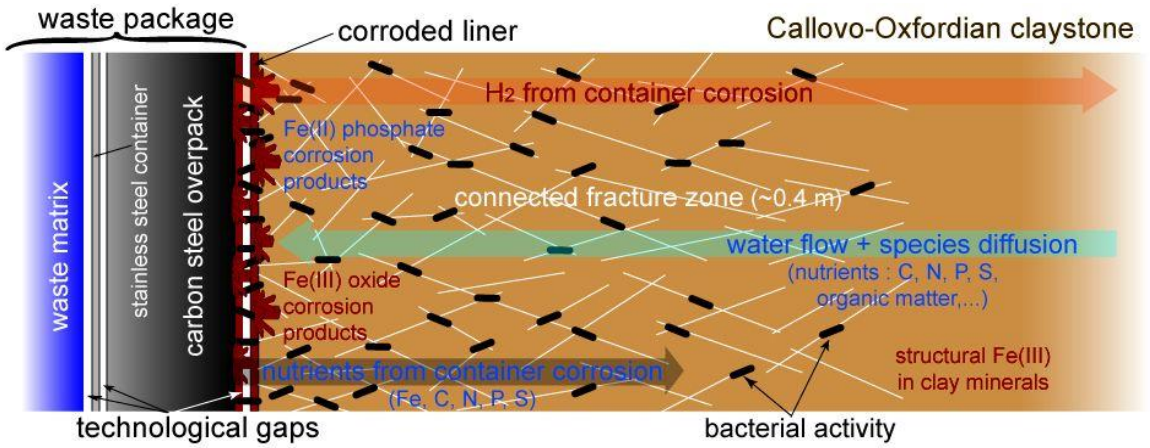

Figure 59: Schéma du champ proche d'une alvéole de stockage des déchets HAVL indiquant la localisation potentiel de l'activité microbienne et le flux de nutriments et substrats énergétiques (pas à l'échelle) (Libert et al., 2013).

Les micro-organismes peuvent modifier (directement ou indirectement) les caractéristiques chimiques et physiques à l'interface métal/environnement et donc influencer le processus de corrosion (Beech and Gaylarde, 1999; Stott, 1993; Videla and Herrera, 2005). Cependant le rôle des micro-organismes sur la corrosion n'est pas encore clairement élucidé dans la littérature, car ils peuvent accélérer ou inhiber la corrosion selon les conditions environnementales.

En termes de biocorrosion, la plupart des mécanismes déjà décrits sont liés au métabolisme de bactéries sulfato-réductrices. Notre étude s'intéresse à l'impact de bactéries ferri-réductrices pour deux raisons: *(i)* les produits de corrosion attendus dans des conditions anoxiques (en particulier, l'H_2 et la magnétite) peuvent potentiellement favoriser ces métabolismes; *(ii)* les bactéries ferri-réductrices sont moins étudiées en terme de corrosion comparées aux bactéries sulfato-réductrices. L'impact attendu de ces bactéries ferri-réductrices sur la corrosion est l'altération des couches d'oxydes de passivation (i.e. la magnétite) par la réduction du Fe(III) structural ce qui pourrait réactiver le processus de corrosion et donc modifier les vitesses de corrosion (Esnault *et al.*, 2011; Herrera and Videla, 2009; Lee and Newman, 2003; Potekhina *et al.*, 1999). En tenant compte de ce contexte scientifique, les objectifs de cette étude sont décrits ci-dessous.

7.3 Objectifs de l'étude

Les objectifs spécifiques sont les suivants:

- évaluer l'impact des **bactéries hydrogénotrophes et ferri-réductrices** sur le processus de corrosion car les produits de corrosion attendus dans des conditions anoxiques (en particulier, l'H_2 et la magnétite) peuvent potentiellement favoriser ces métabolismes et activités;
- évaluer l'influence du **substrat métallique** (poudre de fer et coupon d'acier au carbone) sur le processus de corrosion;
- évaluer le rôle de l'**H_2 comme substrat énergétique** potentiel pour le développement bactérien;
- évaluer la **biodisponibilité du Fe(III)** de la magnétite en présence d'H_2 en tant que donneur d'électrons.

7.4 Démarche scientifique

La démarche scientifique proposée dans cette étude repose sur deux principaux scénarios d'expérimentations qui ont été évalués par des méthodes géochimiques.

Premier scénario (dissolution de la magnétite): expériences avec de l'H_2 (comme donneur d'électrons) à différentes concentrations initiales et de la magnétite (comme accepteur d'électrons) visant à évaluer la biodisponibilité du Fe(III) et donc la stabilité du minéral. Ici, on suppose que la couche de passivation est constituée de magnétite qui pourra être déstabilisée par l'activité bactérienne en utilisant l'H_2 comme énergie.

Deuxième scénario (corrosion métallique): expériences avec des échantillons métalliques en fer (poudre de fer ou coupon d'acier au carbone) visant à *(i)* mesurer principalement le Fe dissous et la production d'H_2 (ou sa consommation par les bactéries); et à *(ii)* caractériser les produits de corrosion solides formés pendant le processus de corrosion.

La bactérie choisie pour cette étude est *Shewanella oneidensis* strain MR-1 considérée comme un micro-organisme modèle pour l'étude des processus de réduction dissimilatrice du Fe(III) en présence d'H_2 comme donneur d'électrons.

Dans cette étude, deux solutions expérimentales qui diffèrent en composition chimique ont été utilisées: un milieu minimal favorable pour le métabolisme de bactéries ferri-réductrices (appelé solution M1) et un milieu simplifié (appelé solution de contrôle).

Le Tableau 12 résume les conditions réactionnelles des principales expériences réalisées dans cette étude, décrites au chapitre 2 et utilisées dans les chapitres 4 et 5.

Tableau 12: Résumé des conditions réactionnelles des principales expériences géochimiques.

Objectif	Echantillon solide	Solution	Conditions	Temps (mois)	Analyse des phases solides
Evaluation de la réduction dissimilatrice du Fe(III)	Magnétite synthétisée ($7\ g.L^{-1}$)	M1 + contrôle (Na_2SO_4) (140 mL)	Anaérobie (3 conditions): H_2 4% (H_2:N_2 / 4:96%) pH_i ~ 7.3 (M1 + contrôle) H_2 10% (H_2:CO_2:N_2 / 10:20:70%) pH_i ~ 6.3 (M1); 6.0 (contrôle) H_2 60% (H_2:CO_2:N_2 / 60:10:30%) pH_i ~ 6.6 (M1); 6.3 (contrôle) 30°C Abiotique + biotique Sans lactate	0-1	DRX FTIR MEB/EDX
Evaluation du processus de corrosion	Poudre de fer ($7\ g.L^{-1}$)	M1 + contrôle (Na_2SO_4) (140 mL)	Anaérobie (N_2:CO_2 / 90:10%) pH_i ~ 6.4 (M1); 6.2 (contrôle) 30°C Abiotique + biotique Sans lactate	0-1	DRX FTIR MEB/EDX
	Coupon en acier au carbone (1; 0.8 cm^2)	M1 + contrôle (Na_2SO_4) (140 mL)	Anaérobie (N_2:CO_2 / 90:10%) pH_i ~ 6.4 (M1); 6.2 (contrôle) 30°C Abiotique + biotique Sans lactate	0-1 0-5	DRX Raman MEB/EDX perte de masse

7.5 Conclusions et perspectives

L'objectif principal de la présente étude était d'évaluer l'impact des activités de bactéries hydrogénotrophes et ferri-réductrices sur le processus de corrosion anoxique. Il a été supposé que le couple redox Fe(III)/H_2 (accepteur d'électrons/donneur d'électrons) est un moteur important pour les activités microbiennes qui peuvent ainsi affecter la vitesse de corrosion par la déstabilisation de la couche de passivation (i.e. la magnétite).

Notre démarche scientifique reposait sur des expériences de laboratoire suivies sur de courtes périodes de temps (1 et 5 mois) en utilisant des indicateurs géochimiques, comme la concentration en Fe dissous et l'H_2 gazeux ainsi que la caractérisation des produits solides en fin d'expérimentations.

En ce qui concerne les expériences avec de l'H_2 et de la magnétite (premier scénario d'expérimentations), les résultats ont montré un effet chimique conduisant à la dissolution de la magnétite en plus de l'effet biologique. Il a été mesuré de faibles quantités de Fe(II) dissous dans des conditions abiotiques en raison de la réduction chimique du Fe(III) de la magnétite avec l'H_2 (en effet, une légère baisse dans la concentration d'H_2 a été observée dans ces expériences).

Cependant l'impact de l'activité bactérienne sur la dissolution de la magnétite a été démontré dans nos expériences en plus de l'effet chimique. Les résultats ont clairement mis en évidence que la magnétite est déstabilisée en présence de bactéries hydrogénotrophes et ferri-réductrices due à la réduction du Fe(III) structural couplée à l'oxydation d'H_2 quelle que soit la solution expérimentale (M1 et contrôle). La quantité de Fe(III) bioréduit est plus élevée en présence de concentrations croissantes en H_2 dans le système: 4% H_2 < 10% H_2 < 60% H_2. Ces résultats confirment le rôle de l'H_2 comme substrat énergétique pour la respiration anaérobie, en particulier dans l'environnement de stockage pauvre en matière organique biodégradable.

En comparant les deux solutions expérimentales (M1 et contrôle) et en faisant abstraction de l'effet chimique sur la dissolution de la magnétite, des quantités similaires de Fe(II) ont été produites, pour les deux solutions, dues à la réduction du Fe(III) par les bactéries: environ 150 µM et 3000 µM avec 10% et 60% d'H_2, respectivement. Cependant la formation de minéraux biogéniques a été observée uniquement avec la solution M1 à 10% et 60% d'H_2. La présence de vivianite a été notée dans ces conditions comme une conséquence directe de l'augmentation du Fe(II) aqueux et de la présence de phosphate dans la solution M1. Cette vivianite apparaît sous forme de grands cristaux isolés, en taille plus importante avec 60% d'H_2 qu'avec 10% d'H_2. Ces phases minérales secondaires n'ont pas été identifiées avec la solution contrôle en conditions abiotiques et biotiques.

Les résultats obtenus dans ce premier scénario d'expérimentations soulignent la biodisponibilité du Fe(III) en présence de gaz H_2 et l'altération de la magnétite affectant ainsi les propriétés de passivation de ces couches d'oxydes. De plus, nous pouvons conclure que la quantité d'H_2 disponible est le paramètre contrôlant sa dissolution. Une corrélation directe entre la concentration d'H_2, l'activité bactérienne et la quantité de Fe(III) bioréduit a été mise en évidence aussi bien dans la solution contrôle (plus pauvre en nutriments) que dans la solution M1. Il semble que les bactéries soient plus actives, indépendamment de la composition de la solution, lorsque de grandes quantités d'H_2 sont disponibles.

En ce qui concerne les expériences sur la corrosion métallique (deuxième scénario d'expérimentations), les résultats ont montré que la réaction de corrosion est différente selon la solution expérimentale. Les concentrations de Fe dissous et d'H_2 sont beaucoup plus élevées en présence de la solution M1 comparées aux concentrations mesurées dans la solution contrôle pour les conditions abiotiques et biotiques et pour tous les échantillons métalliques testés (poudre de fer et coupon d'acier au carbone). Par exemple, dans des conditions abiotiques et pour un temps d'exposition de 1 mois, la vitesse de corrosion de l'acier au carbone est deux fois plus élevée avec la solution M1 (40 $\mu m.y^{-1}$) que pour la solution contrôle (19 $\mu m.y^{-1}$). Ces résultats soulignent l'importance du milieu réactionnel pour les prédictions des phénomènes de corrosion à long terme.

En comparant les coupons en acier et la poudre de fer, la quantité de Fe dissous est significativement plus élevée avec la poudre de fer ayant une surface réactive plus importante. De plus, les produits de corrosion solides sont différents pour chaque échantillon métallique, comme le montre le Tableau 13. A noter que la formation de produits de corrosion solides à la surface de l'acier n'a pas pu être mise en évidence avec la solution contrôle quel que soit le temps d'exposition.

Tableau 13: Produits de corrosion solides identifiés dans les expériences de corrosion.

Echantillon métallique	Temps d'exposition (mois)	Solution	Condition	Produits de corrosion solides
Poudre de fer	0-1	M1	Biotique	Vivianite, sidérite, chukanovite
		M1	Abiotique	Vivianite, sidérite, chukanovite
		Contrôle	Biotique	Sidérite, chukanovite
		Contrôle	Abiotique	Chukanovite
Coupon en acier au carbone	0-1	M1	Biotique	Vivianite
		M1	Abiotique	Vivianite
		Contrôle	Biotique	-
		Contrôle	Abiotique	-
	0-5	M1	Biotique	Vivianite
		M1	Abiotique	Magnétite, vivianite
		Contrôle	Biotique	-
		Contrôle	Abiotique	-

vivianite ($Fe_3(PO_4)_2 \cdot 8H_2O$); sidérite ($FeCO_3$); chukanovite ($Fe_2(OH)_2CO_3$); magnétite (Fe_3O_4)

L'influence de l'activité bactérienne sur le processus de corrosion anoxique a été clairement observée avec la solution M1 et le coupon d'acier après 5 mois de réaction (il est à noter que la solution M1 est représentative des eaux porales de l'argilite des sites de Tournemire et Bure en France). La formation de magnétite n'a été observée que dans des conditions abiotiques, alors que cette phase minérale n'était plus identifiée en présence de bactéries. Ces résultats confirment le mécanisme associé aux bactéries ferri-réductrices: la déstabilisation/dissolution des couches d'oxydes de passivation par la réduction du Fe(III) structural ce qui va accélérer le processus de corrosion. Les vitesses de corrosion estimées dans cette étude confirment ces résultats soit une augmentation quasiment d'un facteur 2 en présence de bactéries après 5 mois de réaction. Cependant aucune différence sur les vitesses de corrosion entre les conditions abiotiques et biotiques n'a été obtenue dans les expériences après 1 mois de suivi, probablement à cause de l'absence de formation de magnétite sur cette période de temps. De même, à ce stade, ce processus de biocorrosion n'a pas été confirmé pour la solution contrôle (Na_2SO_4) où la vitesse de corrosion diminue alors que la présence de magnétite n'a pas pu être mise en évidence (analyses MEB et DRX).

Il est à noter que dans la plupart des conditions réactionnelles une consommation d'H_2 par des bactéries a été observée en mettant de nouveau en évidence le rôle de l'H_2 comme substrat énergétique. La consommation d'H_2 par les bactéries n'a pas été observée pour la solution contrôle et les échantillons sous forme de coupons d'acier probablement à cause de la faible quantité d'H_2 produite conduisant à une faible activité bactérienne. Ces résultats corroborent les résultats relatifs à la dissolution de la magnétite[4]. Il faut ici souligner un effet favorable de la présence de bactéries hydrogénotrophes, car leur consommation d'H_2 pourrait diminuer les risques éventuels de fragilisation par l'H_2 des matériaux métalliques et potentiellement pourrait diminuer l'accumulation de ce gaz dans le site du stockage. Par ailleurs, malgré une diminution de la population bactérienne planctonique au cours du temps pour tous les scénarios d'expérimentations, l'activité bactérienne reste significative. L'activité bactérienne n'est donc pas directement liée à la concentration des bactéries en solution. Ce point devient pertinent dans les expériences où un biofilm peut se former (i.e. surface de coupon en acier).

Ce travail présente une nouvelle approche sur l'étude et la compréhension des phénomènes de biocorrosion, l'identification des mécanismes physico-chimiques et la détermination des paramètres contrôlant la vitesse de corrosion. Une approche géochimique a permis l'obtention de données sur l'évolution des éléments dissous, gazeux et solides permettant ainsi une meilleure connaissance des mécanismes impliqués dans les processus de biocorrosion. Bien que les méthodes électrochimiques n'aient pas été utilisées dans cette étude, il est à noter que les approches géochimiques et électrochimiques peuvent être complémentaires pour les investigations de la biocorrosion, en particulier lorsque les mesures à long terme ne sont pas possibles avec les méthodes électrochimiques.

L'interaction entre les micro-organismes, les matériaux métalliques et le milieu géologique est un système complexe à gérer avec une seule approche scientifique. Une approche intégrative, ajoutant la modélisation, devient nécessaire pour la prédiction du comportement à long terme des matériaux du stockage géologique de déchets radioactifs. Malheureusement cette approche modélisation n'a pas été effectuée dans cette étude. Cependant notre travail apporte des données importantes pour une future modélisation, tels que les valeurs de vitesse de corrosion, les concentrations d'éléments chimiques (Fe, H_2, ...) et l'identification des phases minérales. Nos résultats montrent que l'activité bactérienne peut induire une légère augmentation des vitesses de corrosion (d'un facteur inférieur à 2 dans les conditions de ces expériences). Néanmoins, il faut replacer ces résultats dans le contexte du stockage où la pression d'H_2 maximale attendue est beaucoup plus élevée (~ 50 bars dans le site de Bure en France) par rapport à la pression d'H_2 utilisée dans nos expériences (~ 0,6 bar).

Des questions restent posées, en particulier, quelle est l'influence de la dynamique de l'activité microbienne sur le processus de corrosion à long terme?

D'autres expérimentations pourraient être proposées afin de compléter les résultats actuels:

- des expériences avec de l'acier au carbone et la solution contrôle (Na_2SO_4) en présence de quantités élevées d'H_2 afin d'évaluer si l'H_2 peut favoriser l'activité microbienne et donc une corrosion plus importante;
- des expériences avec des réacteurs à flux continu afin d'éviter les limitations de la croissance microbienne (e.g. l'épuisement des nutriments) et d'étudier des paramètres spécifiques (en conservant les autres paramètres constants). Ce type d'expérience pourrait également permettre l'acquisition de données sur une plus longue période de temps;
- la mise en œuvre d'un modèle global de l'activité microbienne en représentant les principales réactions biologiques dans des modèles prédictifs de transport réactif.

REFERENCES

Amend, J. P. and E. L. Shock (2001). "Energetics of overall metabolic reactions of thermophilic and hyperthermophilic Archaea and bacteria." FEMS Microbiology Reviews **25**(2): 175-243.

Andra. (2005a). Dossier 2005 Argile: Synthesis - Evaluation of the feasibility of a geological repository in an argillaceous formation. Andra Technical Report 266VA.

Andra. (2005b). Dossier 2005 Argile: Tome evolution phenomenologique du stokage geologique. Andra Technical Report.

Andra. (2012). Inventaire national des matières et déchets radioactifs édition 2012 - Les essentiels. Andra Inventaire National.

ASTM (2011). Standard G1-03: Practice for Preparing, Cleaning, and Evaluating Corrosion Test Specimens.

Beech, I. B. (2003). "Sulfate-reducing bacteria in biofilms on metallic materials and corrosion." Microbiology Today **30**: 115-117.

Beech, I. B. and C. C. Gaylarde (1999). "Recent advances in the study of biocorrosion - An overview." Revista de Microbiologia **30**(3): 177-190.

Beech, I. B., V. Zinkevich, L. Hanjangsit, R. Gubner and R. Avci (2000). "The effect of Pseudomonas NCIMB 2021 biofilm on AISI 316 stainless steel." Biofouling **15**(1-3): 3-12.

Behrends, T., E. Krawczyk-Barsch and T. Arnold (2012). "Implementation of microbial processes in the performance assessment of spent nuclear fuel repositories." Applied Geochemistry **27**(2): 453-462.

Bellot-Gurlet, L., D. Neff, S. Reguer, J. Monnier, M. Saheb and P. Dillmann (2009). "Raman Studies of Corrosion Layers Formed on Archaeological Irons in Various Media." Journal of Nano Research **8**: 147-156.

Bennett, D. G. and R. Gens (2008). "Overview of European concepts for high-level waste and spent fuel disposal with special reference waste container corrosion." Journal of Nuclear Materials **379**(1-3): 1-8.

Bildstein, O., L. Trotignon, M. Perronnet and M. Jullien (2006). "Modelling iron-clay interactions in deep geological disposal conditions." Physics and Chemistry of the Earth, Parts A/B/C **31**(10-14): 618-625.

Boivin-Jahns, V., R. Ruimy, A. Bianchi, S. Daumas and R. Christen (1996). "Bacterial Diversity in a Deep-Subsurface Clay Environment." Applied and Environmental Microbiology **62**(9): 3405-3412.

Bonneville, S., P. Van Cappellen and T. Behrends (2004). "Microbial reduction of iron(III) oxyhydroxides: effects of mineral solubility and availability." Chemical Geology **212**(3-4): 255-268.

Castro, L., C. García-Balboa, F. González, A. Ballester, M. L. Blázquez and J. A. Muñoz (2013). "Effectiveness of anaerobic iron bio-reduction of jarosite and the influence of humic substances." Hydrometallurgy **131–132**(0): 29-33.

Cattant, F., D. Crusset and D. Feron (2008). "Corrosion issues in nuclear industry today." Materials Today **11**(10): 32-37.

Combarieu, G., P. Barboux and Y. Minet (2007). "Iron corrosion in Callovo-Oxfordian argilite: From experiments to thermodynamic/kinetic modelling." Physics and Chemistry of the Earth, Parts A/B/C **32**(1-7): 346-358.

Cornell, R. M. and U. Schwertmann (2003). The Iron Oxides: Structure, Properties, Reactions, Occurrences and Uses, Wiley-VCH: Wienheim, Germany.

Coy, C. C. (2013). Biocorrosion of carbon steel in water injection systems of the oil and gas industry: new experimental models from the field. Ph.D thesis, Université de Toulouse.

Da Silva, S., R. Basséguy and A. Bergel (2002). "The role of hydrogenases in the anaerobic microbiologically influenced corrosion of steels." Bioelectrochemistry **56**(1–2): 77-79.

David, D. (2001). Matériaux: Analogues archéologiques et corrosion. Paris Chatenay-Malabry, 304146, Andra

De Windt, W., N. Boon, S. D. Siciliano and W. Verstraete (2003). "Cell density related H_2 consumption in relation to anoxic Fe(0) corrosion and precipitation of corrosion products by *Shewanella oneidensis* MR-1." Environmental Microbiology **5**(11): 1192-1202.

Debruyn, W., J. Dresselaers, P. Vermieren, J. Kelchtermans and H. Tas. (1991). Corrosion of container and infrastructure materials under clay repository conditions. Commission of the European Communities, Technical report, EUR 13667 EN.

Deniau, I., I. Devol-Brown, S. Derenne, F. Behar and C. Largeau (2008). "Comparison of the bulk geochemical features and thermal reactivity of kerogens from Mol (Boom Clay), Bure (Callovo–Oxfordian argillite) and Tournemire (Toarcian shales) underground research laboratories." Science of The Total Environment **389**(2–3): 475-485.

Dong, H. L., J. K. Fredrickson, D. W. Kennedy, J. M. Zachara, R. K. Kukkadapu and T. C. Onstott (2000). "Mineral transformation associated with the microbial reduction of magnetite." Chemical Geology **169**(3-4): 299-318.

Downs, R. T. (2006). The RRUFF Project: an integrated study of the chemistry, crystallography, Raman and infrared spectroscopy of minerals., Program and Abstracts of the 19th General Meeting of the International Mineralogical Association in Kobe, Japan. O03-13.

Dubiel, M., C. H. Hsu, C. C. Chien, F. Mansfeld and D. K. Newman (2002). "Microbial iron respiration can protect steel from corrosion." Applied and Environmental Microbiology **68**(3): 1440-1445.

Duquette, D. J., R. M. Latanision, C. A. W. Di Bella and B. E. Kirstein (2009). "Corrosion Issues Related to Disposal of High-Level Nuclear Waste in the Yucca Mountain Repository - Peer Reviewers' Perspective." Corrosion **65**(4): 272-280.

Ehrlich, H. L. and D. K. Newman (2008). Geomicrobiology, CRC Press.

El Hajj, H., A. Abdelouas, B. Grambow, C. Martin and M. Dion (2010). "Microbial corrosion of P235GH steel under geological conditions." Physics and Chemistry of the Earth, Parts A/B/C **35**(6–8): 248-253.

El Mendili, Y., A. Abdelouas and J. F. Bardeau (2013). "Insight into the mechanism of carbon steel corrosion under aerobic and anaerobic conditions." Physical Chemistry Chemical Physics **15**(23): 9197-9204.

Esnault, L. (2010). Réactivité géomicrobiologique des matériaux et minéraux ferrifères: conséquences sur l'évolution à long terme des matériaux d'un stockage de déchets radioactifs en milieu argileux. Ph.D thesis, Université de Nancy-Henri Poincaré.

Esnault, L., M. Jullien, C. Mustin, O. Bildstein and M. Libert (2011). "Metallic corrosion processes reactivation sustained by iron-reducing bacteria: Implication on long-term stability of protective layers." Physics and Chemistry of the Earth, Parts A/B/C **36**(17–18): 1624-1629.

Esnault, L., M. Libert and O. Bildstein (2013b). "Assessment of microbiological development in nuclear waste geological disposal: a geochemical modeling approach." Procedia Earth and Planetary Science **7**: 244-247.

Esnault, L., M. Libert, O. Bildstein, C. Mustin, F. Marsal and M. Jullien (2013a). "Impact of iron-reducing bacteria on the properties of argillites in the context of radioactive waste geological disposal." Applied Clay Science **83-84**(0): 42-49.

Farelas, F., M. Galicia, B. Brown, S. Nesic and H. Castaneda (2010). "Evolution of dissolution processes at the interface of carbon steel corroding in a CO_2 environment studied by EIS." Corrosion Science **52**(2): 509-517.

Faria, D. L. A., S. V. Silva and M. T. Oliveira (1997). "Raman microspectroscopy of some iron oxides and oxyhydroxides." Journal of Raman Spectroscopy **28**(11): 873-878.

Feron, D., D. Crusset and J. M. Gras (2008). "Corrosion issues in nuclear waste disposal." Journal of Nuclear Materials **379**(1-3): 16-23.

Flemming, H. C. and J. Wingender (2010). "The biofilm matrix." Nature Reviews Microbiology **8**(9): 623-633.

Fredrickson, J. K. and Y. A. Gorby (1996). "Environmental processes mediated by iron-reducing bacteria." Current Opinion in Biotechnology **7**(3): 287-294.

Fredrickson, J. K., J. P. McKinley, B. N. Bjornstad, P. E. Long, D. B. Ringelberg, D. C. White, L. R. Krumholz, J. M. Suflita, F. S. Colwell, R. M. Lehman, T. J. Phelps and T. C. Onstott (1997). "Pore-size constraints on the activity and survival of subsurface bacteria in a late Cretaceous shale-sandstone sequence, northwestern New Mexico." Geomicrobiology Journal **14**(3): 183-202.

Frey, M. (2002). "Hydrogenases: Hydrogen-activating enzymes." ChemBioChem **3**(2-3): 153-160.

Frost, R. L., W. Martens, P. A. Williams and J. T. Kloprogge (2002). "Raman and infrared spectroscopic study of the vivianite-group phosphates vivianite, baricite and bobierrite." Mineralogical Magazine **66**(6): 1063-1073.

Frost, R. L. and M. Weier (2004). "Raman spectroscopic study of vivianites of different origins." Neues Jahrbuch Fur Mineralogie-Monatshefte(10): 445-463.

Gales, G., M. F. Libert, R. Sellier, L. Cournac, V. Chapon and T. Heulin (2004). "Molecular hydrogen from water radiolysis as an energy source for bacterial growth in a basin containing irradiating waste." FEMS Microbiology Letters **240**(2): 155-162.

Gao, M., X. Pang and K. Gao (2011). "The growth mechanism of CO_2 corrosion product films." Corrosion Science **53**(2): 557-568.

Gaucher, E., C. Robelin, J. M. Matray, G. Negral, Y. Gros, J. F. Heitz, A. Vinsot, H. Rebours, A. Cassagnabere and A. Bouchet (2004). "ANDRA underground research laboratory: interpretation of the mineralogical and geochemical data acquired in the Callovian-Oxfordian formation by investigative drilling." Physics and Chemistry of the Earth, Parts A/B/C **29**(1): 55-77.

Gottschalk, G. (1986). Bacterial Metabolism, Springer.

Gralnick, J. A. (2012). "On conducting electron traffic across the periplasm." Biochemical Society Transactions **40**(6): 1178-1180.

Gralnick, J. A. and D. K. Newman (2007). "Extracellular respiration." Molecular Microbiology **65**(1): 1-11.

Grygar, T. (1995). "Kinetics of Electrochemical Reductive Dissolution of Iron(III) Hydroxyoxides." Collection of Czechoslovak Chemical Communications **60**(8): 1261-1273.

Hanesch, M. (2009). "Raman spectroscopy of iron oxides and (oxy)hydroxides at low laser power and possible applications in environmental magnetic studies." Geophysical Journal International **177**(3): 941-948.

Herrera, L. K. and H. A. Videla (2009). "Role of iron-reducing bacteria in corrosion and protection of carbon steel." International Biodeterioration & Biodegradation **63**(7): 891-895.

Hogg, S. (2005). Essential Microbiology, John Wiley & Sons Ltd.

Huang, C. K. and P. K. Kerr (1960). "Infrared study of the carbonate minerals." The American Mineralogist **45**: 311-324.

Jones, D. A. and P. S. Amy (2002). "A thermodynamic interpretation of microbiologically influenced corrosion." Corrosion **58**(8): 638-645.

Keith-Roach, M. J. and F. R. Livens (2002). Microbial interactions with radionuclides - summary and future perspectives. Interactions of microorganisms with radionuclides. M. Keith-Loach and F. Livens, Elsevier**:** 383-391.

Kerber-Schütz, M., M. Libert, M. L. Schlegel, J.-E. Lartigue and O. Bildstein (2013a). "Dissimilatory Iron Reduction in the Presence of Hydrogen: A Case Study of Microbial Activity and Nuclear Waste Disposal." Procedia Earth and Planetary Science **7**(0): 409-412.

Kerber-Schütz, M., R. Moreira, O. Bildstein, J.-E. Lartigue, M. L. Schlegel, B. Tribollet, V. Vivier and M. Libert (2013b). "Combined geochemical and electrochemical methodology to quantify corrosion of carbon steel by bacterial activity." Bioelectrochemistry**, in press**.

Kermani, M. B. and A. Morshed (2003). "Carbon dioxide corrosion in oil and gas production - A compendium." Corrosion **59**: 659-683.

King, F. (2007). Overview of a Carbon Steel Container Corrosion Model for a Deep Geological Repository in Sedimentary Rock. Nuclear Waste Management Organization, Technical report TR-2007-01.

King, F. and S. Stroes-Gascoyne. (2000). An assessment of the long-term corrosion behaviour of C-steel and the impact on the redox conditions inside a nuclear fuel waste disposal container. Ontario Power Generation Nuclear Waste Management Division, Tehnical report 06819-REP-01200-10028.

Kostka, J. E., D. D. Dalton, H. Skelton, S. Dollhopf and J. W. Stucki (2002). "Growth of iron(III)-reducing bacteria on clay minerals as the sole electron acceptor and comparison of growth yields on a variety of oxidized iron forms." Applied and Environmental Microbiology **68**(12): 6256-6262.

Kostka, J. E. and K. H. Nealson (1995). "Dissolution and Reduction of Magnetite by Bacteria." Environmental Science & Technology **29**(10): 2535-2540.

Kostka, J. E. and K. H. Nealson (1998). Isolation, cultivation, and characterization of iron- and manganese-reducing bacteria. Techniques in Microbial Ecology. R. S. Burlage, R. Atlas, D. Stahl, G. Geesey and G. Sayler, Oxford University Press**:** 58-78.

Kostka, J. E., J. W. Stucki, K. H. Nealson and J. Wu (1996). "Reduction of structural Fe(III) in smectite by a pure culture of Shewanella putrefaciens strain MR-1." Clays and Clay Minerals **44**(4): 522-529.

Kostka, J. E., J. Wu, K. H. Nealson and J. W. Stucki (1999). "The impact of structural Fe(III) reduction by bacteria on the surface chemistry of smectite clay minerals." Geochimica et Cosmochimica Acta **63**(22): 3705-3713.

Kursten, B., B. Cornélis, S. Labat and P. Van Iseghem. (1996). Geological disposal of conditioned high-level and long lived radioactive waste. In situ corrosion experiments. SCK-CEN, Technical report R-3121.

Landolt, D., A. Davenport, J. Payer and D. Shoesmith. (2009). A Review of Materials and Corrosion Issues Regarding Canisters for Disposal of Spent Fuel and High-level Waste in Opalinus Clay. Nagra Technical Report NTB 09-02.

Lee, A. K. and D. K. Newman (2003). "Microbial iron respiration: impacts on corrosion processes." Applied Microbiology and Biotechnology **62**(2-3): 134-139.

Lee, S. Y., H. Yoshikawa and T. Matsui (2010). "Biomineralization of Vivianite on the Carbon Steel Surface Attacked by the Iron Reducing Bacteria." MRS Online Proceedings Library **1265**: AA06-01.

Li, X. M., T. X. Liu, F. B. Li, W. Zhang, S. G. Zhou and Y. T. Li (2012). "Reduction of structural Fe(III) in oxyhydroxides by *Shewanella decolorationis* S12 and characterization of the surface properties of iron minerals." Journal of Soils and Sediments **12**(2): 217-227.

Libert, M., O. Bildstein, L. Esnault, M. Jullien and R. Sellier (2011). "Molecular hydrogen: An abundant energy source for bacterial activity in nuclear waste repositories." Physics and Chemistry of the Earth, Parts A/B/C **36**(17-18): 1616-1623.

Libert, M., M. K. Schütz, L. Esnault, D. Feron and O. Bildstein (2013). "Impact of microbial activity on the radioactive waste disposal: long term prediction of biocorrosion processes." Bioelectrochemistry**, in press**.

Lin, L. H., G. F. Slater, B. S. Lollar, G. Lacrampe-Couloume and T. C. Onstott (2005). "The yield and isotopic composition of radiolytic H_2, a potential energy source for the deep subsurface biosphere." Geochimica et Cosmochimica Acta **69**(4): 893-903.

Little, B., P. Wagner, K. Hart, R. Ray, D. Lavoie, K. Nealson and C. Aguilar (1998). "The role of biomineralization in microbiologically influenced corrosion." Biodegradation **9**(1): 1-10.

Liu, D., H. Dong, M. E. Bishop, J. Zhang, H. Wang, S. Xie, S. Wang, L. Huang and D. D. Eberl (2012). "Microbial reduction of structural iron in interstratified illite-smectite minerals by a sulfate-reducing bacterium." Geobiology **10**(2): 150-162.

Liu, T. X., X. M. Li, F. B. Li, W. Zhang, M. J. Chen and S. G. Zhou (2011). "Reduction of iron oxides by *Klebsiella pneumoniae* L17: Kinetics and surface properties." Colloids and Surfaces A: Physicochemical and Engineering Aspects **379**(1-3): 143-150.

Lloyd, J. R. and J. C. Renshaw (2005). "Bioremediation of radioactive waste: radionuclide-microbe interactions in laboratory and field-scale studies." Current Opinion in Biotechnology **16**(3): 254-260.

Lovley, D. R. (2002). "Dissimilatory metal reduction: from early life to bioremediation." ASM News **68**(5): 231-237.

Lovley, D. R. (2005). Potential Role of Dissimilatory Iron Reduction in the Early Evolution of Microbial Respiration. Origins: Genesis, Evolution and Diversity of Life. J. Seckbach, Springer Netherlands**:** 299-313.

Lovley, D. R., J. L. Fraga, J. D. Coates and E. L. Blunt-Harris (1999). "Humics as an electron donor for anaerobic respiration." Environmental Microbiology **1**(1): 89-98.

Lovley, D. R., E. J. P. Phillips and D. J. Lonergan (1989). "Hydrogen and Formate Oxidation Coupled to Dissimilatory Reduction of Iron or Manganese by *Alteromonas putrefaciens*." Applied and Environmental Microbiology **55**(3): 700-706.

Lower, S. K., M. F. Hochella and T. J. Beveridge (2001). "Bacterial recognition of mineral surfaces: Nanoscale interactions between *Shewanella* and alpha-FeOOH." Science **292**(5520): 1360-1363.

Luu, Y. S. and J. A. Ramsay (2003). "Review: microbial mechanisms of accessing insoluble Fe(III) as an energy source." World Journal of Microbiology & Biotechnology **19**(2): 215-225.

Martin, F. A., C. Bataillon and M. L. Schlegel (2008). "Corrosion of iron and low alloyed steel within a water saturated brick of clay under anaerobic deep geological disposal conditions: An integrated experiment." Journal of Nuclear Materials **379**(1-3): 80-90.

Mauclaire, L., J. A. McKenzie, B. Schwyn and P. Bossart (2007). "Detection and cultivation of indigenous microorganisms in Mesozoic claystone core samples from the Opalinus Clay Formation (Mont Terri Rock Laboratory)." Physics and Chemistry of the Earth, Parts A/B/C **32**(1-7): 232-240.

Mehanna, M., R. Basséguy, M.-L. Delia, L. Girbal, M. Demuez and A. Bergel (2008). "New hypotheses for hydrogenase implication in the corrosion of mild steel." Electrochimica Acta **54**(1): 140-147.

Meike, A. and S. Stroes-Gascoyne. (2000). Review of microbial responses to abiotic environmental factors in the context of the proposed Yucca Mountain repository. AECL Technical Report 12101

Meshulam-Simon, G., S. Behrens, A. D. Choo and A. M. Spormann (2007). "Hydrogen metabolism in *Shewanella oneidensis* MR-1." Applied and Environmental Microbiology **73**(4): 1153-1165.

Michelin, A., E. Drouet, E. Foy, J. J. Dynes, D. Neff and P. Dillmann (2013). "Investigation at the nanometre scale on the corrosion mechanisms of archaeological ferrous artefacts by STXM." Journal of Analytical Atomic Spectrometry **28**(1): 59-66.

Moreira, R. L. S. (2013). Étude électrochimique des mécanismes de la biocorrosion à l'interface de l'acier au carbone en présence de bactéries ferri-réductrices et hydrogénotrophes dans le contexte de stockage des déchets nucléaires. Ph.D thesis, Université Pierre et Marie Curie - Paris 6.

Moreira, R. M., M. K. Schütz, M. Libert, B. Tribollet and V. Vivier (2013). "Influence of hydrogen-oxidizing bacteria on the corrosion of low carbon steel: Local electrochemical investigations." Bioelectrochemistry**, in press**.

Motamedi, M., O. Karland and K. Pedersen (1996). "Survival of sulfate reducing bacteria at different water activities in compacted bentonite." FEMS Microbiology Letters **141**(1): 83-87.

Myers, C. R. and K. H. Nealson (1988). "Microbial Reduction of Manganese Oxides - Interactions with Iron and Sulfur." Geochimica et Cosmochimica Acta **52**(11): 2727-2732.

Namduri, H. and S. Nasrazadani (2008). "Quantitative analysis of iron oxides using Fourier transform infrared spectrophotometry." Corrosion Science **50**(9): 2493-2497.

Nealson, K. H., A. Belz and B. McKee (2002). "Breathing metals as a way of life: geobiology in action." Antonie Van Leeuwenhoek International Journal of General and Molecular Microbiology **81**(1-4): 215-222.

Nealson, K. H. and D. Saffarini (1994). "Iron and Manganese in Anaerobic Respiration - Environmental Significance, Physiology, and Regulation." Annual Review of Microbiology **48**: 311-343.

Neff, D., P. Dillmann, M. Descostes and G. Beranger (2006). "Corrosion of iron archaeological artefacts in soil: Estimation of the average corrosion rates involving analytical techniques and thermodynamic calculations." Corrosion Science **48**(10): 2947-2970.

Neff, D., S. Reguer, L. Bellot-Gurlet, P. Dillmann and R. Bertholon (2004). "Structural characterization of corrosion products on archaeological iron: an integrated analytical approach to establish corrosion forms." Journal of Raman Spectroscopy **35**(8-9): 739-745.

Nevin, K. P. and D. R. Lovley (2002). "Mechanisms for Fe(III) oxide reduction in sedimentary environments." Geomicrobiology Journal **19**(2): 141-159.

Newman, D. K. and R. Kolter (2000). "A role for excreted quinones in extracellular electron transfer." Nature **405**(6782): 94-97.

Odziemkowski, M. S., T. T. Schuhmacher, R. W. Gillham and E. J. Reardon (1998). "Mechanism of oxide film formation on iron in simulating groundwater solutions: Raman spectroscopic studies." Corrosion Science **40**(2-3): 371-389.

Oh, S. J., D. C. Cook and H. E. Townsend (1998). "Characterization of iron oxides commonly formed as corrosion products on steel." Hyperfine Interactions **112**(1-4): 59-65.

Oulkadi, D. (2013). Gel de silice hybrides dopés en particules colloïdales de smectites pour l'étude des interactions bactérie/silicate. Ph.D thesis, Université de Lorraine.

Panias, D., M. Taxiarchou, I. Paspaliaris and A. Kontopoulos (1996). "Mechanisms of dissolution of iron oxides in aqueous oxalic acid solutions." Hydrometallurgy **42**(2): 257-265.

Papillon, F., M. Jullien and C. Bataillon (2003). Carbon steel behaviour in compacted clay: two long term tests for corrosion prediction. International Workshop - Prediction of long term corrosion behaviour in nuclear waste systems, London: Maney Pub.

Pedersen, K. (2000). Microbial Processes in Radioactive Waste Disposal. SKB Technical Report TR-00-04.

Pedersen, K. (2002). Microbial processes in the disposal of high level radioactive waste 500 m underground in Fennoscandian Shield rocks. Interactions of microorganisms with radionuclides. M. Keith-Loach and F. Livens, Elsevier**:** 279-311.

Pedersen, K., M. Motamedi and O. Karnland. (1995). Survival of bacteria in nuclear waste buffer materials: the influence of nutrients, temperature and water activity. SKB Technical Report 95-27.

Pekov, I. V., N. Perchiazzi, S. Merlino, N. Vyacheslav, M. Merlini and A. E. Zadov (2007). "Chukanovite, $Fe_2(CO_3)(OH)_2$, a new mineral from the weathered iron meteorite Dronino." European Journal of Mineralogy **19**(6): 891-898.

Philp, J. C., K. J. Taylor and N. Christofi (1991). "Consequences of sulphate-reducing bacterial growth in a lab-simulated waste disposal regime." Experientia **47**(6): 553-559.

Pierre, J. L., M. Fontecave and R. R. Crichton (2002). "Chemistry for an essential biological process: the reduction of ferric iron." Biometals **15**(4): 341-346.

Platts, N., B. D.J. and C. C. Naish. (1994). Anaerobic oxidation of carbon steel in granitic groundwaters: A review of the relevant literature. SKB Technical Report 94-01.

Potekhina, J. S., N. G. Sherisheva, L. P. Povetkina, A. P. Pospelov, T. A. Rakitina, F. Warnecke and G. Gottschalk (1999). "Role of microorganisms in corrosion inhibition of metals in aquatic habitats." Applied Microbiology and Biotechnology **52**(5): 639-646.

Poulain, S., C. Sergeant, M. Simonoff, C. Le Marrec and S. Altmann (2008). "Microbial investigations in Opalinus Clay, an argillaceous formation under evaluation as a potential host rock for a radioactive waste repository." Geomicrobiology Journal **25**(5): 240-249.

Remazeilles, C. and P. Refait (2009). "Fe(II) hydroxycarbonate $Fe_2(OH)_2CO_3$ (chukanovite) as iron corrosion product: Synthesis and study by Fourier Transform Infrared Spectroscopy." Polyhedron **28**(4): 749-756.

Roden, E. E., M. M. Urrutia and C. J. Mann (2000). "Bacterial reductive dissolution of crystalline Fe(III) oxide in continuous-flow column reactors." Applied and Environmental Microbiology **66**(3): 1062-1065.

Russell, J. D. (1979). "Infrared Spectroscopy of Ferrihydrite: Evidence for the Presence of Structural Hydroxyl-Groups." Clay Minerals **14**(2): 109-114.

Saheb, M., D. Neff, P. Dillmann, H. Matthiesen and E. Foy (2008). "Long-term corrosion behaviour of low-carbon steel in anoxic environment: Characterisation of archaeological artefacts." Journal of Nuclear Materials **379**(1–3): 118-123.

Schlegel, M. L., C. Bataillon, K. Benhamida, C. Blanc, D. Menut and J. L. Lacour (2008). "Metal corrosion and argillite transformation at the water-saturated, high-temperature iron-clay interface: A microscopic-scale study." Applied Geochemistry **23**(9): 2619-2633.

Schlegel, M. L., C. Bataillon, C. Blanc, D. Pret and E. Foy (2010). "Anodic Activation of Iron Corrosion in Clay Media under Water-Saturated Conditions at 90°C: Characterization of the Corrosion Interface." Environmental Science & Technology **44**(4): 1503-1508.

Schwertmann, U. and R. M. Cornell (1991). Iron Oxides in the Laboratory: Preparation and Characterization, Weinheim; New York: VCH.

Smart, N. R., D. J. Blackwood and L. O. Werme. (2001). The anaerobic corrosion of carbon steel and cast iron in artificial groundwaters. SKB Technical Report TR-01-22.

Smart, N. R., D. J. Blackwood and L. O. Werme (2002a). "Anaerobic corrosion of carbon steel and cast iron in artificial groundwaters: Part 1 - electrochemical aspects." Corrosion **58**: 547-559.

Smart, N. R., D. J. Blackwood and L. O. Werme (2002b). "Anaerobic corrosion of carbon steel and cast iron in artificial groundwaters: Part 2 - gas generation." Corrosion **58**: 627-637.

Stookey, L. L. (1970). "Ferrozine - a New Spectrophotometric Reagent for Iron." Analytical Chemistry **42**(7): 779-&.

Stott, J. F. D. (1993). "What Progress in the Understanding of Microbially Induced Corrosion Has Been Made in the Last 25 Years? A Personal Viewpoint." Corrosion Science **35**(1-4): 667-673.

Stroes-Gascoyne, S., C. J. Hamon, P. Maak and S. Russell (2010). "The effects of the physical properties of highly compacted smectitic clay (bentonite) on the culturability of indigenous microorganisms." Applied Clay Science **47**(1-2): 155-162.

Stroes-Gascoyne, S. and F. P. Sargent (1998). "The Canadian approach to microbial studies in nuclear waste management and disposal." Journal of Contaminant Hydrology **35**(1-3): 175-190.

Stroes-Gascoyne, S., C. Sergeant, A. Schippers, C. J. Hamon, S. Neble, M. H. Vesvres, V. Barsotti, S. Poulain and C. Le Marrec (2011). "Biogeochemical processes in a clay formation in situ experiment: Part D - Microbial analyses - Synthesis of results." Applied Geochemistry **26**(6): 980-989.

Stroes-Gascoyne, S. and J. M. West (1996). "An overview of microbial research related to high level nuclear waste disposal with emphasis on the Canadian concept for the disposal of nuclear fuel waste." Canadian Journal of Microbiology **42**(4): 349-366.

Taillefert, M., J. S. Beckler, E. Carey, J. L. Burns, C. M. Fennessey and T. J. DiChristina (2007). "*Shewanella putrefaciens* produces an Fe(III)-solubilizing organic ligand during anaerobic respiration on insoluble Fe(III) oxides." Journal of Inorganic Biochemistry **101**(11-12): 1760-1767.

Talandier, J., G. Mayer and J. Croisé (2006). Simulations of the Hydrogen migration out of Intermediate-Level Radioactive Waste disposal drifts using TOUGH2. TOUGH Symposium 2006. California, USE

Thauer, R. K., K. Jungermann and K. Decker (1977). "Energy conservation in chemotrophic anaerobic bacteria." Bacteriological Reviews **41**(1): 100-180.

Turnbull, A. (2009). A Review of the Possible Effects of Hydrogen on Lifetime of Carbon Steel Nuclear Waste Canisters. NAGRA Technical Report 09-04.

Urios, L., F. Marsal, D. Pellegrini and M. Magot (2012). "Microbial diversity of the 180 million-year-old Toarcian argillite from Tournemire, France." Applied Geochemistry **27**(7): 1442-1450.

Urios, L., F. Marsal, D. Pellegrini and M. Magot (2013). "Microbial Diversity at Iron-Clay Interfaces after 10 Years of Interaction Inside a Deep Argillite Geological Formation (Tournemire, France)." Geomicrobiology Journal **30**: 442–453.

Urrutia, M. M., E. E. Roden and J. M. Zachara (1999). "Influence of aqueous and solid-phase Fe(II) complexants on microbial reduction of crystalline iron(III) oxides." Environmental Science & Technology **33**(22): 4022-4028.

Venkateswaran, K., D. P. Moser, M. E. Dollhopf, D. P. Lies, D. A. Saffarini, B. J. MacGregor, D. B. Ringelberg, D. C. White, M. Nishijima, H. Sano, J. Burghardt, E. Stackebrandt and K. H. Nealson (1999). "Polyphasic taxonomy of the genus *Shewanella* and description of *Shewanella oneidensis* sp. nov." International Journal of Systematic Bacteriology **49**: 705-724.

Venzlaff, H., D. Enning, J. Srinivasan, K. J. J. Mayrhofer, A. W. Hassel, F. Widdel and M. Stratmann (2013). "Accelerated cathodic reaction in microbial corrosion of iron due to direct electron uptake by sulfate-reducing bacteria." Corrosion Science **66**(0): 88-96.

Videla, H. A. and L. K. Herrera (2005). "Microbiologically influenced corrosion: looking to the future." International Microbiology **8**(3): 169-180.

Videla, H. A. and L. K. Herrera (2009). "Understanding microbial inhibition of corrosion. A comprehensive overview." International Biodeterioration & Biodegradation **63**(7): 896-900.

Vignais, P. M. and B. Billoud (2007). "Occurrence, classification, and biological function of hydrogenases: An overview." Chemical Reviews **107**(10): 4206-4272.

Vinsot, A., S. Mettler and S. Wechner (2008). "In situ characterization of the Callovo-Oxfordian pore water composition." Physics and Chemistry of the Earth, Parts A/B/C **33**: S75-S86.

Viollier, E., P. W. Inglett, K. Hunter, A. N. Roychoudhury and P. Van Cappellen (2000). "The ferrozine method revisited: Fe(II)/Fe(III) determination in natural waters." Applied Geochemistry **15**(6): 785-790.

Volbeda, A., M. H. Charon, C. Piras, E. C. Hatchikian, M. Frey and J. C. Fontecilla-Camps (1995). "Crystal structure of the nickel-iron hydrogenase from *Desulfovibrio gigas*." Nature **373**(6515): 580-587.

West, J. M., I. G. McKinley and S. Stroes-Gascoyne (2002). Microbial effects on waste repository materials. Interactions of microorganisms with radionuclides. M. Keith-Loach and F. Livens, Elsevier**:** 255-278.

Wigginton, N. S., K. M. Rosso, B. H. Lower, L. Shi and M. F. Hochella Jr (2007). "Electron tunneling properties of outer-membrane decaheme cytochromes from Shewanella oneidensis." Geochimica et Cosmochimica Acta **71**(3): 543-555.

Zuo, R., E. Kus, F. Mansfeld and T. K. Wood (2005). "The importance of live biofilms in corrosion protection." Corrosion Science **47**(2): 279-287.

ANNEXE

Article I

The article I is titled **"*Combined geochemical and electrochemical methodology to quantify corrosion of carbon steel by bacterial activity*"**, which was accepted for publication in the Bioelectrochemistry journal in 2013.

The main objective of this manuscript was to combine geochemical and electrochemical approaches to study the impact of a hydrogenotrophic iron-reducing bacterium (*Shewanella oneidensis* strain MR-1) on the corrosion of carbon steel.

Geochemical analysis allowed the monitoring of the dissolution and the formation of Fe(II,III) solid corrosion products during bacterial oxidation of H_2 produced by corrosion. Local electrochemical techniques allowed to generate a high H_2 concentration for bacterial metabolism and then to probe the bacterial reaction in terms of modification of the local potential.

The results highlighted in this article are part of a joint work between members of the BIOCOR ITN research project. The common point between both studies is the use of the same carbon steel sample, experimental solution (M1) and bacteria for the experiments. Geochemical results were obtained during this PhD work, whereas the electrochemical results were obtained during Rebeca Moreira's PhD work (Moreira, 2013; Moreira *et al.*, 2013).

Both approaches show that the corrosion rate is enhanced by a factor of 2-3 in the presence of *Shewanella oneidensis* strain MR-1. It is suggested that the mechanism likely to influence the corrosion rate is the bioreduction of Fe(III) from magnetite coupled to the H_2 oxidation.

ARTICLE I

Combined geochemical and electrochemical methodology to quantify corrosion of carbon steel by bacterial activity

Marta K. Schütz, Rebeca Moreira, Olivier Bildstein, Jean-Eric Lartigue, Michel L. Schlegel, Bernard Tribollet, Vincent Vivier, Marie Libert

Accepted for publication in the Bioelectrochemistry journal in 2013

Bioelectrochemistry xxx (2013) xxx–xxx

Contents lists available at ScienceDirect

Bioelectrochemistry

journal homepage: www.elsevier.com/locate/bioelechem

Combined geochemical and electrochemical methodology to quantify corrosion of carbon steel by bacterial activity

Marta K. Schütz [a,d,*], Rebeca Moreira [c], Olivier Bildstein [a], Jean-Eric Lartigue [a], Michel L. Schlegel [b], Bernard Tribollet [c], Vincent Vivier [c], Marie Libert [a]

[a] CEA, DEN, DTN/SMTM/LMTE, 13108 Saint Paul lez Durance, France
[b] CEA, DEN, DANS/DPC/SCP/LRSI, F91191 Gif-sur-Yvette, France
[c] UPR 15 du CNRS, Laboratoire Interfaces et Systèmes Electrochimiques, Université Pierre et Marie Curie, T22, 4 Place Jussieu, 75252 Cedex 05 Paris, France
[d] Aix-Marseille Université, Sciences de l'Environnement, 13545 Aix en Provence, France

ARTICLE INFO

Article history:
Received 17 December 2012
Received in revised form 1 June 2013
Accepted 28 July 2013
Available online xxxx

Keywords:
Biocorrosion
Iron-reducing bacteria
Dihydrogen
SEM micrographs
Raman microspectroscopy
Chronoamperometry

ABSTRACT

The availability of respiratory substrates, such as H_2 and Fe(II,III) solid corrosion products within nuclear waste repository, will sustain the activities of hydrogen-oxidizing bacteria (HOB) and iron-reducing bacteria (IRB). This may have a direct effect on the rate of carbon steel corrosion. This study investigates the effects of *Shewanella oneidensis* (an HOB and IRB model organism) on the corrosion rate by looking at carbon steel dissolution in the presence of H_2 as the sole electron donor. Bacterial effect is evaluated by means of geochemical and electrochemical techniques. Both showed that the corrosion rate is enhanced by a factor of 2–3 in the presence of bacteria. The geochemical experiments indicated that the composition and crystallinity of the solid corrosion products (magnetite and vivianite) are modified by bacteria. Moreover, the electrochemical experiments evidenced that the bacterial activity can be stimulated when H_2 is generated in a small confinement volume. In this case, a higher corrosion rate and mineralization (vivianite) on the carbon steel surface were observed. The results suggest that the mechanism likely to influence the corrosion rate is the bioreduction of Fe(III) from magnetite coupled to the H_2 oxidation.

1. Introduction

Disposal of high-level nuclear waste (HLW) in deep geological repositories is increasingly considered as a reliable solution in many countries. In France, for example, the current option explored is to store the vitrified HLW in stainless steel containers, conditioned in carbon steel overpacks which are then emplaced in a deep underground repository (about 500 m deep) in an argillaceous formation (claystone). This is known as a multi-barrier system, designed to ensure long-term radionuclide confinement. One of the purposes of the multi-barrier system is to prevent water circulation around the metallic packages, thus preventing corrosion in water-saturated conditions.

However, knowledge about steel corrosion processes, especially over a long time period, must still be expanded to ensure that geological disposals will remain safe over a period of several hundred thousand years. The main issues related to steel corrosion are the influences of physico-chemical conditions (e.g. water saturation, pressure, temperature, pH, redox potential), and consequently microbial activity on the durability of the different metallic packages.

Several studies reveal the presence of microorganisms in most of the deep clay formations already investigated, such as the Callovo-Oxfordian argillite and Opalinus clay [1,2]. Therefore, an impact of the microbial activity can be expected with respect to the various phenomena that may occur within the repository, such as (i) radionuclide migration through clay formations (including effects of biofilms); (ii) build-up of the gas phase by microbial gas production; and (iii) Microbiologically Influenced Corrosion (MIC) or biocorrosion [3,4] which is discussed in this study.

Energetic substrates and nutrients are available to support microbial activity under geological conditions. Nutrients may be present either as soluble species in the groundwater or in minerals (solid-associated forms). Among the energetic substrates, H_2 is expected to be one of the most efficient substrates (acting as an electron donor) [5]. It can be produced by radiolytic dissociation of water or by anoxic aqueous metallic corrosion [6,7]. Moreover, Fe(III) from clay minerals [8,9] and corrosion products, such as magnetite (Fe_3O_4) [10–14], could be a significant electron acceptor for anaerobic microbial respiration (by dissimilatory processes). The availability of such substrates may sustain the development of hydrogen-oxidizing bacteria (HOB) and iron-reducing bacteria (IRB), which in turn could have an impact on geochemical and corrosion processes in deep geological environments.

Several studies have dealt with the impact of sulfate-reducing bacteria (SRB) [15–18] on corrosion processes. In contrast, the impact of the

* Corresponding author at: CEA, DEN, DTN/SMTM/LMTE, 13108 Saint Paul lez Durance, France. Tel.: +33 4 42254942; fax: +33 4 42256272.
E-mail address: martakerber@gmail.com (M.K. Schütz).

1567-5394/$ – see front matter © 2013 Elsevier B.V. All rights reserved.
http://dx.doi.org/10.1016/j.bioelechem.2013.07.003

IRB species have been only marginally investigated. Their role in biocorrosion is still under debate; either an inducing or an inhibitory effect by formation of a protective biofilm on metal surface has been hypothesized [19–21]. Recent studies have investigated the impact of IRB species on metallic corrosion processes under geological disposal conditions [22–24]. The IRB can use Fe(III) from magnetite or other Fe(III) (hydr)oxides as electron acceptor in the presence of H_2 as electron donor. An alteration of the (hydr)oxide layers with a possible reactivation of the corrosion process may thus occur as a consequence of the Fe(III) bacterial respiration [22].

This study investigates the effect of the HOB and IRB activities on the corrosion rate of carbon steel in the presence of H_2 as the sole electron donor. These investigations are supported by geochemical and electrochemical techniques. Geochemical analysis allows the monitoring of the metal dissolution and the formation of Fe(II,III) solid corrosion products during the bacterial oxidation of H_2 produced by corrosion. Local electrochemical techniques allow to generate a high H_2 concentration for bacterial metabolism and then to probe the bacterial reaction in terms of modification of the local potential.

2. Materials and methods

2.1. Bacterial culture

The *Shewanella oneidensis* strain MR-1 (ATCC 700550™) was chosen as a model of IRB and HOB. Cultures were obtained aerobically at the beginning of the stationary growth phase in a Luria Bertani Broth (LB) medium (5 g L^{-1} NaCl, 10 g L^{-1} tryptone, 5 g L^{-1} yeast extract) after 24 h at 30 °C under sterile conditions. Bacterial cells were harvested from the LB medium by centrifugation (4000 rpm for 20 min), washed once with sterile minimal medium (M1) and then inoculated in the batch reactors (initial concentration 10^8 cells mL^{-1} counted by epifluorescence method with LIVE/DEAD® *Bac*Light™ kit). The chemically defined minimal medium (M1) was prepared according to Kostka and Nealson (1998) [25]. However, minor modifications were made to the composition [22] in order to obtain a representative solution of the groundwater found in the argillaceous formations for geological disposal in France. The final composition is shown in Table 1.

Table 1
M1 minimal medium composition.

Compound	Concentration
$(NH_4)_2SO_4$	9 mM
Na_2SeO_4	11 μM
HEPES	17 mM
$NaHCO_3$	2 mM
K_2HPO_4[a]	0.5 mM
KH_2PO_4[a]	0.3 mM
$CoSO_4.7H_2O$[b]	5 μM
$NiSO_4.6H_2O$[b]	5 μM
NaCl[b]	10 μM
H_3BO_3[c]	45 μM
$ZnSO_4.7H_2O$[c]	0.8 μM
$Na_2MoO_4.2H_2O$[c]	3 μM
$CuSO_4.5H_2O$[c]	0.2 μM
$MnSO_4.H_2O$[c]	1 μM
$MgSO_4.7H_2O$[c]	0.8 mM
$CaCl_2.2H_2O$[c]	0.4 mM
$FeSO_4.7H_2O$[c]	4 μM
Arginine[d]	0.11 mM
Glutamate[d]	0.13 mM
Serine[d]	0.19 mM
Nicotinic acid[e]	0.08 mM
Thiamine-HCl[e]	0.01 mM
Biotine[e]	0.40 μM

[a] Phosphate buffer solution.
[b] Metals supplement solution.
[c] Basal salts solution.
[d] Amino acid solution.
[e] Vitamins solution.

The pH was adjusted to ca. 7 with NaOH and then the medium was sterilized by autoclaving (120 °C for 20 min), except for the thermolabile components (e.g. amino acids) which were filter-sterilized (0.22 μm) and added to the autoclaved medium.

2.2. Carbon steel coupons

Corrosion studies were performed with low carbon steel coupons A37 supplied by the French Alternative Energies and Atomic Energy Commission (CEA). They contain 0.12% C, 0.22% Si, 0.62% Mn, 0.008% Al, 0.012% S, 0.012% P, 0.02% Ni, 0.03% Cr, 0.04% Cu, 0.005% Co and <0.005% Ti. Carbon steel is a corrosion-allowance material which is expected to have nearly-uniform corrosion in a reducing environment, and has been therefore considered as a candidate material for packages used in the geological disposal.

The cylindrical coupons were laterally insulated from the solution by a diallyl phthalate glass-fiber resin (Presi) in order to expose only an active surface of 0.8 cm^2. Then, the coupons were polished with 600 grit SiC abrasive paper and sterilized with ethanol by sonication for 15 min prior to the experiments.

2.3. Batch experiments

All experiments started under strictly sterile conditions in batch reactors at 30 °C under an anaerobic atmosphere. Both abiotic and biotic conditions were investigated.

2.3.1. Geochemical techniques

The geochemical experiments were performed in triplicate in 140 mL of M1 medium under an N_2/CO_2 (90:10%) atmosphere. The corrosion reaction was monitored as a function of time by gas and solution analyses. The aqueous Fe concentration was analyzed by Inductively Coupled Plasma Optical Emission Spectrometry (ICP-OES, Varian, VISTA-MPX) after 0.02 μm filtration and 2% (v/v) HNO_3 acidification. The analysis of H_2 in the headspace was carried out by Micro Gas Chromatography (Varian, CP-4900) using a thermal conductivity detector with N_2 as carrier gas. The total H_2 concentration was calculated as the sum of the concentrations in the gas and the aqueous phases (determined using Henry's law).

2.3.2. Electrochemical techniques

The electrochemical measurements were performed with a homemade Scanning Electrochemical Microscope (SECM) [26,27] in a 4-electrode cell configuration elaborated specifically for anaerobic and sterile conditions. The double wall glass cell was equipped with the carbon steel working electrode (WE1) placed in the bottom of the cell, and with a platinum probe of 50 μm in radius acting as a second mobile working electrode (WE2) for generating H_2. The cell was sealed with a Teflon cover and the platinum WE2 probe was placed through a nitrile flexible support on the cover, perpendicular to WE1, in a way to allow its displacement for the measurements. The WE2 microelectrode was positioned with the help of motorized stages driven by a motion controller (Newport) with Labview software. Both working electrodes used as reference a saturated calomel electrode (SCE) and a platinum grid as counter electrode.

The disassembled cell and the platinum WE2 probe were sterilized prior to the experiments with 70% ethanol solution for 20 min; then rinsed with sterilized water in a laminar flow chamber and finally UV-irradiated for 15 min. The lugging capillary (for holding the reference electrode) and the platinum grid counter electrode were sterilized in autoclave. The cell was assembled under sterile conditions and 230 mL of M1 medium was introduced and deaerated for 2 h under an N_2 atmosphere. The N_2 flow was maintained at the cell headspace (near to the liquid surface) so as to ensure the anaerobic conditions during the whole electrochemical measurements. A supplementary N_2

Please cite this article as: M.K. Schütz, et al., Combined geochemical and electrochemical methodology to quantify corrosion of carbon steel by bacterial activity, Bioelectrochemistry (2013), http://dx.doi.org/10.1016/j.bioelechem.2013.07.003

bubbling of the bulk solution was also carried out during inoculation of the electrochemical cell.

An approach curve was performed at a rate of 7.5 μm s^{-1} with the probe polarized at −0.9 V/SCE and the substrate held at Open Circuit Potential (OCP). Such approach curve allowed the contact point between the steel substrate and the apex of the probe to be determined with a spatial resolution better than a fraction of micrometer. Then, the microelectrode was repositioned at 50 μm from the substrate and polarized for generating locally H_2 (Scheme 1). The use of SECM for generation or collection of H_2 in solution has already been described in the literature [28,29].

2.4. Characterization of the coupon surface

Steel coupon surfaces in the geochemical experiments were analyzed, after 5 months of reaction, by Raman microspectroscopy and Scanning Electron Microscopy (SEM). The coupon surfaces of the electrochemical experiments were analyzed only by SEM. The samples for the Raman analysis were kept in anoxic conditions in small confining boxes and the measurements were performed through a glass window (500 μm thick) using a LabRam HR800 (Horiba Jobin Yvon) spectrometer equipped with a Nd-YAG laser at 532 nm and a 50× long range objective lens. The laser power was 50 mW attenuated by a factor of 100. The acquisition time ranged from 60 to 600 s depending on the spectral quality. The Raman spectra are presented in this study without smoothing or line fitting. The spectra analysis was performed by comparing the significant bands with literature data [30–34]. SEM studies were performed at 20 keV and 5.3 nA with a Leica Stereoscan 440 microscope coupled with Energy Dispersive Spectroscopy (EDS) for elemental semi-quantitative analyses (Princeton Gamma-Tech). The samples were slightly rinsed with deionised water, dried with N_2 gas and stored in plastic containers until analysis. The coupons were carbon coated prior to the SEM analysis.

3. Results and discussion

3.1. Geochemical results

Under anaerobic conditions, carbon steel corrosion (simplified as Fe in the Eqs. (1) & (3)) is described by iron oxidation as the anodic reaction (Eq. (1)) and water reduction as the cathodic reaction (Eq. (2)):

$$Fe \rightarrow Fe^{2+} + 2e^- \quad (1)$$

$$2H_2O + 2e^- \rightarrow 2HO^- + H_2 \quad (2)$$

According to the overall reaction (Eq. (3)), the molecular stoichiometry of Fe:H_2 produced by corrosion is 1:1:

$$Fe + 2H_2O \rightarrow Fe^{2+} + 2OH^- + H_2 \quad (3)$$

Fig. 1 shows the evolution of Fe and H_2 produced by carbon steel corrosion.

In abiotic conditions, equimolar H_2 and dissolved Fe are released, which is in good agreement with the stoichiometry of Eq. (3). Effective biocorrosion was evidenced by the larger amounts of Fe and H_2 produced at about 5 days compared to abiotic conditions. Moreover, in the presence of bacteria, H_2 concentration remains much lower when compared to dissolved Fe concentration. Such evidence suggests that bacteria consume the soluble H_2 in the aqueous phase for respiration. Several studies have indeed shown that H_2 is an important energetic substrate, especially in disposal environments where only low amounts of biodegradable organic matter are available [5,7,35].

The pH in the bulk solution was initially equal to 6.47 and only a slight increase was observed at the end of the experiments for both abiotic and biotic conditions, with values of 6.54 and 6.62, respectively (data not shown).

A black layer and a white precipitate (over the black layer) were progressively formed on the coupon surface in both abiotic and biotic conditions, suggesting a reaction between the surface and species in solution which also resulted in a decrease in the aqueous Fe concentration after 20 days of reaction (results not shown in Fig. 1). The Raman analysis for the solid corrosion products formed in abiotic conditions (Fig. 2a) revealed the presence of vivianite ($Fe_3(PO_4)_2.8H_2O$) (i & iii) and magnetite (ii) as the most abundant mineral phases. In contrast, for the biotic conditions (Fig. 2b), the intensity of vivianite bands is greater (i & iii); the intensity of magnetite band significantly decreases (ii); and relatively intense bands appear in the region 1440 cm^{-1} (iv), which may indicate cellular compounds (e.g. lipids, enzymes like hydrogenase) on the coupon surface. The magnetite band is broad, suggesting formation of a mineral phase with poor crystallinity.

The SEM analysis also revealed vivianite as a corrosion product for both abiotic (Fig. 3a & b) and biotic (Fig. 3e & f) conditions. A modification in the morphology of this mineral was observed in the presence of bacteria. Moreover, in biotic conditions the black layer morphology and chemical composition are modified (Fig. 3g & h), compared to those in

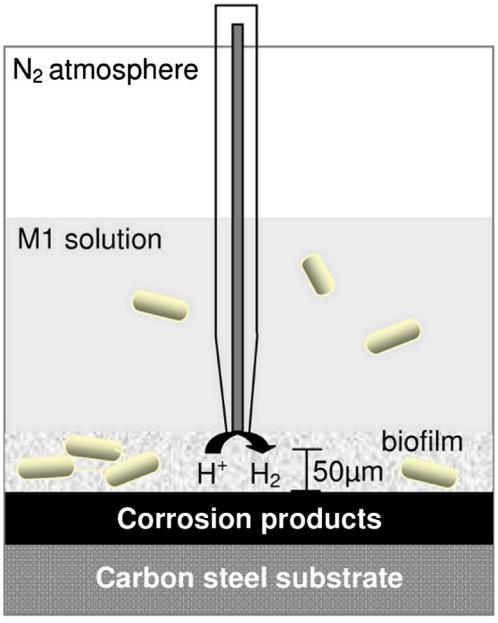

Scheme 1. Sketch of the experimental setup for the local H_2 generation by the platinum probe in a close vicinity of the carbon steel substrate.

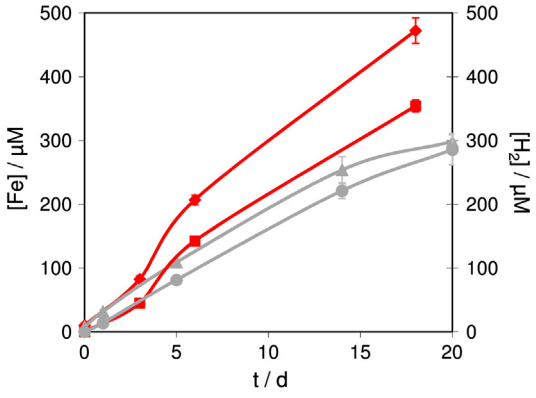

Fig. 1. Production of Fe and H_2 by carbon steel corrosion during the geochemical experiments ($n = 3$): Fe (♦,▲) and H_2 (■,●) concentrations (μM) as function of time (days). Biotic conditions (♦,■) and abiotic conditions (▲,●).

Please cite this article as: M.K. Schütz, et al., Combined geochemical and electrochemical methodology to quantify corrosion of carbon steel by bacterial activity, Bioelectrochemistry (2013), http://dx.doi.org/10.1016/j.bioelechem.2013.07.003

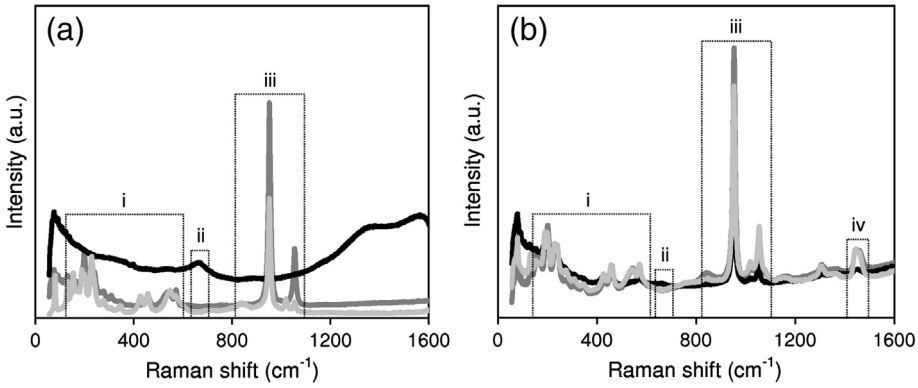

Fig. 2. Raman spectra of corrosion products detected on steel coupons reacted during 5 months in the geochemical experiments. (a) Abiotic conditions: vivianite (i) and (iii); magnetite (ii). (b) Biotic conditions: vivianite (i) and (iii); magnetite (ii); and cellular compounds (iv). Each spectrum in the figures is representative of the signal collected on the sample surface.

abiotic conditions (Fig. 3c & d). Both Raman and SEM analyses point out a modification of the composition and crystallinity of corrosion products by the bacterial activity.

The literature proposes different mechanisms of bacterial-induced corrosion. Widdel's group have hypothesized that, in the case of SRB and methanogenic species, corrosion is enhanced by direct electron transfer from metal to bacterial cells [18,36]. In contrast, we can assume that, in the case of IRB species, dissimilatory reduction of Fe(III) promotes the solubilization and removal of (hydr)oxide layers, exposing carbon steel surfaces to corrosion [21,22]. To date, direct contact, nanowires and electron shuttling have been proposed as strategies for dissimilatory Fe(III) reduction from insoluble substrates [37]. Our results corroborate these findings, showing that *S. oneidensis* can reduce Fe(III) from magnetite using soluble H_2 produced during the corrosion process as an electron donor.

3.2. Electrochemical results

Fig. 4 shows the OCP variation of the carbon steel electrode in the M1 solution. Such measurement indicates the variation of the difference of potential between the carbon steel working electrode and the reference electrodes at the equilibrium state over time. The OCP remains stable at −714 mV/SCE during the first 16 h of the experiment. Then, the supplementary N_2 bubbling of the solution for 1 h is accompanied by a small decrease of the potential (about 23 mV). The OCP is slightly perturbed upon addition of the *S. oneidensis* inoculum, but then it slightly decreases and stabilizes at ca. −718 mV/SCE after a few hours.

After mapping experiments (data not shown), in which the platinum probe was polarized to generate H_2, we noticed a formation of solid phases over the entire surface of the steel substrate (Fig. 5a). SEM micrograph of the substrate at the position where the H_2 was locally generated (target area in Fig. 5a) is shown in Fig. 5b. A more important mineralization was observed on this specific area, in the vicinity of the probe, where H_2 was kept in a confinement volume (ca. 3.9×10^{-8} cm^3). This observation suggests an influence of the corrosion increase in this localized area. Changes in the local pH, redox potential, or even the enhancement of the bacterial activity due to a greater availability of energetic substrate (H_2) can be considered as potential factors for the mineralization effect. The EDS analysis of a single crystal (Fig. 5d & c, respectively) shows the formation of iron phosphate as vivianite.

During the corrosion process two phenomena take place simultaneously — the anodic reaction (Eq. (1)) and the cathodic reaction (Eq. (2)). At the equilibrium (OCP), the net current in the substrate is zero. When the potential of the steel electrode is set to a value greater than the OCP, the anodic dissolution of the substrate is favored. We thus biased the substrate state in order to control the kinetics of dissolution and we locally generated H_2 through the probe brought to the vicinity of the substrate. The distance between the steel substrate and the probe was set at 50 μm by performing a preliminary approach curve [38]. With such a device (sketched in Scheme 1), it was possible to reproduce and to control the different processes that usually take place simultaneously on the steel electrode.

The steel dissolution was monitored over 5 days for different corrosion conditions by measuring the total current of the electrode in order to reveal the influence of the local H_2 concentration (Fig. 6). The corrosion rate was shown to depend on the presence of both bacteria and the H_2 that was generated. When the potential of the steel electrode is biased at OCP, in the abiotic conditions and without H_2 generation (Fig. 6, curve a), the current remains in the range of 0.5 μA cm^{-2}. In contrast, when H_2 is generated, the current of the steel electrode increases to about 1 μA cm^{-2} and remains in a quasi steady-state regime (Fig. 6, curve b). The positive feedback regime that takes place between the probe and the substrate explains this behavior [38]. In biotic conditions, a steady increase of the current is observed during 5 days (Fig. 6, curve c).

The integration of the anodic current of each experiment provides the exchanged charge during the corrosion process (Table 2). These results clearly indicate that in biotic conditions and with local H_2 generation, the corrosion magnitude is significantly increased due to an increase of the bacterial activity (the more dihydrogen is produced, the more the consumption of iron by the bacteria). It is noteworthy that these experiments do not allow the measurements of the H_2 produced by the corrosion process, only the H_2 generated by the probe.

Again, the carbon steel surface exhibited a mineralization as iron phosphate. It should also be mentioned that longer experiments (more than 5 days) are usually difficult to perform in such experimental conditions, since the distance between the probe and the substrate is small (50 μm) so as to confine the H_2 generation. Hence, the biocorrosion can lead to accumulation of corrosion or biological products between the probe and the substrate. Bacterial adhesion on the carbon steel surface can also be observed after the experiments, as shown in Fig. 7, which is another indication of the bacterial action on the corrosion process.

3.3. Corrosion rate results

The corrosion rates were obtained from the results of the geochemical and electrochemical experiments. In the case of geochemical measurements, the corrosion rate was estimated from the aqueous Fe concentration (shown in Fig. 1), according to Eq. (3) and assuming no precipitation of corrosion products during the first 20 days of reaction. In contrast, in the case of electrochemical measurements, the charges for steel corrosion obtained for 5 days were converted considering the

Please cite this article as: M.K. Schütz, et al., Combined geochemical and electrochemical methodology to quantify corrosion of carbon steel by bacterial activity, Bioelectrochemistry (2013), http://dx.doi.org/10.1016/j.bioelechem.2013.07.003

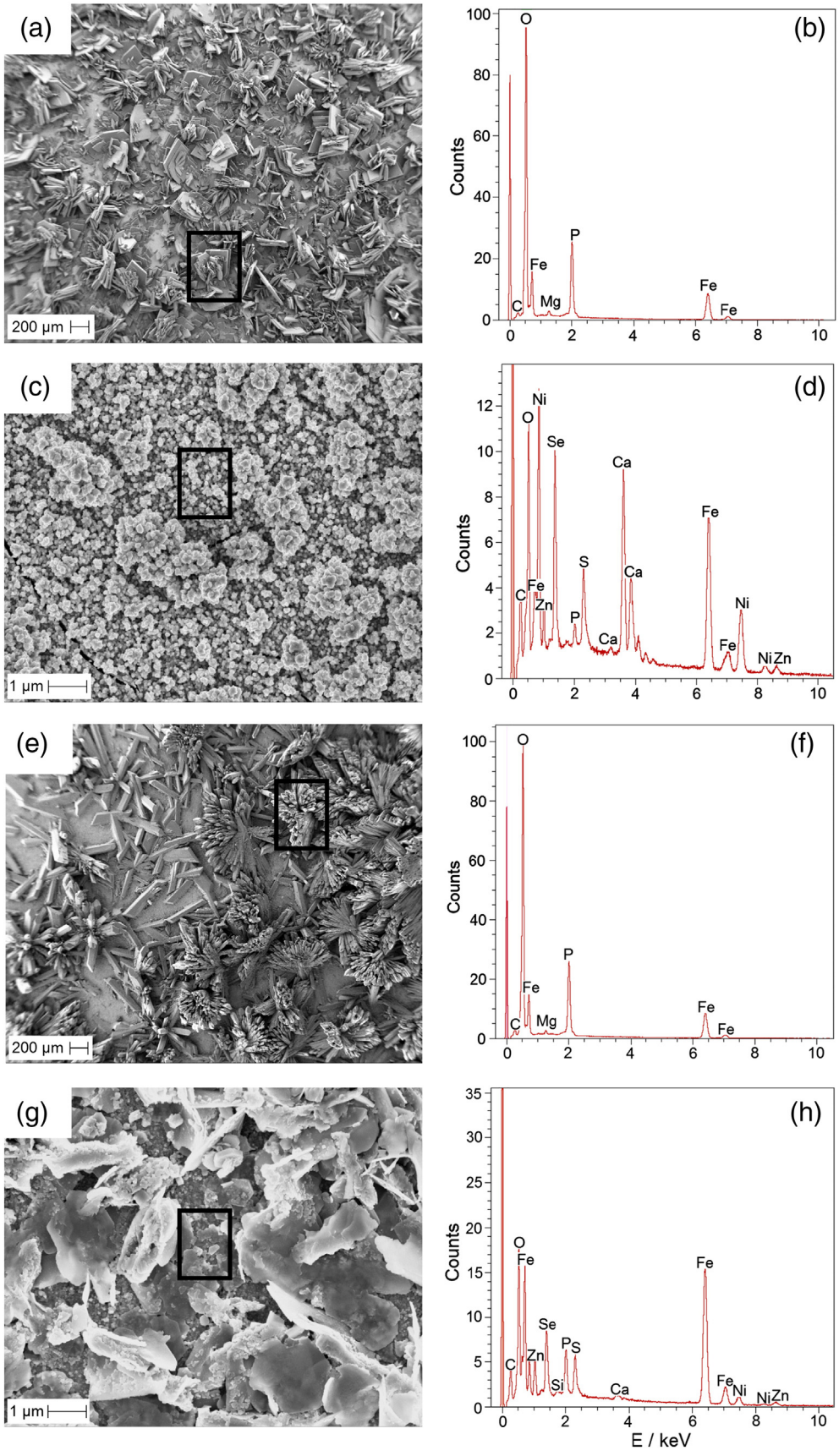

Fig. 3. SEM micrographs and EDS spectra of corrosion products formed by carbon steel corrosion after 5 months in the geochemical experiments. (a–d) Abiotic conditions: precipitate formed over the black layer (a, b) and black layer (c, d). (e–h) Biotic conditions: precipitate formed over the black layer (e, f) and black layer (g, h). The rectangle on SEM images corresponds to the areas analyzed by EDS.

Please cite this article as: M.K. Schütz, et al., Combined geochemical and electrochemical methodology to quantify corrosion of carbon steel by bacterial activity, Bioelectrochemistry (2013), http://dx.doi.org/10.1016/j.bioelechem.2013.07.003

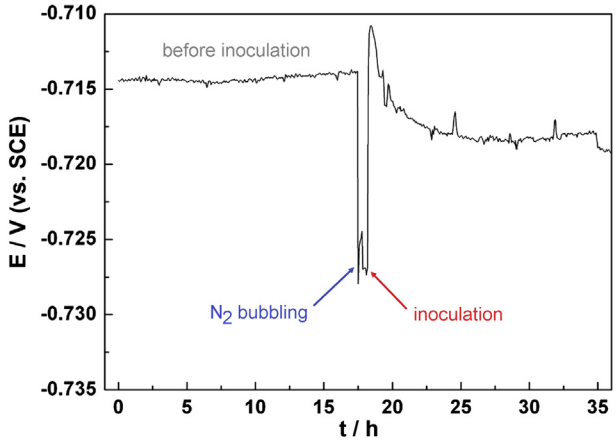

Fig. 4. Evolution of the OCP (V vs. SCE) as function of time (hours) of the carbon steel substrate before and after inoculation of *Shewanella oneidensis* during the electrochemical experiments.

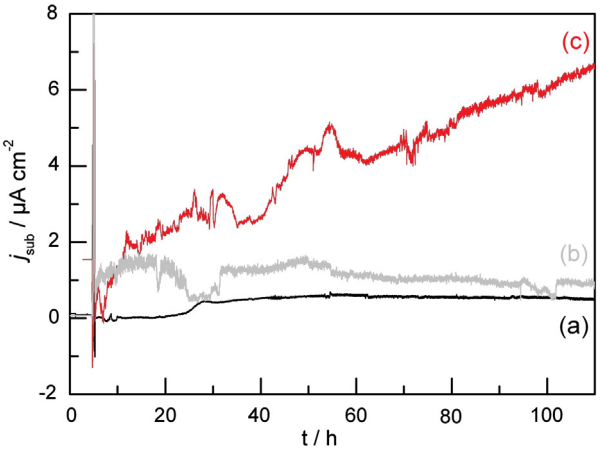

Fig. 6. Chronoamperometric response (μA cm^{-2}) as function of time (hours) of the carbon steel substrate in biotic conditions for electrochemical experiments. (a) No local H_2 generation by the probe. (b) Without *Shewanella oneidensis* under a local H_2 generation by the probe. (c) With both *Shewanella oneidensis* and local H_2 generation by the probe.

general value for steel (j = 86.3 μA cm^{-2} equals a corrosion rate of 1 mm $year^{-1}$) [39].

Fig. 8 and Table 2 show the corrosion rates obtained from the geochemical and electrochemical results, respectively. Fig. 8 shows that the short-term corrosion rate is higher than the long-term one for both abiotic and biotic conditions. The bacterial effect on the corrosion rate tends to decrease with time, suggesting a depletion of nutrients because of experimental conditions (batch reactors) leading to a limitation of bacterial development. Average rates are estimated at 100 μm $year^{-1}$ and 30 μm $year^{-1}$ for biotic and abiotic conditions, respectively, after a period of about 20 days.

The corrosion rates obtained by the electrochemical results (Table 2) show values that are significantly smaller when compared to the geochemical results because of the choice of the potential applied for the measurements. At OCP, anodic and cathodic currents are contributing to the overall reaction and, in this case, the cathodic reaction (water reduction) is not taken into account and the anodic current (steel dissolution) value is therefore underestimated. Although the corrosion rate

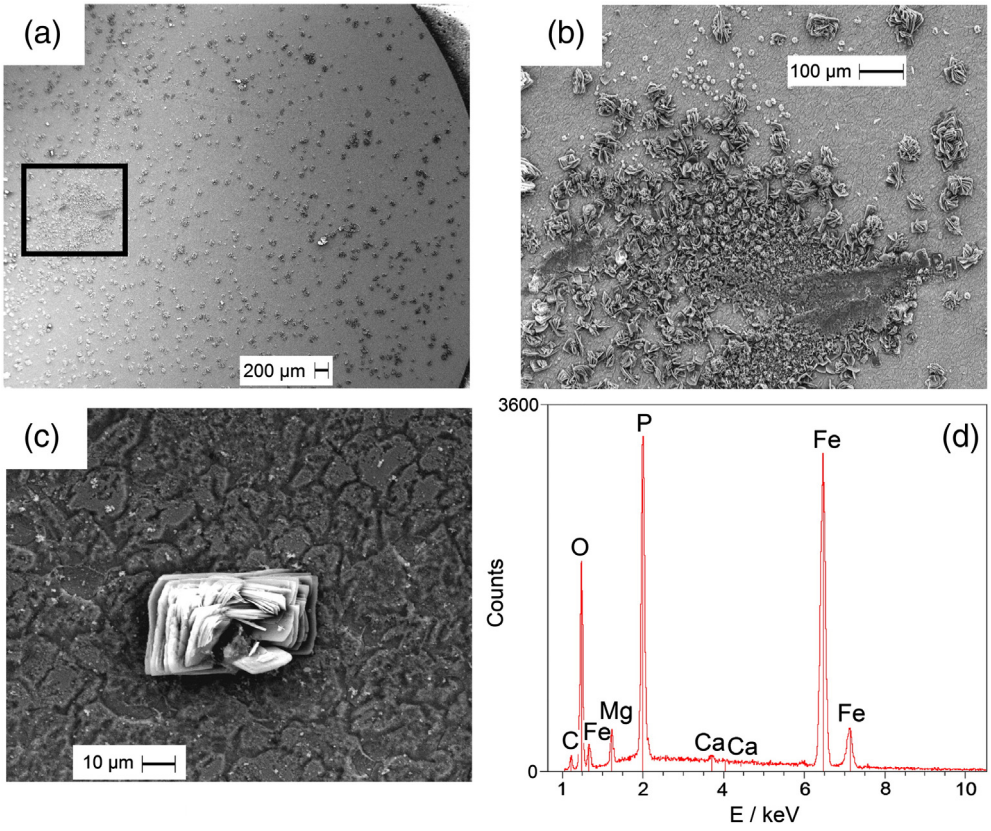

Fig. 5. SEM micrographs of carbon steel coupon reacted during 3 days in biotic conditions in the electrochemical experiments. (a) Global view of the coupon surface. (b) View of the center where the H_2 generating probe was placed. (c) View of a single crystal formed. (d) EDS spectrum of the crystal shown in Figure c.

Please cite this article as: M.K. Schütz, et al., Combined geochemical and electrochemical methodology to quantify corrosion of carbon steel by bacterial activity, Bioelectrochemistry (2013), http://dx.doi.org/10.1016/j.bioelechem.2013.07.003

Table 2
Determination of the exchanged charge (in millicoulomb) during the corrosion in different conditions (calculated from results presented in Fig. 6) with the respective corrosion rates.

Experiment	q (st corr) / (mC)[a]	q (H_2 generation) / (mC)[b]	v (corr) / (μm/y)[c]
With bacteria without probe (Fig. 6a)	216 ± 11	–	7.3 ± 0.4
With probe without bacteria (Fig. 6b)	430 ± 22	100 ± 5	14.5 ± 0.7
With probe and bacteria (Fig. 6c)	1400 ± 70	100 ± 5	48.0 ± 2.4

[a] Charge (steel corrosion).
[b] Charge (H_2 generation).
[c] Corrosion rate.

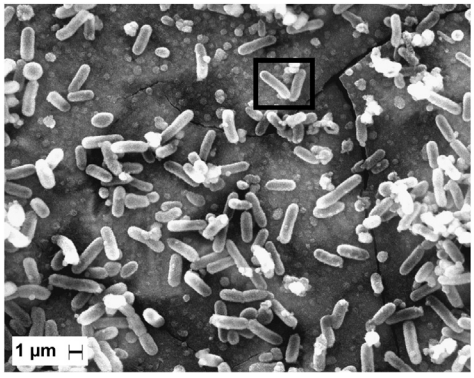

Fig. 7. SEM micrograph showing attachment of bacteria on the carbon steel surface after 10 days in the electrochemical experiments. The rectangle on SEM image indicates the cells of *Shewanella oneidensis*. No fixation treatment was performed for the analysis.

values obtained in the electrochemical and geochemical experiments cannot be directly compared, they demonstrate a clear influence of the bacterial activity. The corrosion rates are shown to be greater in biotic than abiotic conditions with both techniques.

4. Conclusions

Safe disposal of HLW is a key issue of waste management. The current disposal concept relies on a multi-barrier system which includes different metallic packages (stainless steel, carbon steel). Over time, production of H_2 and Fe(II,III) solid corrosion products is expected due to the anoxic aqueous corrosion. Such corrosion products can provide respiratory substrates for bacterial activities. Therefore, the influence of the biological parameter on corrosion has to be also evaluated in order to demonstrate the safety of the disposal system.

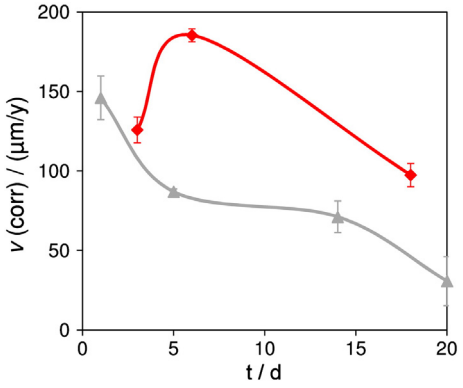

Fig. 8. Corrosion rate (μm $year^{-1}$) as function of time (days) measured at the outset of the geochemical experiments ($n = 3$): biotic (♦); and abiotic (▲) conditions.

This study demonstrates that the corrosion process is enhanced by a factor of 2–3 in presence of bacteria. The geochemical results showed that after 5 days a greater amount of Fe and H_2 is produced during corrosion in comparison with abiotic conditions. Moreover, the consumption of the soluble H_2 in the aqueous phase by bacteria is evidenced as well as a modification in the composition and crystallinity of the solid corrosion products (magnetite and vivianite) on the carbon steel surface. Still, the electrochemical results showed a higher mineralization (vivianite) and corrosion rate in the presence of bacteria when H_2 is generated in a small confinement volume (ca. 3.9×10^{-8} cm^3). So, our results suggest that *S. oneidensis* likely induces corrosion by reduction of Fe(III) from magnetite using soluble H_2 produced by the corrosion process as electron donor.

However, it remains to be determined if the bacterial activity will have a similar long-term effect on the corrosion rate under disposal conditions. A modeling approach, including calibrated parameters according to the results of the short-term experiments, could be used to extrapolate the corrosion kinetics and predict biocorrosion processes on a long-term scale.

Acknowledgments

The authors thank Damien Féron (CEA Saclay, France) for the carbon steel samples, Paul Soreau (IBEB, CEA Cadarache, France) for the ICP-OES analysis and Françoise Pillier (LISE, UPR15, France) for the SEM analysis. This research has received funding from the European Community's Seventh Framework Programme (FP7/2007-2013) under grant agreement n° 238579 by the BIOCOR ITN project (website: www.biocor.eu/).

References

[1] S. Stroes-Gascoyne, C.J. Hamon, D.A. Dixon, J.B. Martino, Microbial analysis of samples from the tunnel sealing experiment at AECL's Underground Research Laboratory, Phys. Chem. Earth. 32 (2007) 219–231.
[2] S. Poulain, C. Sergeant, M. Simonoff, C. Le Marrec, S. Altmann, Microbial investigation of Opalinus clay, an argillaceous formation under evaluation as a potential host rock for a radioactive waste repository, Geomicrobiol. J. 25 (2008) 240–249.
[3] M.J. Keith-Roach, F.R. Livens, Microbial interactions with radionuclides — summary and future perspectives, Interactions of Microorganisms with Radionuclides, Elsevier, 2002, pp. 383–391.
[4] S. Stroes-Gascoyne, J.M. West, An overview of microbial research related to high-level nuclear waste disposal with emphasis on the Canadian concept for the disposal of nuclear fuel waste, Can. J. Microbiol. 42 (1996) 349–366.
[5] L.H. Lin, G.F. Slater, B.S. Lollar, G. Lacrampe-Couloume, T.C. Onstott, The yield and isotopic composition of radiolytic H_2, a potential energy source for the deep subsurface biosphere, Geochim. Cosmochim. Acta 69 (2005) 893–903.
[6] G. Galès, M.F. Libert, R. Sellier, L. Cournac, V. Chapon, T. Heulin, Molecular hydrogen from water radiolysis as an energy source for bacterial growth in a basin containing irradiating waste, FEMS Microbiol. Lett. 240 (2004) 155–162.
[7] M. Libert, O. Bildstein, L. Esnault, R. Sellier, Molecular hydrogen: an abundant energy source for bacterial activity in nuclear waste repositories, Phys. Chem. Earth. 36 (2011) 1616–1623.
[8] J.E. Kostka, J.W. Stucki, K.H. Nealson, J. Wu, Reduction of structural Fe(III) in smectite by a pure culture of *Shewanella putrefaciens* strain MR-1, Clays Clay Miner. 44 (1996) 522–529.
[9] J.E. Kostka, J. Wu, K.H. Nealson, J.W. Stucki, The impact of structural Fe(III) reduction by bacteria on the surface chemistry of smectite clay minerals, Geochim. Cosmochim. Acta 63 (1999) 3705–3713.
[10] J.E. Kostka, K.H. Nealson, Dissolution and reduction of magnetite by bacteria, Environ. Sci. Technol. 29 (1995) 2535–2540.
[11] M.K. Schütz, M. Libert, M.L. Schlegel, J.E. Lartigue, O. Bildstein, Dissimilatory iron reduction in presence of hydrogen: a case of microbial activity in the nuclear waste disposal, Procedia Earth Planet. Sci. 7 (2013) 409–412.
[12] O. Bildstein, L. Trotignon, M. Perronnet, M. Jullien, Modelling iron-clay interactions in deep geological disposal conditions, Phys. Chem. Earth. 31 (2006) 618–625.
[13] F.A. Martin, C. Bataillon, M.L. Schlegel, Corrosion of iron and low alloyed steel within a water saturated brick of clay under anaerobic deep geological disposal conditions: an integrated experiment, J. Nucl. Mater. 379 (2008) 80–90.
[14] M.L. Schlegel, C. Bataillon, K. Benhamida, C. Blanc, D. Menut, J.-L. Lacour, Metal corrosion and argillite transformation at the water-saturated, high temperature iron-clay interface: a microscopic-scale study, Appl. Geochem. 23 (2008) 2619–2633.
[15] V.L. Rainha, I.T.E. Fonseca, Kinetic studies on the SRB influenced corrosion of steel: a first approach, Corros. Sci. 39 (1997) 807–813.
[16] D. Féron, I. Dupont, G. Novel, Influence of microorganisms on the free corrosion potential of stainless steels in natural seawaters, in: D. Thierry (Ed.), Aspects of Microbiologically Induced Corrosion, The Institute of Material, London, 1997, pp. 103–139.

[17] I.B. Beech, Sulfate-reducing bacteria in biofilms on metallic materials and corrosion, Microb. Today 30 (2003) 115–117.
[18] H. Venzlaff, D. Enning, J. Srinivasan, K.J.J. Mayrhofer, A.W. Hassel, F. Widdel, M. Stratmann, Accelerated cathodic reaction in microbial corrosion of iron due to direct electron uptake by sulfate-reducing bacteria, Corros. Sci. 66 (2013) 88–96.
[19] M. Dubiel, C.H. Hsu, C.C. Chien, F. Mansfeld, D.K. Newman, Microbial iron respiration can protect steel from corrosion, Appl. Environ. Microb. 68 (2002) 1440–1445.
[20] K. Lee, D.K. Newman, Microbial iron respiration: impacts on corrosion processes, Appl. Microbiol. Biotechnol. 62 (2003) 134–139.
[21] L.K. Herrera, H.A. Videla, Role of iron-reducing bacteria in corrosion and protection of carbon steel, Int. Biodeterior. Biodegrad. 63 (2009) 891–895.
[22] L. Esnault, M. Jullien, C. Mustin, O. Bildstein, M. Libert, Metallic corrosion processes reactivation sustained by iron-reducing bacteria: implication on long-term stability of protective layers, Phys. Chem. Earth. 36 (2011) 1624–1629.
[23] M. Libert, L. Esnault, D. Féron, Biocorrosion en conditions de stockage géologique de déchets radioactifs, Mater. Tech. 99 (2011) 581–589.
[24] R. Moreira, M.K. Schütz, M. Libert, B. Tribollet, V. Vivier, Local Electrochemical Measurements Applied to Biocorrosion, Bioelectrochem, 2013. (this issue).
[25] J.E. Kostka, K.H. Nealson, Isolation, cultivation, and characterization of iron- and manganese-reducing bacteria, Techniques in Microbial Ecology, Oxford University Press, New York, 1998, p. 468.
[26] C. Gabrielli, S. Joiret, M. Keddam, H. Perrot, N. Portail, P. Rousseau, V. Vivier, A SECM assisted EQCM study of iron pitting, Electrochim. Acta 52 (2007) 7706–7714.
[27] M. Keddam, N. Portail, D. Trinh, V. Vivier, Progress in scanning electrochemical microscopy by coupling with electrochemical impedance and quartz crystal microbalance, Chem. Phys. Chem. 10 (2009) 3175–3182.
[28] P.G. Nicholson, S. Zhou, G. Hinds, A.J. Wain, A. Turnbull, Electrocatalytic activity mapping of model fuel cell catalyst films using scanning electrochemical microscopy, Electrochim. Acta 54 (2009) 4525–4533.
[29] D. Trinh, M. Keddam, X.R. Novoa, V. Vivier, Alternating current measurements in scanning electrochemical microscopy, part 2: detection of adsorbates, Chem. Phys. Chem. 12 (2011) 2177–2183.
[30] D.L.A. Faria, S.V. Silva, M.T. Oliveira, Raman microspectroscopy of some iron oxides and oxyhydroxides, J. Raman Spectrosc. 28 (1997) 873–878.
[31] M. Hanesch, Raman spectroscopy of iron oxides and (oxy)hydroxides at low laser power and possible applications in environmental magnetic studies, Geophys. J. Int. 177 (2009) 941–948.
[32] L. Bellot-Gurlet, D. Neff, S. Réguer, J. Monnier, M. Saheb, P. Dillmann, Raman studies of corrosion layers formed on archaeological irons in various media, J. Nano Res. 8 (2009) 147–156.
[33] R.L. Frost, W. Martens, P.A. Williams, J.T. Kloprogge, Raman and infrared spectroscopic study of the vivianite-group phosphates vivianite, baricite and bobierrite, Mineral. Mag. 66 (2002) 1063–1073.
[34] R.L. Frost, M.L. Weier, Raman spectroscopic study of vivianites of different origins, Neues Jb. Mineral. Monat. 10 (2004) 445–463.
[35] F.H. Chapelle, K. O'Neill, P.M. Bradley, B.A. Methé, S.A. Ciufo, L.L. Knobel, D.R. Lovley, A hydrogen-based subsurface microbial community dominated by methanogens, Nature 415 (2002) 312–315.
[36] H.T. Dinh, J. Kuever, M. Mußmann, A.W. Hassel, M. Stratmann, F. Widdel, Iron corrosion by novel anaerobic microorganisms, Nature 427 (2004) 829–832.
[37] Y.-S. Luu, J.A. Ramsay, Review: microbial mechanisms of accessing insoluble Fe(III) as an energy source, World J. Microb. Biotechnol. 19 (2003) 215–225.
[38] J. Kwak, A.J. Bard, Scanning electrochemical microscopy. Theory of the feedback mode, Anal. Chem. 61 (1989) 1221–1227.
[39] C. Lemaitre, N. Pébère, D. Festy, Biodétérioration des matériaux, EDP Sciences, 1998.

Marta K. Schütz received a BS degree in Industrial Chemistry from the Catholic University of Rio Grande do Sul, Porto Alegre, Brazil in 2007; completed her MSc in Materials Science and Engineering in March 2010 at the same University. Now she is a PhD student at the French Commission for Atomic Energy and Alternative Energies (CEA). She is working on biocorrosion phenomena implicated on the radioactive waste geological disposal. The overall objective of her study is to better understand the impact of bacterial activities (notably IRB species) on the corrosion products (dihydrogen and iron (hydr)oxides) and on the rate of anoxic corrosion.

Rebeca Moreira has graduated in Food Engineering with a Master degree in Quality Control in Food and Drink Industries in Rio de Janeiro, Brazil. Started the PhD study in 2010 as a member of the BIOCOR Program at the Laboratory of Interfaces and Electrochemical Systems (University Pierre et Marie Curie), Paris, France. The subject of her work is the study of biocorrosion of carbon steel using local electrochemical techniques.

Olivier Bildstein received his PhD in geochemistry (1998) from the University of Strasbourg. He is a senior research engineer at the French Commission for Atomic Energy and Alternative Energies (CEA) since 2000, after a postdoctoral stay at LLNL (California, USA). His previous affiliations include a doctoral fellowship at the French Institute for Petroleum (1994–1998) and a position as hydrogeologist at the French Geological Survey (BRGM) (1993). His research focuses on numerical modeling of reactive, multicomponent, and multiphase flow and transport with application to long term evolution of materials in radioactive waste disposal, subsurface pollution/remediation, and potential bacteria mediated processes.

Jean-Eric Lartigue received his PhD in experimental geochemistry (1994) from the University of Marseille (France). He is a research engineer at the French Commission for Atomic Energy and Alternative Energies (CEA) since 1998 after a postdoctoral fellowship at CEA (1995–1998). His research focuses on water rock-interactions with: a) experimental measurements of minerals and conditioning matrices for long live radionuclide dissolution kinetic rates law and b) reactive-transport modeling of materials' long term behavior in a radioactive waste disposal context.

Michel L. Schlegel was received at the Ecole Normale Supérieure of Lyon in 1992. He received his PhD degree at the University of Grenoble in 2000 and worked as a postdoctoral fellow at the University of Colorado at Boulder from 2000 to 2001. He is now a research engineer and a senior expert at the Commissariat à l'Energie Atomique et aux Energies Alternatives. His research topics include metal corrosion and speciation of trace (radio)elements in complex environmental matrices (complexation, interaction with mineral surfaces).

Bernard Tribollet after his graduation from the "Ecole Supérieure d'Electricité" (1973), joined the laboratory of I. Epelboin (now LISE-CNRS UPR 15) where he prepared a PhD under his supervision. In 1981, with the support of a NSF fellowship, he spent one year as a visiting scientist at the University of California, Berkeley under the supervision of Prof. John Newman. His current research field concerns different problems: mass transport, electrodissolution, corrosion and in particular biocorrosion. He co-authored, with Prof. Mark Orazem of the University of Florida, a textbook on impedance spectroscopy published in 2008 as part of the Electrochemical Society Series (Wiley).

Vincent Vivier was born in Saint-Maur (France) in 1971. He received his PhD in 2000 under the supervision of Dr. L.T. Yu in Thiais (France). In 2002, he joined the Laboratoire Interfaces et Systèmes Électrochimiques (CNRS-UPR 15). His current research field concerns the characterization of heterogeneous interface reactivity by means of local electrochemical techniques and electrochemical impedance spectroscopy.

Marie Libert received her PhD in biochemistry (1986) from the University of Technology of Compiegne-France. She is a senior research engineer at the French Commission for Atomic Energy and Alternative Energies (CEA) since 1998. Her previous affiliation includes a doctoral fellowship at the same university. Her research focuses on different fields such as the effect of microorganisms on long term behavior of materials used in nuclear repository, biocorrosion, impact of radioactive emission on biota, and anaerobic microbiology. She was and she is a European expert on several international research programs.

Please cite this article as: M.K. Schütz, et al., Combined geochemical and electrochemical methodology to quantify corrosion of carbon steel by bacterial activity, Bioelectrochemistry (2013), http://dx.doi.org/10.1016/j.bioelechem.2013.07.003

Article II

The article II is titled **"*Dissimilatory iron reduction in the presence of hydrogen: a case study of microbial activity and nuclear waste disposal*"**, which was accepted for publication in the Procedia Earth and Planetary Science journal in 2013.

The main objective of this manuscript was to evaluate the impact of microbial activity (*Shewanella oneidensis* strain MR-1) on the reduction of structural Fe(III) from synthetic magnetite sample in presence of high H_2 concentration (H_2:CO_2:N_2 / 60:10:30%). Chemical monitoring was performed and the first results were discussed.

The results show that 2.4% of the total amount of Fe(III) is reduced from magnetite in the presence of bacteria and H_2 as the sole electron donor, indicating that a crystalline Fe oxide of mixed oxidation state is bioavailable for anaerobic respiration.

This article is part of the proceedings of the Fourteenth International Symposium on Water-Rock Interaction (WRI 14), 2013, Avignon, France.

ARTICLE II

Dissimilatory iron reduction in the presence of hydrogen: a case study of microbial activity and nuclear waste disposal

Marta K. Schütz, Marie Libert, Michel L. Schlegel, Jean-Eric Lartigue, Olivier Bildstein

Published in the Procedia Earth and Planetary Science journal, 2013

Available online at www.sciencedirect.com

SciVerse ScienceDirect

Procedia Earth and Planetary Science 7 (2013) 409 – 412

Procedia
Earth and Planetary Science

Water Rock Interaction [WRI 14]

Dissimilatory iron reduction in the presence of hydrogen: a case study of microbial activity and nuclear waste disposal

Marta K. Schütz[a,c]*, Marie Libert[a], Michel L. Schlegel[b], Jean-Eric Lartigue[a], Olivier Bildstein[a]

[a]*CEA Cadarache, DEN, DTN/SMTM/LMTE, 13108 Saint Paul lez Durance, France*
[b]*CEA Saclay, DEN, DANS/DPC/SCP/LRSI, F91191 Gif-sur-Yvette, France*
[c]*Aix-Marseille Université, Sciences de l'Environnement, 13545 Aix en Provence, France*

Abstract

Long-term corrosion in water-saturated conditions is the main factor responsible for the alteration of nuclear waste packages. However, the formation of passive layers (e.g. magnetite) on the metal surface can generally be considered a protective mechanism against corrosion. Understanding the impact of living microorganisms on the long-term durability of metallic packages is still an open issue, especially with regard to microbiologically influenced corrosion (MIC) processes. This study examines the impact of microbial activity on the reduction of structural Fe(III) in magnetite. The results demonstrate that such Fe oxides are available as electron acceptors using H_2 as electron donor for microbial metabolism, which may have a direct effect on the rates of corrosion.

Selection and/or peer-review under responsibility of the Organizing and Scientific Committee of WRI 14 – 2013

Keywords: hydrogen; magnetite; iron-reducing bacteria; anoxic metallic corrosion; nuclear waste geological disposal.

1. Introduction

The French concept of high-level radioactive waste disposal relies on a multi-barrier system. The waste is confined in a glass matrix packaged into multiple metallic envelopes buried at 500 m depth in natural clay formations. Such system has been designed in order to prevent the migration of radionuclides as well as to prevent water penetration into the radioactive waste repository [1].

The environmental conditions within the repository will change with time. After the closure, the conditions will be warm and oxidizing (10 to 100 years). The temperature will then decrease and the

* Corresponding author. Tel.: +33 4 42254942; fax: +33 4 42256272.
E-mail address: martakerber@gmail.com.

1878-5220
Selection and/or peer-review under responsibility of the Organizing and Scientific Committee of WRI 14 – 2013
doi:10.1016/j.proeps.2013.03.177

conditions will change to anoxic because the radiation rate is reduced and oxygen is consumed, for example, by aerobic corrosion and microbial activities. A re-saturation of the repository by interstitial water of the geological formation will ultimately occur [1], with concomitant corrosion of the metallic envelopes. A better understanding about these processes, especially over a long time, is needed to ensure a safe disposal.

Several studies have demonstrated that bacteria and archaea are present in most of the deep geological formations already investigated, surviving even under extreme conditions [2,3]. In addition, introduction of microorganisms into disposal repository is also expected as a consequence of the human activities during the construction and operational phases. Within nuclear waste repository, metallic corrosion can be considered as a source of nutritional and energetic substrates for microbial growth. Under anoxic conditions, hydrogen will be produced and iron (hydr)oxides (e.g. magnetite, Fe_3O_4) will be formed on the metal surface, which can act as a protective way against corrosion (as passive layer). Therefore, the activities of hydrogen-oxidizing bacteria (HOB) and iron-reducing bacteria (IRB) become parameters that also need to be evaluated regarding the safety of the current disposal concept.

This paper investigates the microbial activity in presence of hydrogen (as electron donor) and magnetite (as electron acceptor) through a series of experiments. The goal is to evaluate if *Shewanella oneidensis* strain MR-1 (IRB and HOB model organism) is capable of reducing the structural Fe(III) from magnetite coupled to H_2 oxidation for respiration. Such Fe(III) bioavailability in iron (hydr)oxides can likely alter the protective properties of passive layers, which could enhance the anoxic corrosion rate.

2. Materials and Methods

All experiments were performed under strictly sterile conditions in batch reactors at 30°C under an anaerobic $H_2/N_2/CO_2$ (60:30:10%, respectively) atmosphere. Both abiotic and biotic conditions were carried out.

2.1. Bacteria

Shewanella oneidensis strain MR-1 (ATCC 700550™) was chosen as model of IRB and HOB. Cultures were grown aerobically to a stationary growth phase in Luria Bertani Broth (LB) medium (5 $g.L^{-1}$ NaCl, 10 $g.L^{-1}$ tryptone, 5 $g.L^{-1}$ yeast extract) for 24 h at 30°C. Bacterial cells were harvested from the LB medium by centrifugation (4000 rpm/20 min), washed once with sterile minimal medium (M1) and then inoculated into the reactors (initial concentration $8x10^7$ $cells.mL^{-1}$ counted by epifluorescence method with LIVE/DEAD® *Bac*Light™ kit).

2.2. Experimental medium

A chemically defined minimal medium (M1) was prepared according to Kostka and Nealson (1998) [4]. However, minor modifications were made to the composition [5] in order to obtain a representative solution of the groundwater found in the clay formations for geological disposal in France. The final composition was the following: 9 mM $(NH_4)_2SO_4$, 0.5 mM K_2HPO_4, 0.3 mM KH_2PO_4, 2 mM $NaHCO_3$, 0.8 mM $MgSO_4.7H_2O$, 0.4 mM $CaCl_2.2H_2O$, 45 µM H_3BO_3, 10 µM NaCl, 4 µM $FeSO_4.7H_2O$, 5 µM $CoSO_4.7H_2O$, 5 µM $NiSO_4.6H_2O$, 3 µM $Na_2MoO_4.2H_2O$, 11 µM Na_2SeO_4, 1 µM $MnSO_4.H_2O$, 0.8 µM $ZnSO_4.7H_2O$, 0.2 µM $CuSO_4.5H_2O$, 17 mM HEPES buffer; amino acids (0.11 M arginine, 0.13 M glutamate, 0.19 M serine); and vitamins (0.08 mM nicotinic acid, 0.01 mM thiamine-HCl, 0.40 µM biotine). The pH was adjusted to approximately 7 with NaOH and then the medium was sterilized by

autoclaving (120°C for 20 min) or filtration (0.22 µm), depending on the presence of components that cannot resist to heating (e.g. amino acids).

2.3. Magnetite

Magnetite ($FeO:Fe_2O_3 = Fe_3O_4$) is an iron oxide of mixed oxidation state [Fe(II), Fe(III)]. Samples were prepared using the synthesis method described by Schwertmann and Cornell (1991) [6]. A solution of 0.3 M $FeSO_4.7H_2O$ (560 mL) was heated to 90°C and then a mixture (240 mL) of 0.27 M in KNO_3 and 3.33 M in KOH was added dropwise. The suspension was maintained at 90°C for 1 h with continuous stirring and cooled overnight. All synthesis was carried out under N_2 atmosphere. At the end, a dark black solid was obtained, which was washed several times with degassed Milli-Q water followed by freeze drying. The samples were sterilized by UV irradiation for 30 min under anaerobic conditions and an amount of 7 $g.L^{-1}$ was added into the reactors.

2.4. Fe(II)/Fe(III) speciation

Fe(II)/Fe(III) speciation in solution was analyzed colorimetrically using the Ferrozine assay [7], which was extensively described by Viollier et al. (2000) [8]. Sampled suspensions were filtered through 0.02 µm into 0.5 N HCl (50:50 v/v). This filtrate was considered as the soluble Fe(II) fraction. Since Fe(III) cannot be analyzed directly, a reducing reagent (hydroxylamine) was used under strongly acidic conditions in order to obtain the total Fe concentration. Consequently, Fe(III) concentrations were obtained using the difference between total Fe and Fe(II) concentrations. The absorbance of the samples was determined by spectroscopy at 562 nm (Tecan, Infinite M1000).

3. Results and Discussion

Our results demonstrate the ability of *Shewanella oneidensis* to reduce Fe(III) from magnetite in presence of H_2 as the sole electron donor. Figure 1 shows total Fe concentration with Fe(II)/Fe(III) speciation for abiotic (Fig. 1a) and biotic (Fig. 1b) conditions.

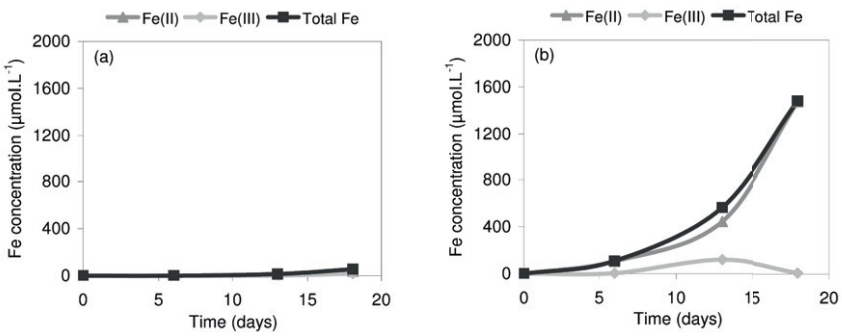

Fig. 1. Magnetite bioreduction: Fe(II) (▲), Fe(III) (◆) and total Fe (■) concentrations; (a) abiotic and (b) biotic conditions.

No magnetite dissolution/reduction was observed in abiotic conditions (Fe concentrations remain constant over 18 days). In contrast, an effect of the bacterial activity was evidenced with respect to Fe(II)

production. The rate of magnetite reduction was initially slow followed by a rapid increase after 10 days, showing an increase with time of soluble Fe(II). The bioreduction was followed by a slight increase in the pH (results not shown), which is in agreement with the literature [9,10]. The pH reached a final value of 6.8 with a starting pH of 6.6 (pH remains constant for abiotic conditions).

The results showed that 1500 $\mu mol.L^{-1}$ of Fe(III) was reduced over 18 days, assuming that 1 mol of Fe(II) was produced for each mol of Fe(III) reduced. Therefore, 2.4% of the total amount of Fe(III) was reduced from magnetite (initial amount 62 $mmol.L^{-1}$). H_2 was not completely consumed by *Shewanella oneidensis* (results not shown), suggesting that at higher concentrations (in this study 80 $mmol.L^{-1}$), the efficiency of H_2 oxidation coupled to Fe(III) reduction is significantly decreased. Similar results were reported by Fredrickson et al. (2003) [10] using lactate (20 $mmol.L^{-1}$) as the sole electron donor; an amount of 52% of lactate oxidation was observed for 50 $mmol.L^{-1}$ of 2-line ferrihydrite. Lactate oxidation was greater at low concentrations (e.g. 93% for 1 $mmol.L^{-1}$ lactate).

4. Conclusion

The activity of iron-reducing bacteria has implications for natural biogeochemical processes as well as for fate and transport of multivalent metals and radionuclides. The results presented herein demonstrate that a crystalline Fe oxide of mixed oxidation state is available as electron acceptor for bacterial metabolism. Regarding the issues related to metallic corrosion within nuclear waste repository, it is evidenced that such Fe(III) bioavailability in addition to the presence of H_2 can potentially alter the protective properties of passive layers, which may have a direct effect on anoxic corrosion rate. The new mineral phases formed by magnetite reduction have still to be investigated in order to better understand the biomineralization processes involved.

Acknowledgements

This research was funded by a grant (n° 238579) from the European Community's Seventh Framework Programme (FP7/2007-2013).

References

[1] Andra. Dossier Argile: Synthesis - Evaluation of the feasibility of a geological repository in an argillaceous formation. Reference 266VA, 2005.

[2] Pedersen K. Microbial processes in the disposal of high level radioactive waste 500 m underground in Fennoscandian Shield rocks. In: *Interactions of Microorganisms with Radionuclides*, Elsevier; 2002, p. 279–311.

[3] Stroes-Gascoyne S, Hamon CJ, Dixon DA, Martino JB. Microbial analysis of samples from the tunnel sealing experiment at AECL's Underground Research Laboratory. *Phys Chem Earth* 2007; **32**: 219–231.

[4] Kostka JE, Nealson KH. Isolation, cultivation, and characterization of iron- and manganese-reducing bacteria. In: *Techniques in Microbial Ecology*, Oxford University Press, New York, 1998, p. 468.

[5] Esnault L, Jullien M, Mustin C, Bildstein O, Libert M. Metallic corrosion processes reactivation sustained by iron-reducing bacteria: Implication on long-term stability of protective layers. *Phys Chem Earth* 2011; **36**: 1624–9.

[6] Schwertmann U, Cornell RM. *Iron Oxides in the Laboratory: Preparation and Characterization*. New York: Weinheim; 1991.

[7] Stookey LL. Ferrozine - A New Spectrophotometric Reagent for Iron. *Anal Chem* 1970; **42**: 779–781.

[8] Viollier E, Inglett PW, Hunter K, Roychoudhury AN, Van Cappellen P. The Ferrozine method revisited: Fe(II)/Fe(III) determination in natural waters. *Appl Geochem* 2000; **15(6)**: 785–790.

[9] Dong H, Fredrickson JK, Kennedy DW, Zachara JM, Kukkadapu RK, Onstott TC. Mineral Transformation Associated with the Microbial Reduction of Magnetite. *Chem Geol* 2000; **169**: 299–318.

[10] Fredrickson JK, Kota S, Kukkadapu RK, Liu C, Zachara JM. Influence of Electron Donor/Acceptor Concentrations on Hydrous Ferric Oxide (HFO) Bioreduction. *Biodegr* 2003; **14**: 91–103.

ABSTRACT

The nuclear industry must to demonstrate the feasibility and safety of high level nuclear waste (HLNW) disposal. The generally recognised strategy for HLNW disposal is based on a multi-barrier system made by metallic packages surrounded by geological formation. The nuclear waste repository will be water re-saturated with time, and then the metallic corrosion process will take place. The aqueous corrosion will produce dihydrogen (H_2) that represents a new energetic source (electron donor) for microbial development. Moreover, the formation of Fe(II,III) solid corrosion products, such as magnetite (Fe_3O_4), will provide electron acceptors favoring the development of iron-reducing bacteria (IRB). The activity of hydrogenotrophic and IRB can potentially alter the protective properties of passivating oxide layers (i.e. magnetite) which could reactivate corrosion.

The main objective of this study is to evaluate the role of hydrogenotrophic and IRB activities on anoxic corrosion process by using geochemical indicators. *Shewanella oneidensis* strain MR-1 was chosen as model organism, and both abiotic and biotic conditions were investigated.

In a first setup of experiments, our results indicate that synthetic magnetite is destabilized in the presence of hydrogenotrophic IRB due to structural Fe(III) reduction coupled to H_2 oxidation. The extent of Fe(III) bioreduction is notably enhanced with the increase in the H_2 concentration in the system: 4% H_2 < 10% H_2 < 60% H_2. In a second setup of experiments, our results indicate that corrosion extent changes according to the solution composition and the surface of metallic sample (iron powder and carbon steel coupon). Moreover, the solid corrosion products are different for each sample: vivianite, siderite and chukanovite are the main mineral phases identified in the experiments with iron powder, while vivianite and magnetite are identified with carbon steel coupons. Our results demonstrate that corrosion rate is increased almost two-fold in the presence of bacteria after 5 months of reaction. The mechanism likely to enhance corrosion is the destabilization/dissolution of magnetite by structural Fe(III) reduction coupled to H_2 oxidation.

This study gives new insights regarding the understanding of biocorrosion phenomena, identification of physicochemical mechanisms, and determination of key parameters controlling the corrosion rate.

Keywords: biocorrosion, dihydrogen, magnetite, iron-reducing bacteria, hydrogenotrophic bacteria, geochemical approach, geological disposal

RESUME

L'industrie nucléaire se doit de démontrer la faisabilité et la sûreté du stockage de déchets nucléaires de haute activité et à vie longue (HAVL). La stratégie généralement reconnue pour le stockage de déchets HAVL est basée sur un concept multi-barrières utilisant des containers métalliques confinés dans une formation géologique. Au cours du temps, la resaturation en eau du site de stockage va initier les mécanismes de corrosion métallique. La corrosion aqueuse du fer des composants métalliques va produire du dihydrogène (H_2) connu pour être un des plus importants substrats énergétiques (donneur d'électrons) permettant le développement de micro-organismes. De plus, la formation de produits de corrosion solides, tels que la magnétite (Fe_3O_4), va fournir du Fe(III) espèce susceptible de jouer le rôle accepteur d'électrons pour le développement de bactéries ferri-réductrices. L'activité de bactéries hydrogénotrophes et ferri-réductrices peut potentiellement altérer les propriétés protectrices des couches d'oxydes (i.e. la magnétite) et donc réactiver la corrosion.

L'objectif principal de cette étude est d'évaluer le rôle de l'activité de bactéries hydrogénotrophes et ferri-réductrices sur le processus de corrosion anoxique en utilisant des indicateurs géochimiques. *Shewanella oneidensis* strain MR-1 a été choisi comme micro-organisme modèle et des conditions abiotiques et biotiques ont été mises en œuvre.

Dans un premier système d'expérimentations, les résultats indiquent que la magnétite de synthèse est déstabilisée en présence de bactéries hydrogénotrophes et ferri-réductrices due à la réduction du Fe(III) structural couplée à l'oxydation de l'H_2. La quantité de Fe(III) bioréduit est augmentée en présence de concentrations croissantes en H_2 dans le système: 4% H_2 < 10% H_2 < 60% H_2. Dans un second système d'expérimentations, les résultats indiquent que la réaction de corrosion est différente selon la composition de la solution et la surface de contact de l'échantillon métallique (poudre de fer ou coupon en acier au carbone). De plus, les produits de corrosion solides sont différents pour chaque échantillon étudié: vivianite, sidérite et chukanovite sont les principales phases minérales identifiées dans les expériences avec de la poudre de fer, tandis que vivianite et magnétite sont identifiées en présence de coupons en acier au carbone. Les résultats montrent que la vitesse de corrosion est quasiment deux fois plus importante en présence de bactéries après 5 mois de réaction. Le mécanisme probable de biocorrosion est la déstabilisation de la magnétite par réduction du Fe(III) structural couplée à l'oxydation de l'H_2.

Cette étude apporte une nouvelle approche sur la compréhension des phénomènes de biocorrosion, l'identification des mécanismes physico-chimiques et la détermination des paramètres contrôlant la vitesse de corrosion.

Mots clés: biocorrosion, dihydrogène, magnétite, bactérie ferri-réductrice, bactérie hydrogénotrophe, approche géochimique, stockage géologique